European Journal of Taxonomy 1011: 1–79
https://doi.org/10.5852/ejt.2025.1011.3023

europeanjournaloftaxonomy.eu
ISSN 2118-9773
2025 · Weber D. *et al.*

Received: 8 January 2025 • Accepted: 11 June 2025 • Published: 25 August 2025

Topic editor: Magalie Castelin • Section editor: Fabio Stoch • Desk editor: Kristiaan Hoedemakers

Monograph

urn:lsid:zoobank.org:pub:09569CAD-967D-482F-A675-B4BCB7723F6F

Water diviners described: six new species of the *Niphargus aquilex* complex (Crustacea, Amphipoda)

Dieter WEBER [1,*,†], Traian BRAD [2,*,†] & Alexander M. WEIGAND [3]

[1] Senckenberg Deutsches Entomologisches Institut,
Eberswalder Straße 90, 15374 Müncheberg, Germany.
[1,3] Fondation faune-flore, 25 rue Munster, 2160 Luxembourg, Luxembourg.
[2] Institutul de Speologie "Emil Racoviță", Department of Cluj-Napoca,
Str. Clinicilor Nr. 5–7, 400006 Cluj-Napoca, Romania.
[3] Musée national d'histoire naturelle du Luxembourg, 25 rue Munster,
2160 Luxembourg, Luxembourg.

[*] Corresponding authors: dieter.weber124@gmx.de, traian.brad@acad-cj.ro
[3] Email: Alexander.Weigand@mnhn.lu

[†] These authors contributed equally to this work.

Abstract. With the onset of molecular taxonomy, it has been recognized that groundwater crustaceans in the family Niphargidae Bousfield, 1977 (Crustacea, Amphipoda) can demonstrate either highly variable or static phenotypes. Thus, it is recommended that new species descriptions follow an integrative taxonomic approach, considering morphotaxonomic and molecular characteristics to establish new taxa. The morphospecies *Niphargus aquilex* Schiødte, 1855 has its main distribution area in Central Europe, spanning southern England, the northern half of France, the Benelux countries, Germany and the Czech Republic. Genetic analyses have shown that it comprises a highly diverse species complex, including amongst others the well-recognized morphospecies *Niphargus schellenbergi* S. Karaman, 1932. In this study, we describe six new species based on available adult males and females – *Niphargus luxemburgensis* Weber, Weigand & Brad sp. nov., *N. palatinensis* Weber & Brad sp. nov., *N. normandiensis* Weber & Brad sp. nov., *N. wasgauensis* Weber & Brad sp. nov., *N. saraviensis* Weber & Brad sp. nov., *N. lotharingiensis* Weber & Brad sp. nov. – taking a re-evaluated published genetic backbone as a further reference into account. The six newly described species appeared pseudocryptic, as minor morphological differences were noticed. A short discussion of the morphological and molecular delimitations is provided.

Keywords. Cryptic diversity, *Niphargus*, integrative taxonomy, groundwater fauna, species complex.

Weber D., Brad T. & Weigand A.M. 2025. Water diviners described: six new species of the *Niphargus aquilex* complex (Crustacea, Amphipoda). *European Journal of Taxonomy* 1011: 1–79.
https://doi.org/10.5852/ejt.2025.1011.3023

Introduction

The family Niphargidae Bousfield, 1977 (Crustacea, Amphipoda) comprises more than 440 formally described species (Horton *et al.* 2023) found nearly all over Europe and parts of Asia, from Spain (Karaman 2017) to Iran (Esmaeili-Rineh *et al.* 2017). They are usually stygobionts, that is, adapted and most often restricted to subterranean life in groundwater and groundwater-dependent habitats (e.g., springs, interstitials). Species show typical troglomorphic characteristics by lacking eyes and body pigmentation, but bearing elongated appendages in most cases. While the majority of the species were described based on their morphology alone, it was revealed that Niphargidae harbors a plethora of cryptic or pseudocryptic species (Fišer & Zagmajster 2009; Delić *et al.* 2017; Eme *et al.* 2018), which can be attributed to widely stable or largely overlapping morphological characteristics. Describing new species by integrating DNA sequences has become a standard for nearly ten years in *Niphargus* taxonomy (Brad *et al.* 2015; Delić *et al.* 2017; Fišer *et al.* 2017, 2018).

The *Niphargus aquilex* species complex ("*aquilex*" "water diviner" in Latin) includes multiple cryptic species, and can serve as a prime example to witness past and current taxonomic challenges (McInerney *et al.* 2014; Weber *et al.* 2023). Westwood (1853) was the first to recognize *N. aquilex* Schiødte, 1855 as a species new to science, although he assigned his material to the first recording of *Niphargus stygius* (Schiødte, 1847) in England. *Niphargus aquilex* was redescribed based on specimens from the neotype locality Crowborough (United Kingdom), which were deposited in the British Museum (Karaman 1980). Another taxon of the *N. aquilex* species complex, *Niphargus schellenbergi* S. Karaman, 1932, was first described from Gännsbrünnle, in the south of Sendelbach (Bavaria, Germany). In the same year, *N. schellenbergi* was redescribed as a subspecies of *N. aquilex* (Schellenberg 1933), whereas from 1972 onwards, it was again considered a species distinct from *N. aquilex* sensu stricto (Straškraba 1972).

Niphargus schellenbergi was always regarded as a single taxonomic entity (either at species or subspecies level), but even prior the age of DNA sequencing it was suspected that *N. aquilex* might actually represent a species complex (Gerecke *et al.* 2005). Several subspecies of *N. aquilex* were described: *N. a. vejdowskyi* (Wrześniowski 1890; Schellenberg 1932), *N. a. tauri* (Schellenberg 1933), *N. a. moldavicus* (Dobreanu *et al.* 1953), *N. a. dobati* (Sket 1999). While the systematic position of the first is still uncertain, the other three taxa have been elevated to the species level (Fišer *et al.* 2009a). Their taxonomic position was corroborated by molecular analyses performed by McInerney *et al.* (2014), who delineated several genetic lineages within the *N. aquilex* species complex. Recently, Weber *et al.* (2023) provided a comprehensive update on the taxonomic situation within the *N. aquilex* species complex. By investigating the mitochondrial cytochrome *c* oxidase subunit I (COI) and nuclear 28S ribosomal RNA (28S rDNA) genes and by applying a set of different molecular delineation methods, the authors were able to conservatively define eight molecular entities under the taxonomic umbrella of *N. aquilex* (annotated as lineages A, B, NDJ, F, G, H, KL, I). Two taxa were identified in the morphospecies *N. schellenbergi* (R, S) (Weber *et al.* 2023). Group B thereby referred to *N. aquilex* sensu stricto, and group S to *N. schellenbergi* sensu stricto. The nomenclature of the molecular lineages used herein follows that of McInerney *et al.* (2014) and extended by Weber *et al.* (2023). We recommend that all subsequent studies report the annotations of taxonomically undescribed molecular lineages.

In this study, and by referring to the molecular delimitation results of Weber *et al.* (2023) as a taxonomic backbone, we provide here an integrative taxonomic framework and the formal description of six of the molecularly identified species within the *N. aquilex* species complex, that is, group A, NDJ, F, G, I, and R sensu Weber *et al.* (2023). At the same time, because a much larger set of DNA sequences was available (Weber *et al.* 2022; Weber & Weigand 2023), which was partly enriched by sequences obtained during fieldwork conducted within the scope of this study, we have reviewed all species delimitation results of Weber *et al.* (2023), but limited our work to a minimum interpretation necessary for the formal description of these six new species.

We provide a list of all available genetic sequences stored in GenBank (Sayers *et al*. 2021) for reference purposes, referring to the *N. aquilex* and *N. schellenbergi* morphospecies (Supp. file 1). Furthermore, genetic sequences for several clades of the *N. aquilex* species complex were named after and published using different annotation systems. We provide a compilation of this historic referencing (Supp. file 2), thus allowing readers to compare our data with those in older publications.

Material and methods

Sampling

In addition to the published data in GenBank (Weber *et al.* 2023; Weber & Weigand 2023), extensive sampling of *Niphargus* specimens was performed in many regions of Germany, Belgium, Luxembourg, and France. Sampling of springs was performed by sieving the sediment and debris present at the point where water emerges from the subsurface through various meshes. Here, specimens of *Niphargus*, which are washed out with the groundwater, hide and live among sediment particles, dead leaves, or other types of debris. When the current of the spring water is not very strong, specimens of *Niphargus* can migrate towards the surface and back, most probably for feeding (Kureck 1967; Husmann 1976). Sampling of *Niphargus* in caves and artificial cavities was performed by simple manual picking of specimens using tweezers or by placing baits with chicken liver for one day. The specimens were individually sampled in 2 mL vials containing 96% ethanol. To simplify retrieving the type localities in the future, photographs of each of the six type localities of the newly described species, as well as a photograph of the site close to the type locality where we collected *N. schellenbergi*, were made (Supp. file 3).

To estimate the preferred habitat of the individual species, we categorized the collection sites into springs, large underground cavities, and interstitial areas (Supp. file 4) for all species where we had more than ten occurrences. Among the springs, we distinguished four groups (cf. Thienemann 1922): 1. A rheocrene spring had a localized outlet with a directly visible discharge. 2. A helocrene spring has several small outlets of groundwater that are often not directly recognizable; they are collected in a sump to form an effluent. 3. A limnocrene springs from the bottom of a pond, and the water flows over the water rim. 4. The term “basin” is not commonly used in the literature. Groundwater is often channeled artificially via a pipe into an artificial trough that has been investigated. Large underground cavities were divided into caves, which are of natural origin, mines, in which material was mined, wells, vertical pipes driven into the rock for water catchment, and souterrains, which refer to all other human-made objects not used for mining. Interstitial is a fine-grained system between gravels, where we only sampled interstitial habitats close to a river (Weber & Weigand 2023).

DNA analysis

DNA was extracted from one pereopod using the DNeasy Blood & Tissue Kit (Qiagen) or the NucleoSpin Tissue Kit (Macherey-Nagel, Düren, Germany), according to the manufacturer’s instructions. DNA isolates were stored at -20°C in the collections of the Evolutionary Biology and Ecology research unit of the Université libre de Bruxelles (Belgium), the Musée national d’histoire naturelle du Luxembourg (Luxembourg), and the Senckenberg German Entomological Institute (Germany).

Polymerase chain reaction (PCR) was performed to amplify the standard barcoding fragment of the cytochrome *c* oxidase subunit 1 gene (COI) (Folmer *et al.* 1994) using the primer pair HCO2198 and LCO1490 (Folmer *et al.* 1994) or the primer pair HCO2198-JJ and LCO1490-JJ (Astrin & Stüben 2008) (10 pmol/µL), premixed at a ratio of 1 : 1. For COI, the PCR mix contained 1.5 µL DNA extract (with varying concentrations, not measured), 1 µL of primer mix, 5 µL of “DreamTaq DNA Polymerase” (Thermo Scientific, Macquarie Park, Australia) and 5 µL of ultrapure water. PCR cycling conditions were an initial 5 min denaturation step at 95°C, 38 cycles of 30 s of denaturation at 95°C, 90 s of annealing at 49°C, 60 s of extension at 72°C and a final elongation step of 30 min at 68°C.

A fragment of the nuclear 28S ribosomal RNA gene (28S rDNA) was analyzed using the PCR primers Niph15 and Niph16 (Verovnik *et al.* 2005). The PCR mixture for the 28S rDNA marker contained 2 µL of DNA extract (with varying concentration, not measured), 1 µL of each primer (10 pmol/µL), 0.2 µL of REDTaq polymerase (Sigma-Aldrich, St. Louis, MI, USA), 5 µL of REDTaq reaction buffer and 15.8 µL of ultrapure water. PCR cycling conditions for 28S rDNA were an initial 3-minute denaturation at 95°C, 56 cycles of 30 s of denaturation at 94°C, 60 s of annealing at 45°C, and 90 s of extension at 72°C.

Bidirectional Sanger sequencing was performed at Genoscreen (Lille, France), Macrogen (Amsterdam and Maastricht, Amsterdam, The Netherlands), or at the Musée national d'histoire naturelle du Luxembourg. For COI, the same primers used for PCR amplification were used. Moreover, 28S rDNA was sequenced with three primers: Niph15 (Verovnik *et al.* 2005), alternatively Niph15i (Weber *et al.* 2023), Niph20, and Niph21 (Flot *et al.* 2010). The sequences were deposited in the NCBI GenBank database and the accession numbers are present successively in Supp. file 6 (COI) and Supp. file 9 (28S rRNA). A list of primers, together with their nucleotide sequence, for both PCR and sequencing is provided in Supp. file 5.

Molecular species delimitation and diagnosis

We used enriched molecular sequence data (COI and 28S rDNA) to re-evaluate the established molecular lineages within the *N. aquilex* species complex sensu Weber *et al.* (2023), which served as the taxonomic backbone for our integrative species descriptions using molecular and morphological data. Molecular sequence data were also analyzed to infer DNA characteristics (that is, individual pure diagnostic nucleotides or species-specific DNA sequence variants, that is, DNA barcodes or nuclear alleles), enabling a supporting differential molecular diagnosis of the delineated species in the *N. aquilex* species complex.

On 26 August 2023, all available COI sequences for *N. aquilex* and *N. schellenbergi* were downloaded from Genbank, enriched by the dataset from Weber, Weigand & Weigand (unpublished) and our newly obtained sequences herein. Thus, the initial COI dataset thus contained 1284 entries. These entries corresponded to 1319 individual COI sequences collected from 894 sampling sites (Supp. file 6). This discrepancy in the number of COI sequences exists because McInerney *et al.* (2014) stored a single COI sequence in GenBank for specimens from different locations when their COI sequences were identical. All incomplete sequences (i.e., sequences missing nucleotides at one or both ends) were removed from dataset 1, as well as those that contained any ambiguous characters (e.g., a single 'N')), resulting in 1115 final COI sequences (dataset 2). Dataset 1 was used to generate distribution maps and establish a phylogenetic framework for the molecular identification of specimens missing in dataset 2. The phylogenetic tree hypothesis was constructed using MEGA-X (Kumar *et al.* 2018). Seven short sequences were removed from dataset 1 and a neighbor-joining tree with 1000 bootstrap replications was generated (Supp. file 7 with description of the method in Supp. file 8). Dataset 2 was used for the distance-based molecular species delimitation approach ASAP (assemble species by automatic partitioning) (Puillandre *et al.* 2021), referring to its online version (https://bioinfo.mnhn.fr/abi/public/asap/asapweb.html) and standard settings under the Jukes-Cantor (JC69) substitution model for computing genetic distances. We primarily used partition 1 for final species delimitation, but also compared these results with partitions 2 and 3.

The data for the 28S rDNA dataset originated from multiple sources and comprised 404 sequences (referring to 415 specimens, since McInerney *et al*. (2014) deposited a single sequence for specimens with identical 28S rDNA sequences), all of which are provided in Supp. file 9, which comprises full 28S rDNA fragment available, 2 sequences (A in column N); only part of 28S rDNA fragment available, 78 sequences (B in column N); data from Weber *et al*. (2023), full 28S rDNA fragment and full COI available, 195 sequences (C in column N); new data within this study, full 28S rDNA fragment available,

138 sequences (D in column N); and new data within this study, only part of 28S rDNA fragment available, 2 sequences (E in column N).

The COI dataset 2 was used to infer molecular diagnostic DNA characters and sequence variants for the delineated species. The'removedup' function of the srnatoolbox webserver (https://arn.ugr.es/srnatoolbox/helper/removedup/; Aparicio-Puerta *et al.* 2022) was used to remove identical sequences (n = 674) in the COI alignment, resulting in 442 distinct COI sequence variants (= DNA barcodes). The alignment was manually inspected for pure diagnostic nucleotide positions (Jörger & Schrödl 2014), i.e., conserved nucleotides within a species, but with distinct character states in all sequence variants of all the other species. However, in addition to relying on (a few) individual diagnostic nucleotide positions, species-specific sets of diagnostic DNA barcodes are used in the differential diagnosis sections of the respective species. Additionally, the 28S rDNA dataset was investigated to identify diagnostic nuclear sequences (alleles) for the newly described species. Molecular diagnostic characteristics are provided in the diagnosis section of each species separately.

Morphological analysis

In the laboratory, one male and one female paratype were selected for further dissection, inspection, and description of the morphological characters. For inspection of the intraspecific morphological variability, we inspected 2–3 more paratypes for each species. The holotype and paratype specimens were not genetically analyzed but originated from a pool of specimens from a single locality, of which specimens have been genetically analyzed for their DNA sequence variants (COI and 28S). Special care was taken to ensure that the genetically analyzed specimens, the specimens selected for dissection, and the specimens deposited as intact holotypes and paratypes did not exhibit any morphological discrepancies. The specimens selected for morphological analysis were immersed in glycerol, dissected body appendages were mounted on slides in glycerol, and the slide cover glasses were sealed with varnish. The slides were inspected with an Olympus SZX16 stereo microscope equipped with an Olympus SC180 camera, and with an Olympus BX51 microscope equipped with an Olympus SC50 camera. The drawings were performed on printed photographs via manual inking and continuous inspection of the slides under the microscope. The terminology used for body parts and the choice of appendages considered for measurements are those previously described (Fišer *et al.* 2009b). The mandibular palp chaetotaxy nomenclature followed Karaman (1993). A table containing all measured appendages for all species described herein is presented in Supp. file 10.

Repository material

The specimens (types and paratypes), or microscope slides containing specimens appendages, used for species descriptions in this study were deposited in the Musée national d'histoire naturelle du Luxembourg (MNHNL) and in the Institutul de Speologie "Emil Racoviță" (ISER) in Cluj-Napoca, Romania. In the case of each described species, all specimens received an inventory number and are presented and explained in detail in the designated chapters in the results section below.

Results

Molecular species delimitation

ASAP analysis of COI, partition 1 with recursion and an ASAP-Score of 4.0, identified 16 species; partition 2 with recursion and an ASAP-Score of 5.0, 21 species; and partition 3 with recursion and an ASAP-Score of 5.5, 23 species (Supp. file 6). ASAP analysis of 28S rDNA from a limited dataset resulted in the identification of 10 putative species (Weber *et al.* 2023). Species A, B, and I are undisputed in all methods.

The situation around species D + N is more complex. Eight specimens of the molecular entity D+N had identical 28S rDNA alleles, and therefore belonged to the same species. According to all models, it is undisputed that it is a separate species from all other species, but partitions 2 and 3 of the ASAP of COI define three species within the D+N complex, identical in partitions 2 and 3, and the 28S rDNA of all specimens under consideration are identical.

Partition 1 of ASAP of COI of the species F + F' assumes a single species. Only the less likely partitions 2 and 3 assume two separate species. 28S rDNA contains two heterozygous individuals that include both F and F'.

According to all models, it is undisputed that species G is a separate species from all other species, but partitions 2 and 3 of the ASAP of COI define a single specimen as an additional separate species.

Species R and S were identified as a single species by partition 1, as two separate species by partition 2, and as three different species by partition 3. The large number of 28S rDNA sequences, 29 for species R and 681 for species S, did not show any heterozygous individuals between the two putative species.

In two cases, F+F' for *N. luxemburgensis* sp. nov. and D+N for *N. normandiensis* sp. nov., molecular entities comprised two well-separated molecular clades each. For these two species, their respective molecular clades are annotated with different symbols but in the same species-specific color when presenting their distribution maps.

Species descriptions

In this chapter, six species of the *N. aquilex* species complex are formally described, and information on *N. aquilex* sensu stricto and *N. schellenbergi* sensu stricto is provided. Distribution maps were generated in QGIS ver. 3.34.8-Prizren (QGIS Development Team 2025) and Inkscape ver. 0.92 (2017), with colors corresponding to Weber *et al.* (2023) and follow https://www.w3schools.com/colors/colors_names.asp (Supp. file 2). We were able to define the type of habitat for 855 sampling sites (Supp. file 4), allowing for a rough inspection of the species' preferred ecology.

Class Malacostraca Latreille, 1802
Order Amphipoda Latreille, 1816
Family Niphargidae Bousfield, 1977
Genus *Niphargus* Schiødte, 1849

Niphargus aquilex Schiødte, 1855
Fig. 1

Remarks

Weber *et al.* (2023) treated this species as *N. aquilex* B, which can be considered *N. aquilex* sensu stricto. The species was regularly found in nearly all types of biotopes, but surprisingly often in helocrene springs (Supp. file 4.1). It is widespread and common in Western Germany, with more scattered records in Luxembourg, Belgium, and along the Channel Coast in France and Great Britain (Fig. 1). A neotype locality was established by Karaman (1980) from Crowborough (United Kingdom) without mentioning precise coordinates. We sampled the region of Crowborough, and our specimens and sequences can therefore be considered to originate from the neotype locality.

The drawing of Schiødte (1855) shows two of the characteristics of *N. aquilex*, that is, the single seta on the dactylus of the gnathopods and the rounded 3rd epimeral plate. Karaman (1980) re-described *N. aquilex* in detail, but he did not take into consideration that *N. aquilex* might comprise a species

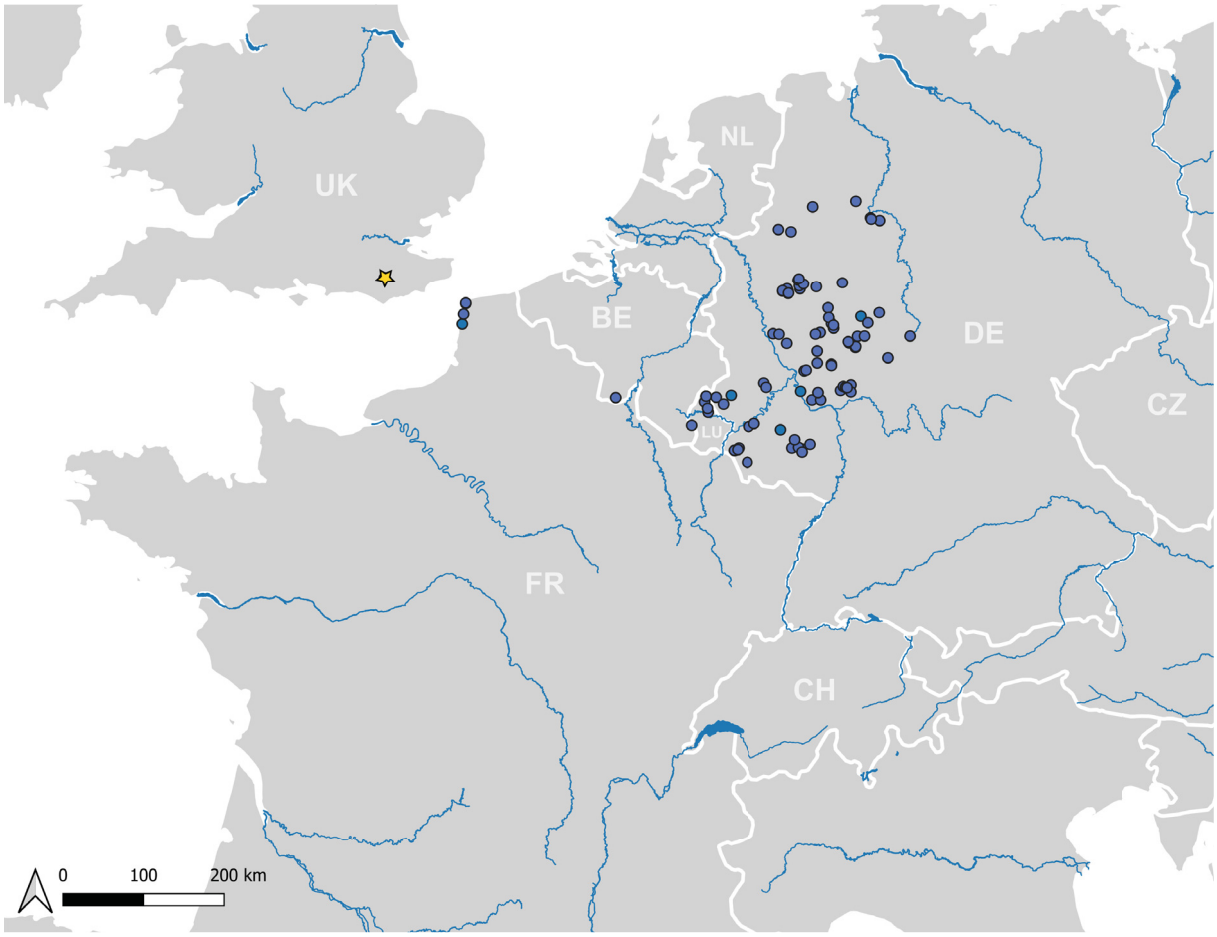

Fig. 1. Distribution of *Niphargus aquilex* Schiødte, 1855 sensu stricto, confirmed by molecular data. The neotype locality in Crowborough (United Kingdom) is marked by a yellow star, overlaying one site record. Very large freshwater bodies are indicated; country codes follow the ISO 3166 standard alpha-2 format.

complex of morphological similar (pseudocryptic) or identical (cryptic) taxa. Karaman's specimens are now >40 years old, and we thus did not try to sequence them. Nevertheless, we obtained three freshly collected specimens from Crowborough and sequenced two COI and three 28S rDNA sequences. All the sequences corresponded to the former species B senus Weber *et al.* (2023), which was already delineated by McInerney *et al.* (2014).

Niphargus schellenbergi Karaman, 1932
Fig. 2

Remarks

Weber *et al*. (2023) treated this species as *N. schellenbergi*, which can be considered *N. schellenbergi* sensu stricto, given that we also included specimens very close to the type locality in our analyses. The species is widespread from Central to Western Germany, Luxembourg, Belgium (Wallonia), the Netherlands (Limburg), and Eastern France (Fig. 2). While in the first description it was assumed that *N. schellenbergi* mainly inhabits springs (Karaman 1932), we found it regularly in caves, artificial caverns, meadow drainages, springs, wells, and in the interstitial (Supp. file 4.2). Karaman (1932) set

the Gänsbrünnle in the South of Sendelbach (Bavaria, Germany) as type locality, referring to a well along the southern margin of its inferred distribution range in Central Germany, but he did not define any type material. We collected specimens in a spring very close to Gänsbrünnle (Supp. file 3.1). More southern distribution records, particularly in Central-East to South-Eastern France, most likely belong to the newly described sister species *Niphargus lotharingiensis* sp. nov.

The drawing in Karaman (1932) shows well the characteristics of *N. schellenbergi*, i.e., the gnathopod II nearly in square-form with its 3 setae on its dactylus. The two drawings of the telson exhibit significant discrepancies and are of limited value for taxonomic determination. The same is true of the two drawings of uropod I, in which the outer ramus is longer in one instance and the inner ramus is longer in the other. A drawing of the entire specimen is missing.

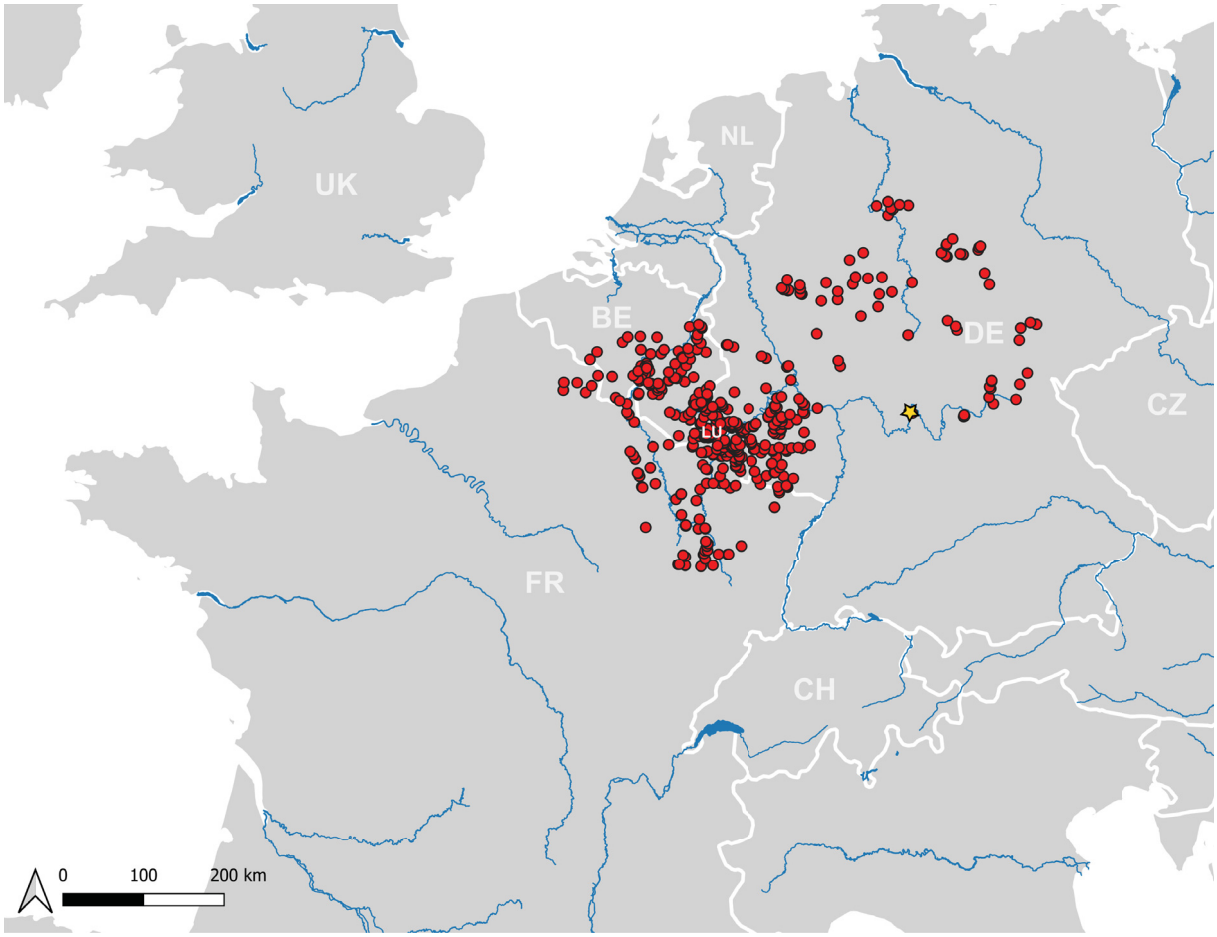

Fig. 2. Distribution of *Niphargus schellenbergi* S. Karaman, 1932 sensu stricto, confirmed by molecular data. The type locality at Gänsbrünnle (Germany) is marked by a yellow star, overlaying two site records. Very large freshwater bodies are indicated; country codes follow the ISO 3166 standard alpha-2 format.

Niphargus luxemburgensis Weber, Weigand & Brad sp. nov.
urn:lsid:zoobank.org:act:1522BA40-BBC2-44B7-9E92-D0AE85085217
Figs 3–11

Diagnosis

Medium-sized *Niphargus* species, poorly setose. Right posteroventral angle of epimeral plates. Outer 6 spines of maxilla I on outer lobe with 1 tooth each; 1 spine with several smaller teeth. Mandibular palp with small number (1–2) of B setae. Gnathopods with 1 seta along outer margin of dactylopodites. Pereiopod VII, the longest leg, almost half of total body length. Pleopods retinaculum with 2 hooks. Uropod I, longer exopodite. Uropod II, longer endopodite. Uropod III sexually dimorphic, exopodite elongated in males. Telson with 3 apical spines on each lobe. The COI marker shows two pure diagnostic sites at positions 55 (C) and 358 (C). Six 28S rDNA alleles are diagnostic (with 13 heterozygous specimens) as well as 79 COI barcodes.

Etymology

The species name derives from the Grand Duchy of Luxembourg, where it was first discovered. In Weber *et al*. (2023), this species was treated as *N. aquilex* F, F'.

Material examined

Holotype

LUXEMBOURG • ♂; Girst, Gutland, basin of a spring in the center of the hamlet of Girsterklaus; 49.7847° N, 6.4989° E; 19 Mar. 2018; Dieter Weber leg.; kept intact in 96% ethanol; 180319-10; MNHNL130574.

Paratypes

LUXEMBOURG • 1 ♂; same collection data as for holotype; 30 Jan. 2018; dissected and appendages drawn; 180130-32; ISER microscope slide DW180130-32 • 1 ♀; same collection data as for preceding; dissected and appendages drawn; 180130-45; ISER microscope slide DW180130-45 • 1 ♂; same collection data as for holotype; 27 Mar. 2017; ISER DW170327-02 • 1 ♀; same collection data as for holotype; 19 Mar. 2018; ISER DW180319-09 • 1 ♀; same collection data as for holotype; 19 Mar. 2018; ISER DW180319-13 • 1 ♀; same collection data as for holotype; 27 Mar. 2017; ISER DW 170327-06; MNHNL130575.

Molecular data

COI and 28S rDNA sequences of specimens belonging to *Niphargus luxemburgensis* sp. nov. were deposited in GenBank. COI and 28S rRNA accession numbers are present in Supp. file 6 and Supp. file 9, respectively.

Description (male paratype ISER DW180130-32)

Measurements

Total body length 7.7 mm (Fig. 3).

Head

Head (Fig. 3) 8.60% of total body length. Eyes and rostrum absent.

Antennae

Antenna I (Fig. 4A): with the main flagellum formed of 18 articles representing 41% of total body length. Peduncle length ⅓ of total length of antenna I. The accessory flagellum (Fig. 4B) biarticulated; proximal article slightly longer than first article of main flagellum; distal article ¼ of total length of accessory flagellum, with 2 apical setae of different lengths and 1 aesthetasc. Aesthetascs ⅓ of respective flagellum articles (Fig. 4C).

Antenna II (Fig. 4D): flagellum formed of 8 articles and representing 40% of total length of antenna II. Most flagellum articles bear 1 short aesthetasc.

Mouthparts

Labium (Fig. 5A): large inner lobes with no setae. Outer lobes with 1 row of fine setae subapically on inner sides. Labrum (not shown) typical, subovoid shape.

Maxilla I (Fig. 5B): with 4 apical setae on distal article of palp. Six spines of outer lobe with 1 tooth each and 1 spine with several small teeth. Inner lobe with 1 apical seta.

Maxilla II (Fig. 5C): with inner lobe slightly shorter than outer lobe. 1 apical row of setae and 1 subapical seta on each lobe.

Left mandible (Fig. 5D): 5 teeth on incisor process. 5 teeth on lacinia mobilis. 5 serrated setae, alternated with 6 trifid setae, between lacinia mobilis and molar process.

Right mandible (Fig. 5E): 5 teeth on incisor process. 7 small teeth on lacinia mobilis. 3 serrated and 2 trifid setae between lacinia mobilis and molar process. Long seta on molar process.

Mandibular palps (Fig. 5D–E): highly similar and of same length. 3 articles account for 19% (article 1), 39% (article 2) and 42% (article 3) of total length of palp. Proximal article without setae, median article

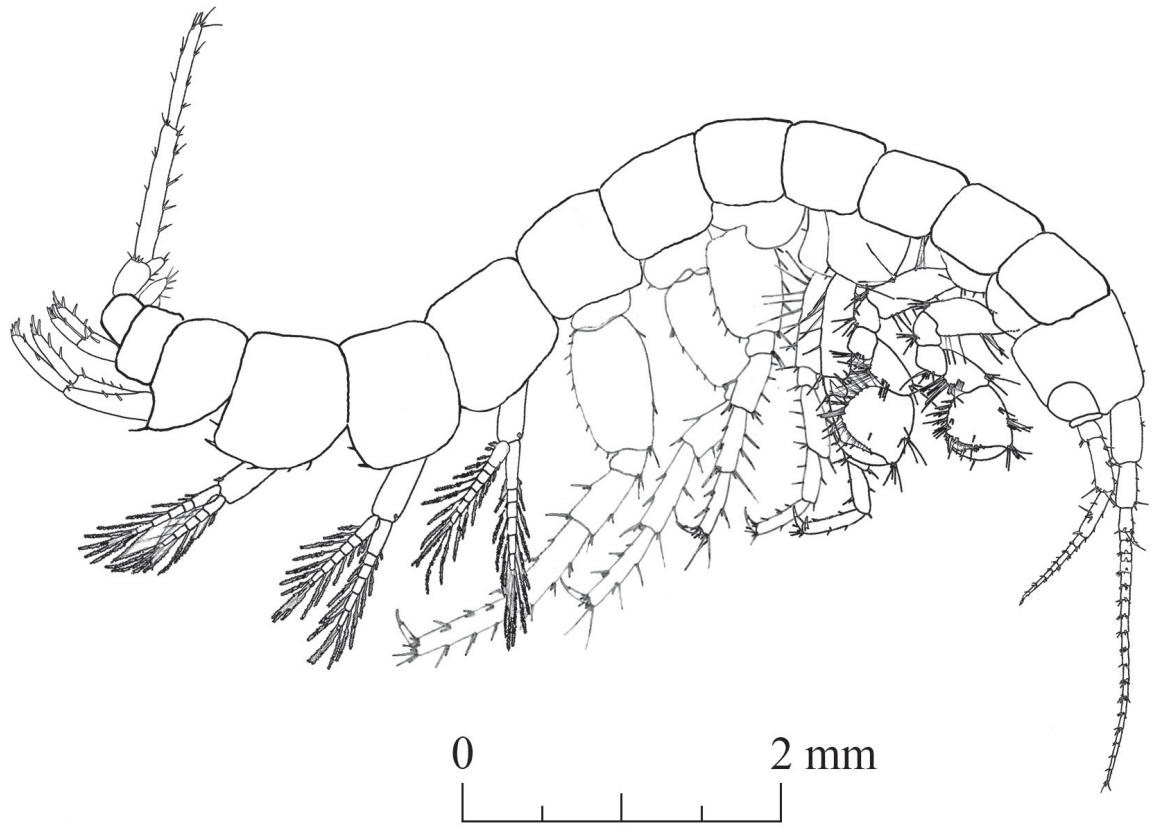

Fig. 3. *Niphargus luxemburgensis* Weber, Weigand & Brad sp. nov., paratype, ♂ (ISER DW180130-32); general appearance.

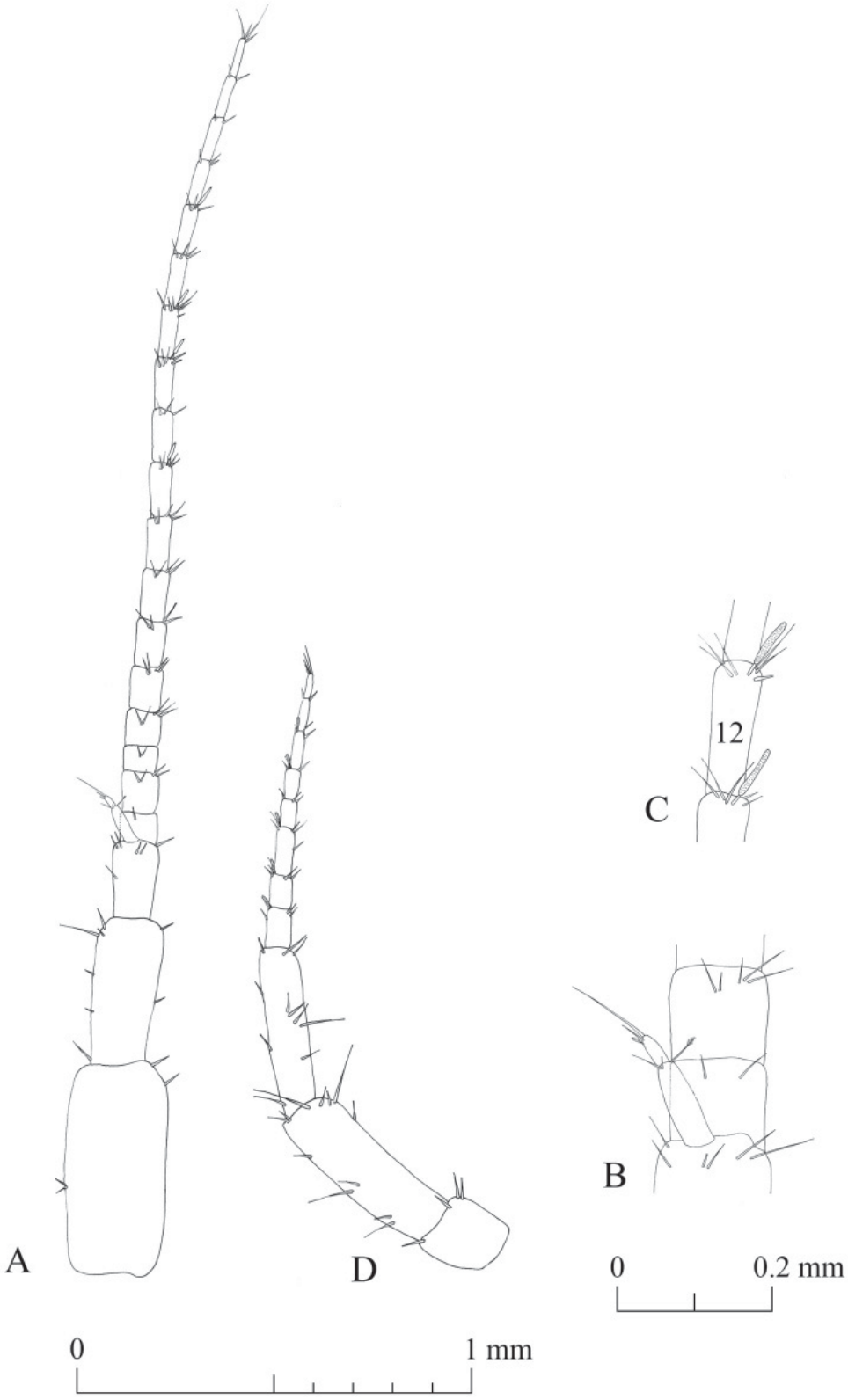

Fig. 4. *Niphargus luxemburgensis* Weber, Weigand & Brad sp. nov., paratype, ♂ (ISER DW180130-32). **A**. Antenna I. **B**. Antenna I, details of accessory flagellum. **C**. Antenna I, details of aesthetascs. **D**. Antenna II.

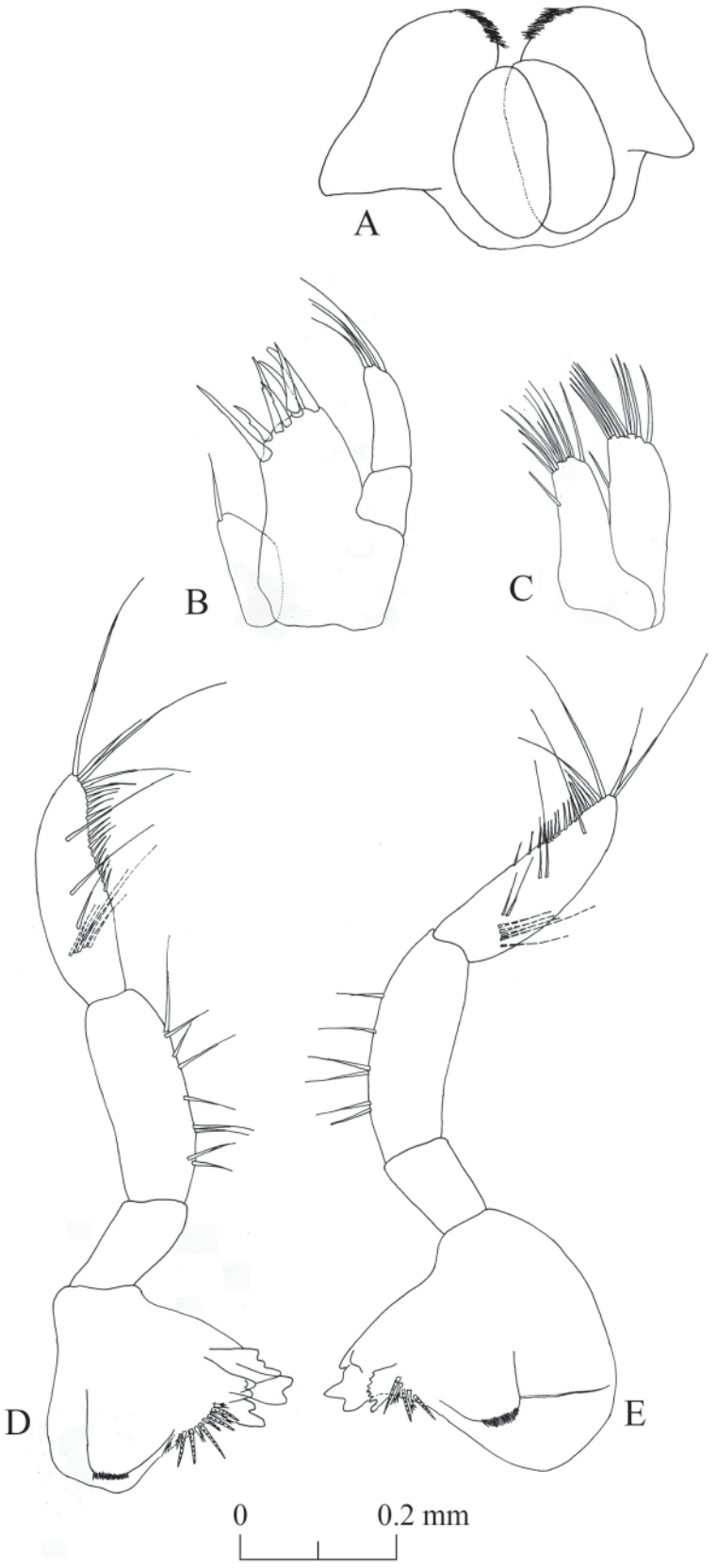

Fig. 5. *Niphargus luxemburgensis* Weber, Weigand & Brad sp. nov., paratype, ♂ (ISER DW180130-32). **A**. Labium. **B**. Maxilla I. **C**. Maxilla II. **D**. Left mandible. **E**. Right mandible.

with 6–9 ventral setae. Distal article of palp with one group of 5 A setae, three groups with 1–2 B setae, 14 D setae and 4 E setae.

Maxilliped (Fig. 6A): with palp formed of 4 articles. Article 1 asetose. Article 2 with 18 setae aligned along inner margin. Article 3 with 5 apical setae, one group of 8 dorsal setae and one group of 5 setae on inner margin. Article 4 with 1 seta located on outer margin and 2 setae at nail insertion. Outer lobe with 7 apical setae and 8 flattened setae on inner margin. Inner lobe with 6 apical setae.

Gnathopods

Gnathopod I (Fig. 6B): coxal plate in shape of rectangular trapezoid, with depth larger than width (ratio depth : width 1.0 : 0.85). Basis length : width ratio 1.0 : 0.43. Ischiopodite with one posteroventral group of 5 setae. Basis length : carpus length ratio 1.0 : 0.54. Carpus with row of 10 setae of various lengths along ventral margin, group of 4 setae located anterodorsally and two groups of 3–5 setae on carpus surface close to ventral margin. Propodite nearly as long as wide, five groups of 2–4 setae on ventral margin, one group of 2 setae on dorsal margin, one group of 6 anterodorsal setae, one group of 6 anteroapical setae, 1 mesial seta on lateral surface, one group of 2 setae on lateral surface close to ventral margin and one group of 2 setae close to palmar corner. 1 strong palmar spine, 1 supporting spine and 2 denticulate spines present in palmar corner. Dactylopodite with claw 35% of total dactylopodite length and 1 seta along outer margin.

Gnathopod II (Fig. 6C): slightly larger than gnathopod I, with coxal plate in shape of rectangular trapezoid; coxal plate width almost similar in length with depth (ratio width : depth 1.0 : 0.95). Ovoid gill. Basis length : width ratio is 1.0 : 0.34. Ischiopodite with one posteroventral group of 5 setae. Basis length : carpus length ratio 1.0 : 0.56. Carpus with row of 12 setae of various lengths along ventral margin, group of 3 setae located anterodorsally and one group of 4 setae on carpus surface close to ventral margin. Propodite as long as wide, 6 groups of 2–5 setae on ventral margin, 1 seta on dorsal margin, one group of 4 anterodorsal setae and 5 anteroapical setae. 1 mesial seta on lateral surface, 2 setae close to palmar corner. 1 strong palmar spine, 1 supporting spine and 2 denticulate spines present in palmar corner. Dactylopodite with claw 37% of total dactylopodite length and 1 seta along outer margin.

Pereopods

Pereopod III (Fig. 7A): coxal plate in shape of rectangular trapezoid, ratio width-depth 1.0 : 0.9. Propodite length : dactylus length ratio 1.0 : 0.4. Dactylus, with nail measuring half of total length of dactylus, 1 dorsal seta with plumose tip. Pereopod III equal in length to pereopod IV (pereopod III length : pereopod IV length ratio 1.0 : 1.0).

Pereopod IV (Fig. 7B): relatively rectangular coxal plate, with concavity on posterior margin, width : depth ratio 1.0 : 0.82. Propodite length : dactylus length ratio 1.0 : 0.46. Robust dactylus, with nail measuring 0.44% of total length of dactylus; 1 dorsal seta with plumose tip and 1 seta at nail base.

Pereopod V (Fig. 8A): coxal plate of irregular shape, with deep concavity on ventral side and 1 anterior seta. Basis ovoid-rectangular shaped, length : width ratio 1.0 : 0.66, 6 setae on posterior margin, 4 setae on anterior margin, 3 anteroapical setae of different lengths. Dactylus with one dorsal seta with plumose tip, 1 seta and 1 spine at nail base, which represents ⅓ of total dactylus length. Propodite length : dactylus length ratio 1.0 : 0.45.

Pereopod VI (Fig. 8B): coxal plate smaller than that of pereopod V, but highly similar in shape and 1 posterior seta. Basis ovoid-rectangular shaped, length : width ratio 1.0 : 0.67, 6 setae on posterior margin, 5 setae on anterior margin, 3 anteroapical setae of different lengths. Dactylus with 1 plumose seta on outer margin and 1 spine near nail base. Nail length slightly more than ⅓ of total dactylus length. Ratio propodite length : dactylus length 1.0 : 0.4.

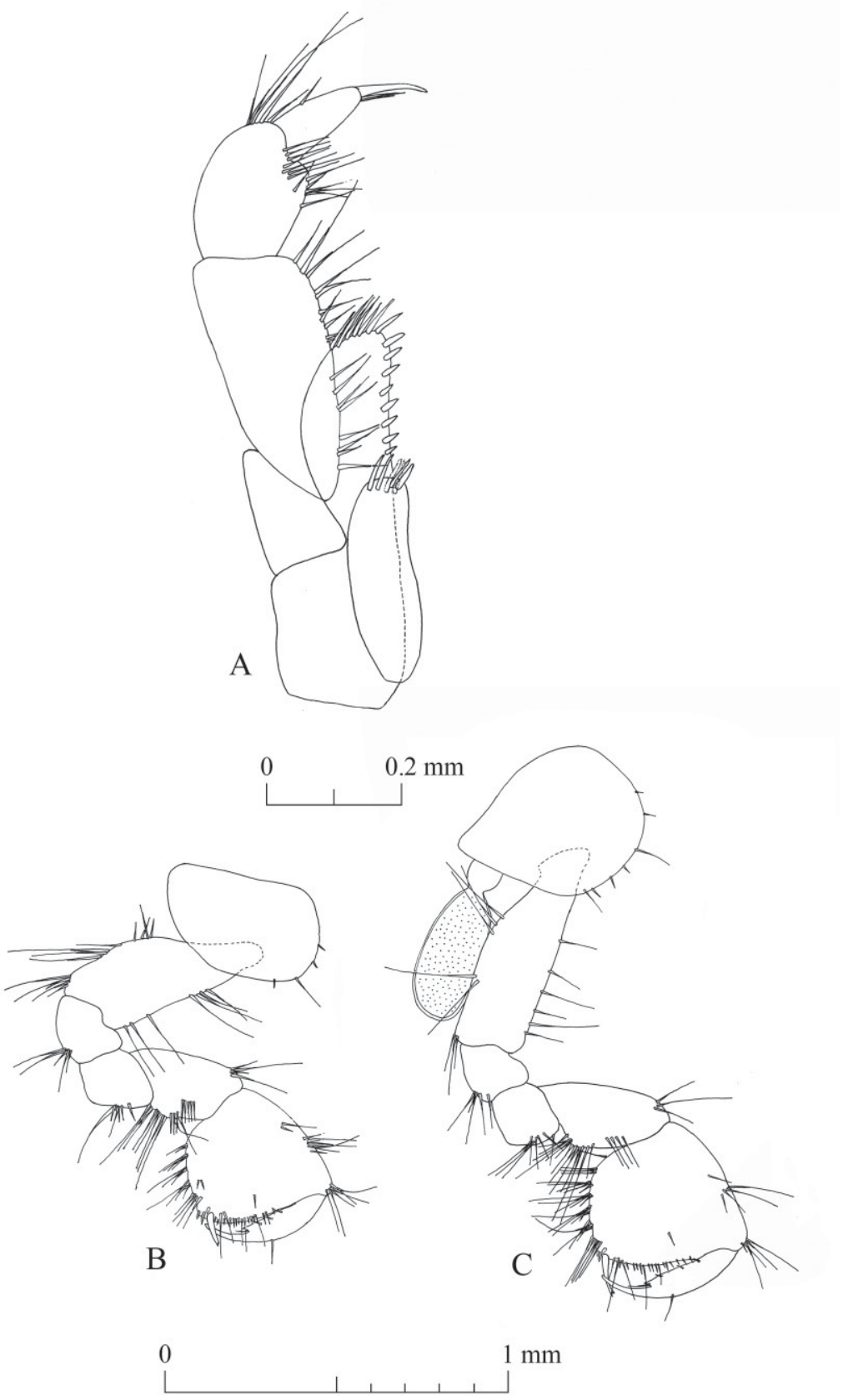

Fig. 6. *Niphargus luxemburgensis* Weber, Weigand & Brad sp. nov., paratype, ♂ (ISER DW180130-32). **A**. Maxilliped. **B**. Gnathopod I. **C**. Gnathopod II.

Pereopod VII (Fig. 8C): longest leg (3.1 mm) of inspected paratype male. Coxal plate trapezoidal, with 1 seta on posterior margin. Basis ovoid-rectangular, ratio length : width 1.0 : 0.6, 8 setae on posterior margin, 2 setae on anterior margin and 3 anteroapical setae of different lengths. Dactylus with 1 plumose seta on outer margin and 1 spine near nail base. Nail length slightly more than ⅓ of total dactylus length. Ratio propodite length : dactylus length 1.0 : 0.36.

Pereopods V : VI : VII ratio 1.0 : 1.34 : 1.49.

Pleopods

Similar in shape and size (pleopod I depicted in Fig. 9A), with unequal rami and 2 hooks on retinaculum.

Epimeral plates (Fig. 9B)

Epimeral plate I with right postero-ventral angle, relatively straight ventral margin, convex posterior margin with 5 setae. Epimeral plate II with right postero-ventral angle, relatively straight ventral margin with 2 spines, convex posterior margin with 6 setae. Epimeral plate III with right posteroventral angle, relative straight ventral margin with 1 spine, convex posterior margin with 6 setae.

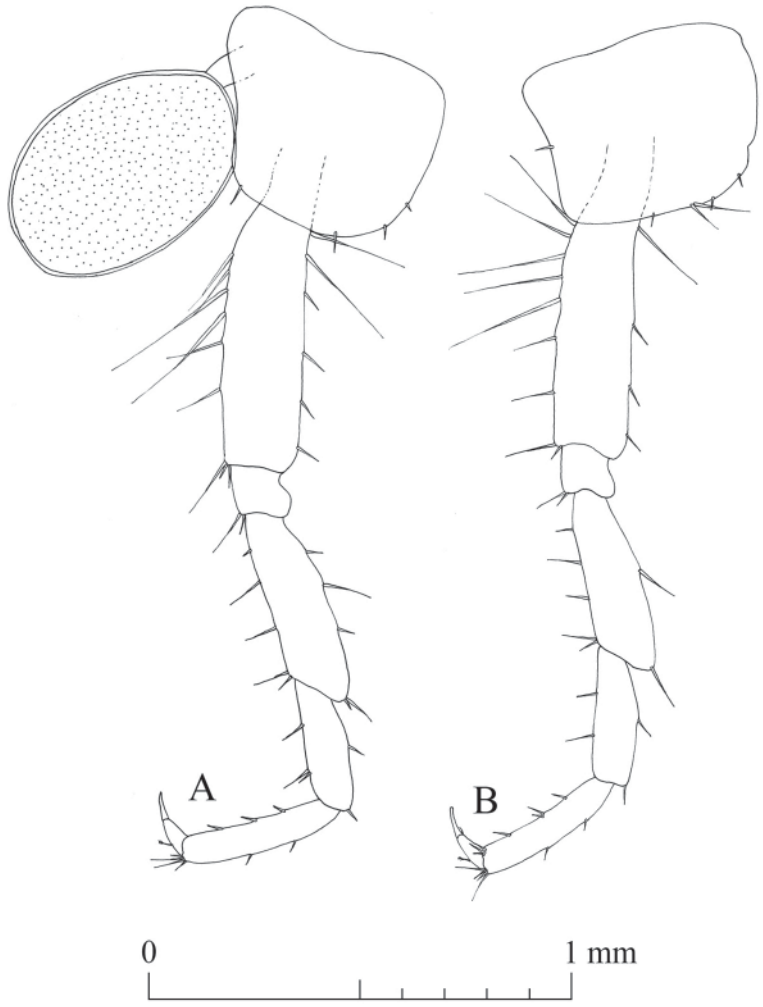

Fig. 7. *Niphargus luxemburgensis* Weber, Weigand & Brad sp. nov., paratype, ♂ (ISER DW180130-32). **A**. Pereopod III. **B**. Pereopod IV.

Uropods

Uropod I (Fig. 10A): with two dorso-lateral rows of 4 spines on peduncle. Exopodite slightly longer than endopodite, and ratio of exopodite length : endopodite length 1.0 : 0.85. 1 strong spine at base of uropod I.

Uropod II (Fig. 10B): with 1 dorsal spine and 3 apical spines. Endopodite longer than exopodite, endopodite length : exopodite length ratio 1.0 : 0.81, both rami with low number of spines.

Uropod III (Fig. 10C): sexually differentiated, longer in males. Peduncle with 4 apical spiniform setae. Short endopodite about half the length of peduncle, with 2 apical setae. Proximal segment of exopodite longer than distal segment (ratio 1.0 : 0.77). Anterior margin of proximal segment of exopodite with 5

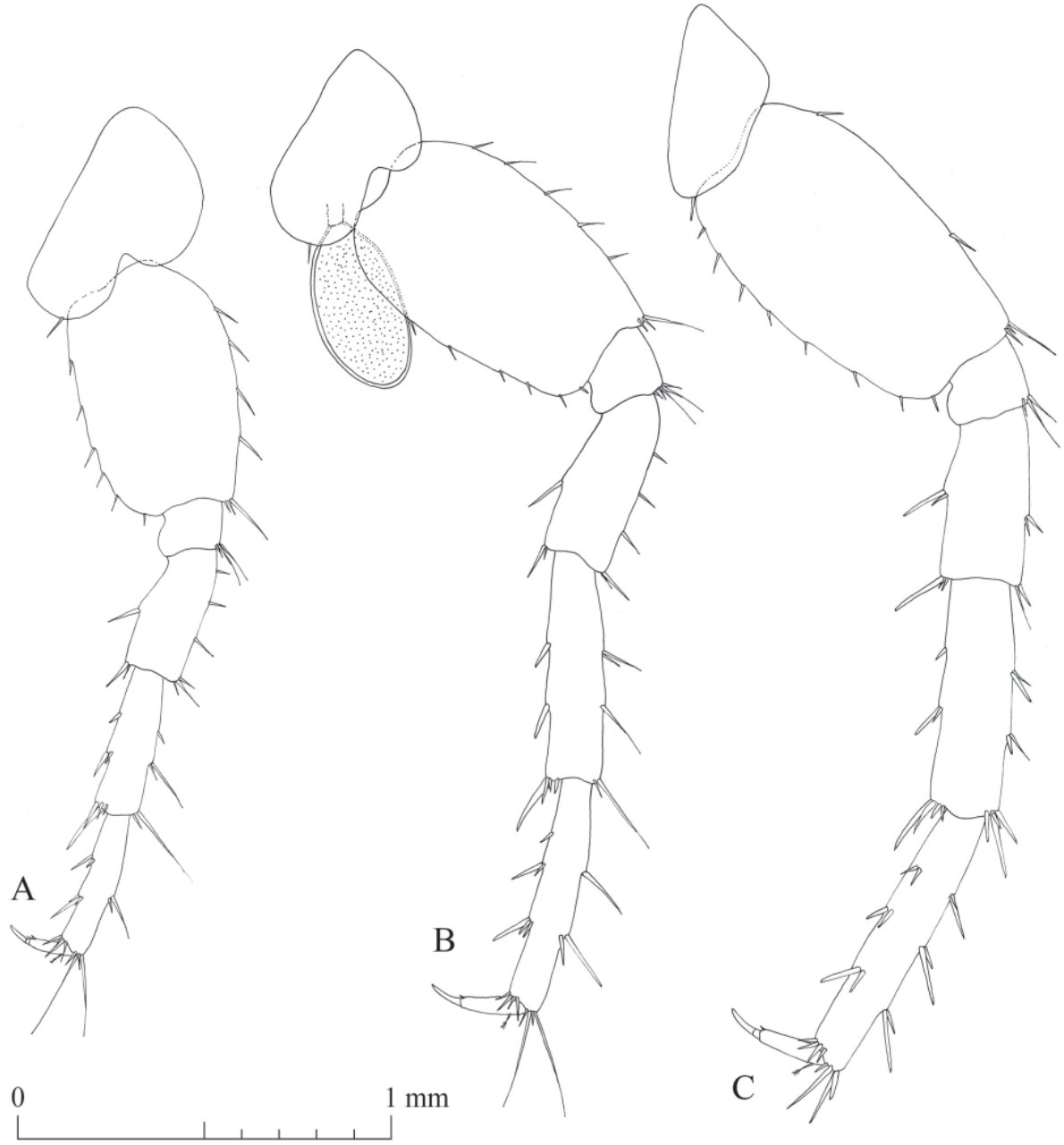

Fig. 8. *Niphargus luxemburgensis* Weber, Weigand & Brad sp. nov., paratype, ♂ (ISER DW180130-32). **A**. Pereopod V. **B**. Pereopod VI. **C**. Pereopod VII.

groups of 2–3 setae; posterior margin of exopodite with 3 groups of 1–2 setae; one group of 3 postero-apical setae. Distal segment of exopodite with 3 groups of 2 setae on anterior margin, 3 groups of 1–2 setae on posterior margin and 4 apical setae of different lengths.

Telson

Telson (Fig. 10E) nearly as wide as long (width : length ratio 0.95), with 1 subapical and 3 apical spines of different lengths on each lobe. Longest spine almost half of telson length. 2 thin setae of different lengths and plumose tip, 1 seta medially on 1 lobe.

Sexual dimorphism

The examined male and female are highly similar. Besides the usual sexual dimorphism (e.g., slightly smaller gnathopods, presence of oostegites, and slightly deeper coxal plates I–VI in females), in *N. luxemburgensis* sp. nov., female uropod III (Fig. 10D) is shorter compared to that of male. Female telson similar to that of the male, but smaller (Fig. 10F).

Intraspecific and interspecific variability

The intraspecific morphological variability of *N. luxemburgensis* sp. nov. appears to be very low. All morphological characters were nearly identical in all inspected specimens (data not shown).

Type locality, ecology and distribution

The type locality is the basin of a spring in the center of the hamlet of Girsterklaus (community of Girst, Gutland, Luxembourg) at 49.7847° N, 6.4989° E (Supp. file 3.2 & 3.3). The artificial basin is made of sandstone. The water contains algae; the bottom of the basin is covered with mud. Specimens of *Niphargus luxemburgensis* sp. nov. were found in the mud as well as among the algae. The water has a hardness of 15°GH (where one degree equals to 17.9 mg/l $CaCO_3$) and a slightly acidic pH of 6.7. There is no human access, neither to the actual spring, nor to the groundwater. We confirm the permanent

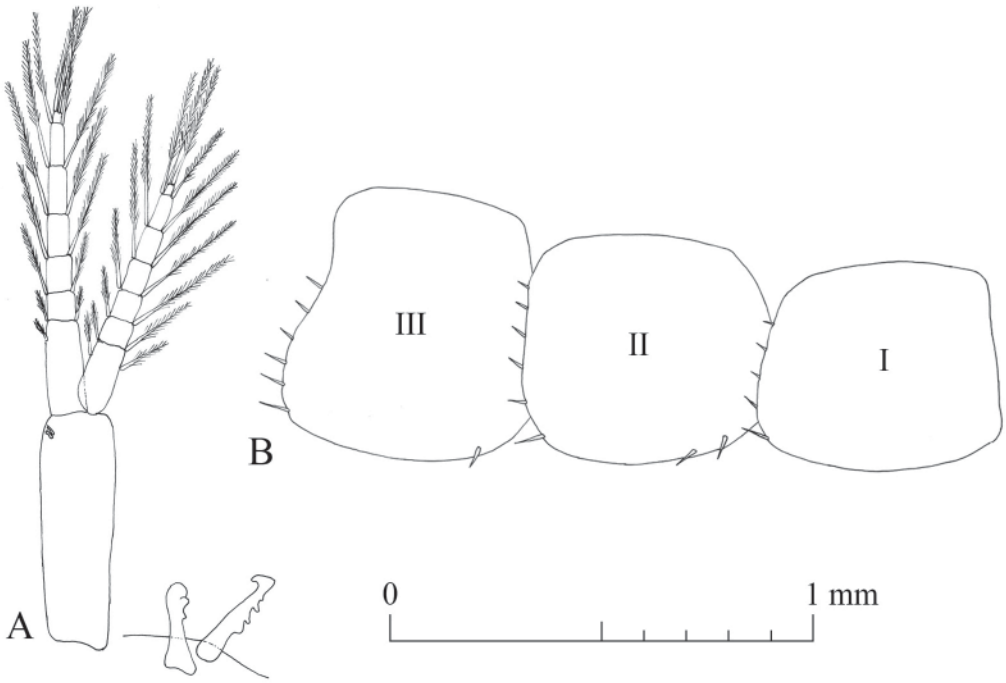

Fig. 9. *Niphargus luxemburgensis* Weber, Weigand & Brad sp. nov., paratype, ♂ (ISER DW180130-32). **A**. Pleopod I, detail of the retinaculum. **B**. Detail of the epimeral plates.

presence of this species in the type locality as it was found on 10 July 2016, 4 September 2016, 30 January 2018, 17 February 2018 and 19 May 2018. In the same basin of the spring, *N. schellenbergi* sensu stricto was also found. We successfully collected 82 specimens of *N. schellenbergi* in 15 springs and 1 mine, at a distance of maximum 10 km around the type locality, in Luxembourg and in Germany, but could not find *N. luxemburgensis* there. The type locality was free of gammarids (Amphipoda, Gammaridae) during the periods of collection. *Niphargus luxemburgensis* seems to be a typical species of the interstitial environment (Supp. file 4.3). It is widely distributed from the UK and North to Central France, Belgium, Germany to the Czech Republic in the East (Fig. 11). The frequent presence in Luxembourg and bordering Germany (Rhineland-Palatinate, Saarland) must be most likely attributed to a more intense sampling in those regions.

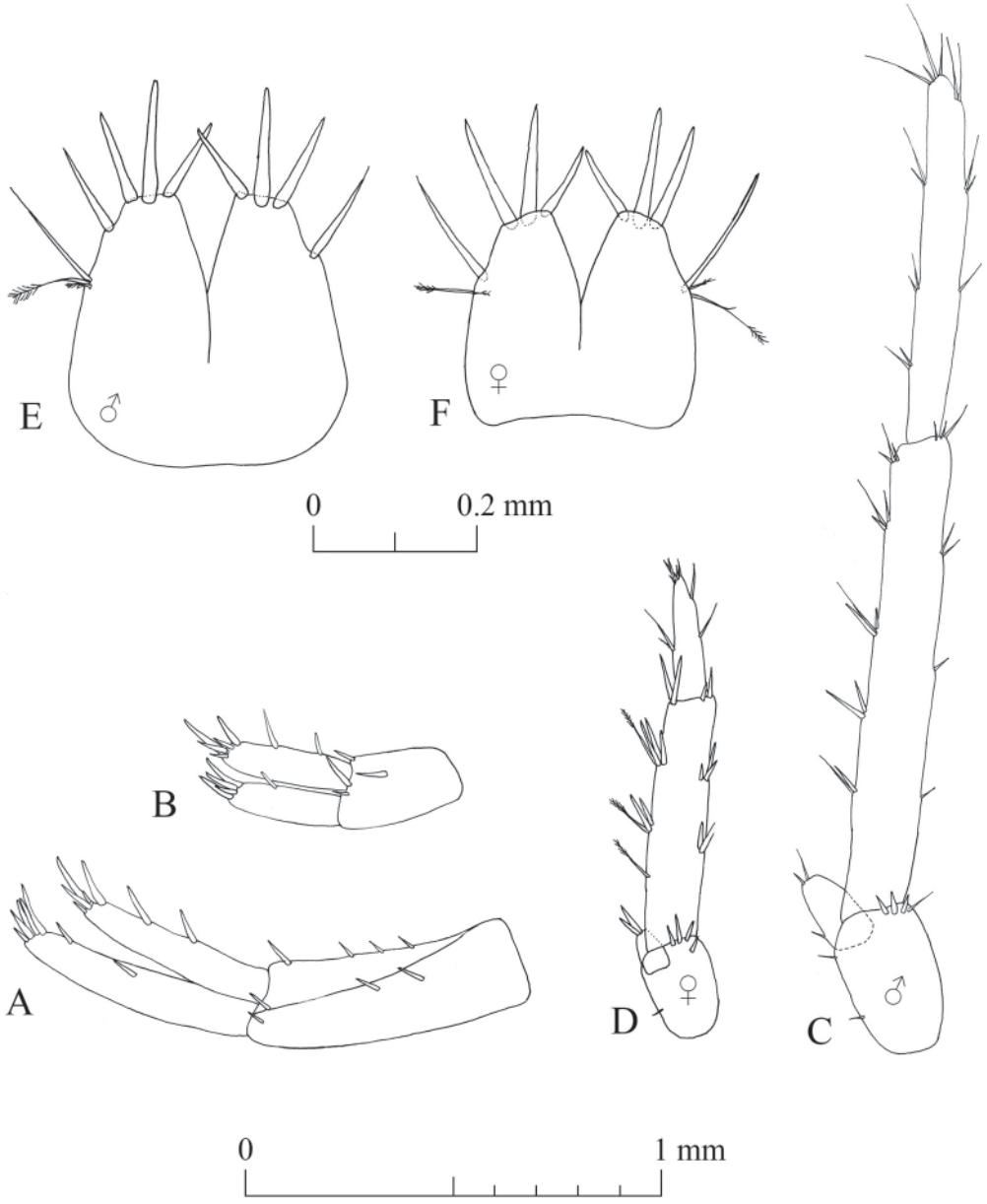

Fig. 10. *Niphargus luxemburgensis* Weber, Weigand & Brad sp. nov., paratype, ♂ (ISER DW180130-32) and paratype, ♀ (ISER DW180130-45). **A**. Male uropod I. **B**. Male uropod II. **C**. Male uropod III. **D**. Female uropod III. **E**. Male telson. **F**. Female telson.

Niphargus luxemburgensis sp. nov. is the only species described herein with two strongly divided subclades (F and F'). Although the genetic distance is relatively large, the connection in the haplotype network identifies both as belonging to the same species. The two clades cannot be distinguished morphologically. Nevertheless, they are geographically separated with only a small overlap: Clade F', including the type locality, has its distribution in the North-Eastern half of France, Belgium, Luxembourg and the very West of Germany (Fig. 11). Clade F is distributed in southern England, the very North of France, Belgium, Luxemburg, all over Germany without the North and the South, up to the Czech Republic (Fig. 11). The geographic overlap of both clades includes Belgium, Luxembourg, and the very West of Germany. The higher number of sites for clade F might be a sampling artefact, as our dataset comprised many more sites in Germany than in France. It can be assumed that the two subclades of *N. luxemburgensis* are in the process of ecological speciation.

Niphargus luxemburgensis sp. nov. has a moderate geographical overlap with *Niphargus vejdovskyi* Wrześniowski, 1890 in the very East of its distribution range, with the latter having been described as *N. puteanus* var. *vejdovskyi* from wells in Prague (Wrześniowski 1890), the village of Bechlín close to Roudnice and from the wells between Kralupy and Vodolka in Bohemia (Czech Republic). Wrześniowski's drawings are difficult to understand but show some similarities to the *N. aquilex* species

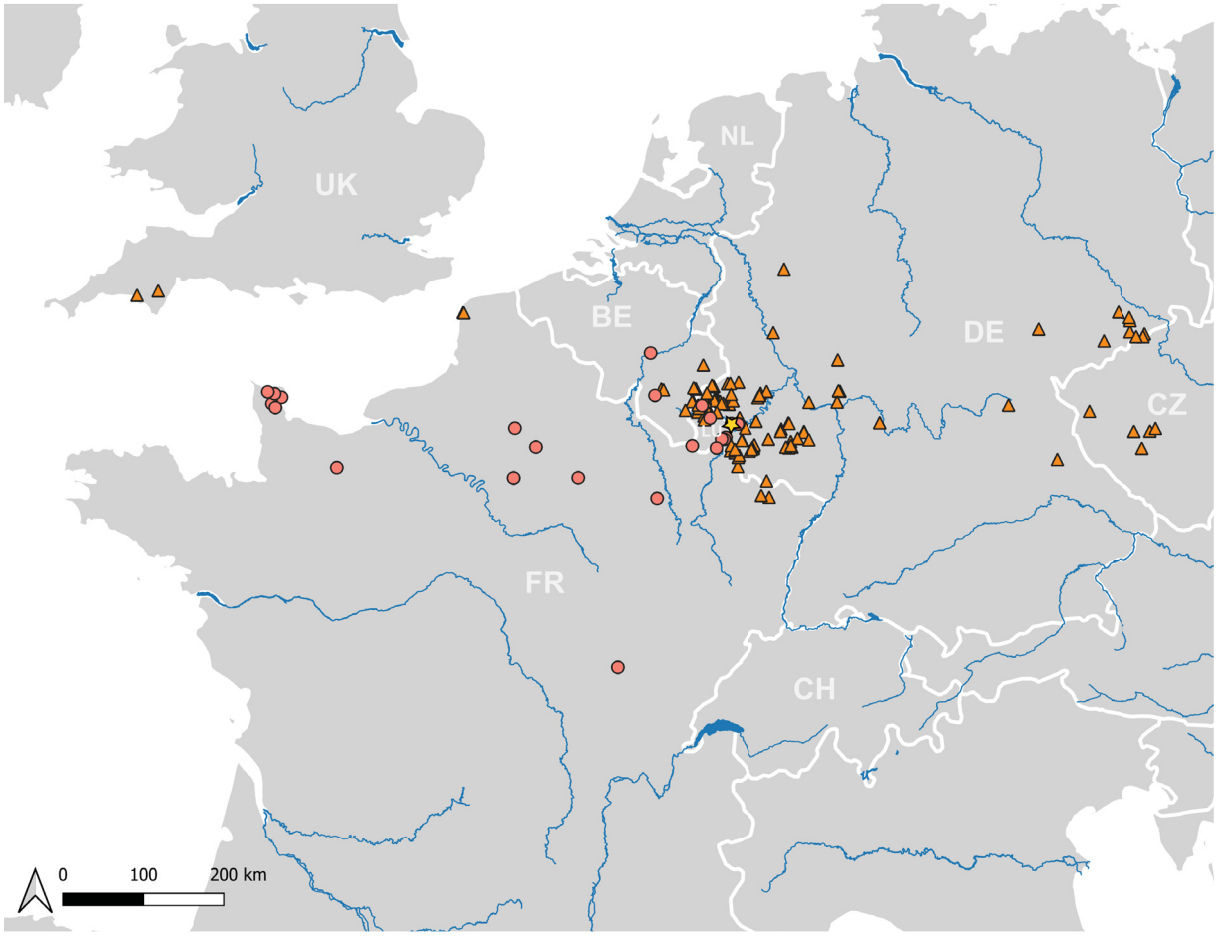

Fig. 11. Distribution of *Niphargus luxemburgensis* Weber, Weigand & Brad sp. nov. confirmed by molecular data. The type locality at Girsterklaus (Luxembourg) is marked by a yellow star, overlaying one site record. The two molecular clades F and F' within *N. luxemburgensis* are referred to by circles and triangles, respectively. Very large freshwater bodies are indicated; country codes follow the ISO 3166 standard alpha-2 format.

group. This taxon was re-described as *N. aquilex vejdovskyi* and synonymised with *N. aquilex* var. *bohemica* Ortmann (Schellenberg 1932), based on material from Schneeberg in the Ore Mountains (Saxony, Germany), from Brunersdorf (Saxony, Germany). Schellenberg assumed that three females from Heligoland (Schleswig-Holstein, Germany) also belong to this species. The inner lobe of the maxilla I of the specimens from Heligoland has 3 to 6 apical setae (Schellenberg 1932), while *N. luxemburgensis* (as well as all other newly described species herein) has 1 apical seta only. *Niphargus vejdovskyi* is therefore not identical to *N. luxemburgensis*, but DNA sequences of the former are not yet available.

Niphargus palatinensis Weber & Brad sp. nov.
urn:lsid:zoobank.org:act:5DA10A74-7763-41C9-B0ED-76AD156C03D4
Figs 12–20

Diagnosis

Medium-sized *Niphargus* species, poorly setose. Right postero-ventral angle of epimeral plates. Six spines of maxilla I outer lobe with 1–3 teeth each; 1 spine with several smaller teeth. Mandibular palp with small number (1–2) of B setae. Gnathopods with 1 seta along outer margin of dactylopodites. Pereiopod VII, the longest leg, almost half of total body length. Pleopods retinaculum with 3 hooks. Uropod I, longer exopodite. Uropod II, longer endopodite. Uropod III sexually dimorphic, exopodite elongated in males. Telson with 4 apical spines on each lobe. The COI marker shows six pure diagnostic sites at positions 31 (C), 184 (C), 223 (G), 353 (G), 358 (G) and 391 (A). A single 28S rDNA allele is diagnostic as well as 21 COI barcodes.

Etymology

The species name derives from the German Federal State of Rhineland-Palatinate, where the type locality is located. In Weber *et al*. (2023), this species was treated as *N. aquilex* A.

Material examined

Holotype

GERMANY • ♂; Rhineland-Palatinate, Waldleiningen, Felsenbrunnen in the Palatinate Forest in the Middle Buntsandstein; rheocrene spring; 49.2881° N, 7.8467° E; 14 Dec. 2016; Dieter Weber leg.; kept intact in 96% ethanol; 161214-02; MNHNL130574.

Paratypes

GERMANY • 1 ♂; same collection data as for holotype; 14 Dec. 2016; dissected and appendages drawn; 161214-01; ISER microscope slide DW161214-01 • 1 ♀; same collection data as for holotype; 8 Aug. 2017; dissected and appendages drawn; 170808-13; ISER microscope slide DW170808-13.

Molecular data

COI and 28S rDNA sequences of specimens belonging to *Niphargus palatinensis* sp. nov. were deposited in GenBank. COI and 28S rRNA accession numbers are present in Supp. file 6 and Supp. file 9, respectively.

Description (male paratype ISER DW161214-01)

Measurements

Total body length 6.92 mm (Fig. 12).

Head

Head (Fig. 12) 8% of total body length. Eyes and rostrum absent.

Antennae

Antenna I (Fig. 13A): with main flagellum formed of 20 articles, representing 50% of total body length. Peduncle length 35% of total length of antenna I. The accessory flagellum (Fig. 13B). Biarticulated; proximal article shorter than first article of main flagellum; distal article 27% of total length of accessory flagellum, with 4 apical setae of different lengths and 1 aesthetasc. Aesthetascs ¾ of respective main flagellum articles (Fig. 13C).

Antenna II (Fig. 13D): flagellum formed of 10 articles and representing 50% of total length of antenna II. Most flagellum articles bear 1 aesthetasc, longer than half of respective flagellum articles.

Mouthparts

Labrum (Fig. 14A): typical, subovoid shape. Labium (Fig. 14B). Large inner lobes with 1 row of fine setae on inner sides. Outer lobes with 2 rows of fine setae subapically on inner sides.

Maxilla I (Fig. 14C): with 3 apical setae on distal article of palp. 6 spines of outer lobe with 1–3 teeth each and 1 spine with several small teeth. Inner lobe with 1 apical seta.

Maxilla II (Fig. 14D): with inner lobe slightly shorter than outer lobe. 1 apical row of setae and 4 setae on inner margin of each lobe.

Left mandible (Fig. 14E): 6 teeth on incisor process. 5 teeth on lacinia mobilis. 8 serrated setae intercalated with 4 trifid setae, between lacinia mobilis and molar process.

Right mandible (Fig. 14F): 5 teeth on incisor process. Lacinia mobilis with several smaller teeth. 7 serrated and 2 trifid setae between lacinia mobilis and molar process. A long seta on molar process.

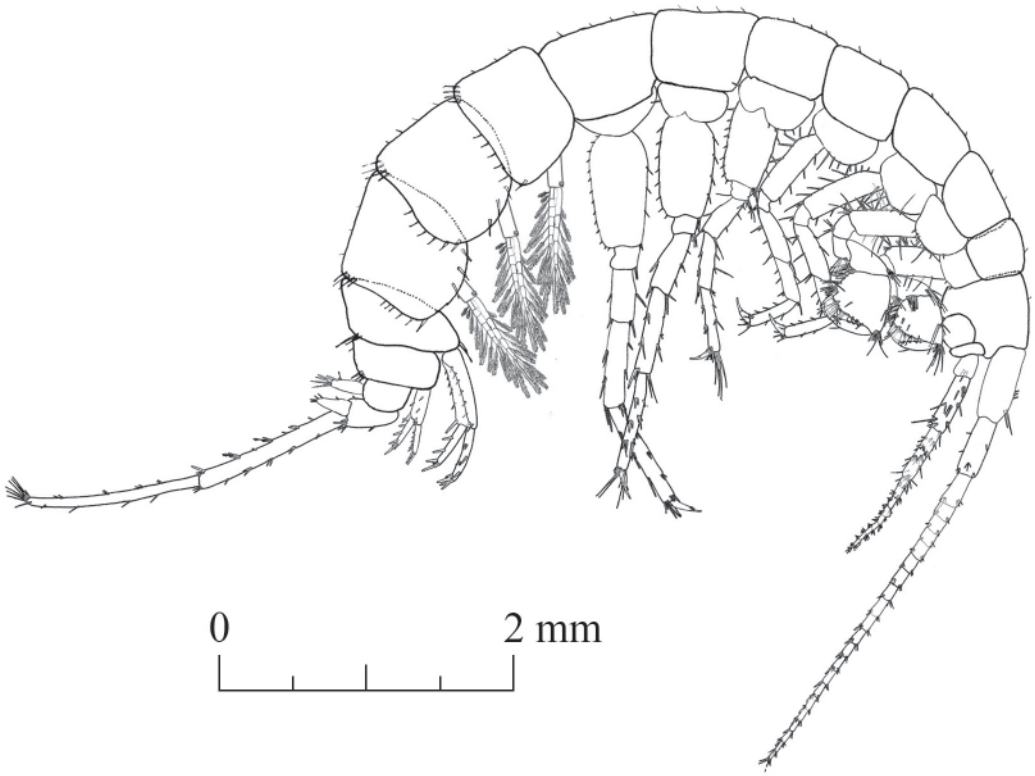

Fig. 12. *Niphargus palatinensis* Weber & Brad sp. nov., paratype, ♂ (ISER DW161214-01); general appearance.

Fig. 13. *Niphargus palatinensis* Weber & Brad sp. nov., paratype, ♂ (ISER DW161214-01). **A**. Antenna I. **B**. Antenna I, details of accessory flagellum. **C**. Antenna I, details of aesthetascs. **D**. Antenna II.

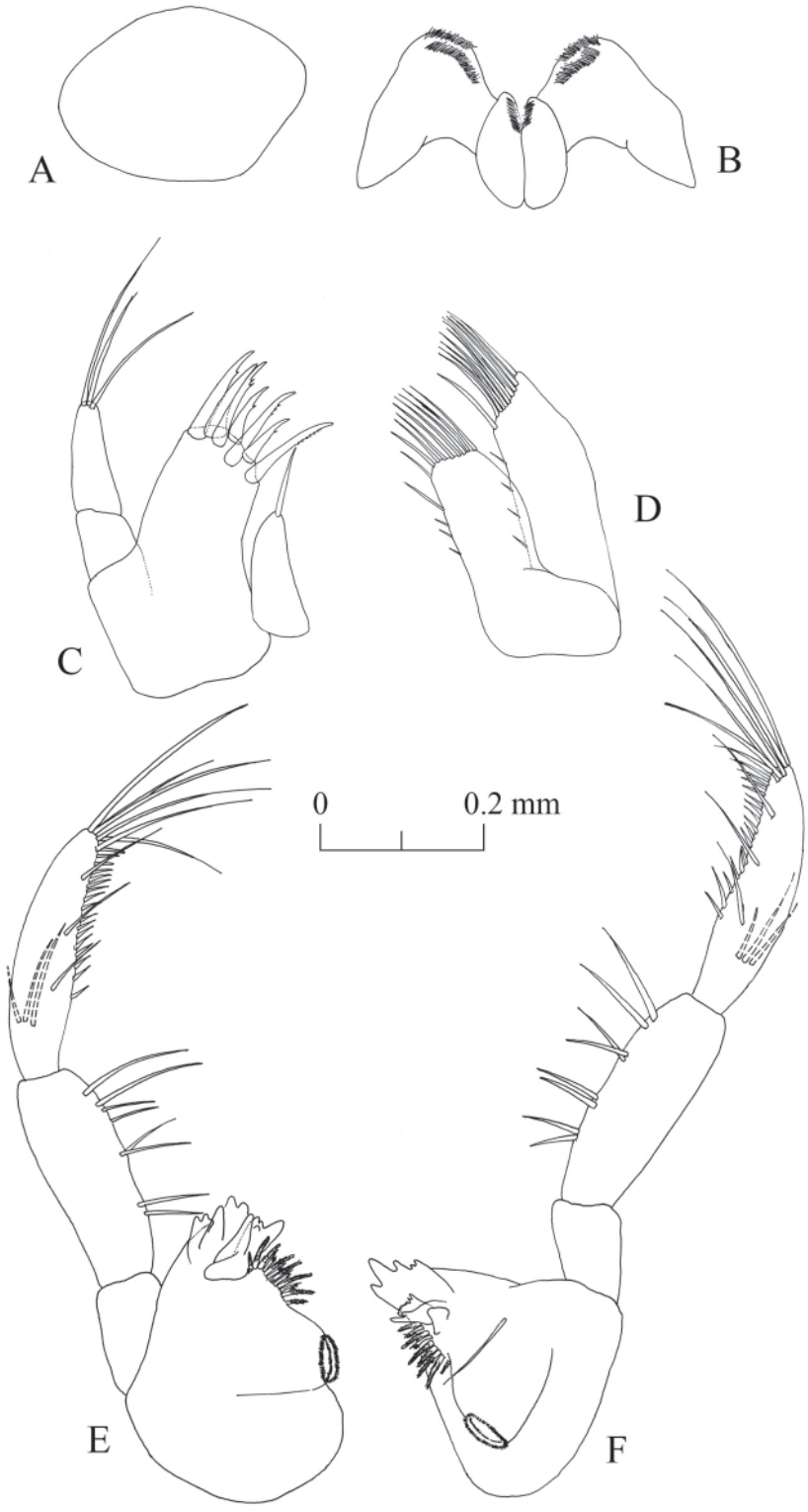

Fig. 14. *Niphargus palatinensis* Weber & Brad sp. nov., paratype, ♂ (ISER DW161214-01). **A**. Labrum. **B**. Labium. **C**. Maxilla I. **D**. Maxilla II. **E**. Left mandible. **F**. Right mandible.

Mandibular palps (Fig. 14E–F): highly similar and of same length. 3 articles account for 17% (article 1), 39% (article 2) and 44% (article 3) of total length of palp. Proximal article without setae, median article with 8 ventral setae. Distal article of palp with one group of 3 A setae, three groups with 1 B setae, 17 D setae and 5–6 E setae.

Maxilliped (Fig. 15A): with palp formed of 4 articles. Article 1 with 2 setae on inner margin. Article 2 with 23 setae aligned along inner margin. Article 3 with 4 apical setae, one group of 6 dorsal setae and one group of 7 setae on inner margin. Article 4 with 1 seta located on outer margin and 2 fine setae at nail insertion. Outer lobe with 5 apical setae and 9 flattened setae on inner margin. Inner lobe provided apically with 3 setae, 1 flattened seta and 2 dorsal setae.

Gnathopods

Gnathopod I (Fig. 15B): coxal plate in shape of rectangular trapezoid, with depth larger than width (ratio depth : width 1.0 : 0.64). Basis length : width ratio 1.0 : 0.44. Ischiopodite with one posteroventral group of 3 setae. Basis : carpus length ratio 1.0 : 0.58. Carpus with row of 7 setae along ventral margin, group of 5 setae located anterodorsally and one group of 8 setae on carpus surface close to ventral margin. Propodite as long as wide, three groups of 3–4 setae on ventral margin, one group of 4 setae on dorsal margin, one group of 10 anteroapical setae, 3 mesial setae on lateral surface, and one group of 3 setae close to palmar corner. 1 strong palmar spine, 1 supporting spine and 2 denticulate spines present in palmar corner. Dactylopodite with claw 26% of te total dactylopodite length and 1 seta along outer margin.

Gnathopod II (Fig. 15C): slightly larger than gnathopod I, with coxal plate in shape of trapezoid; coxal plate width larger than depth (ratio width : depth 1.0 : 0.7). Basis length : width ratio 1.0 : 0.31. Ischiopodite with one posteroventral group of 4 setae. Basis : carpus length ratio 1.0 : 0.54. Carpus with row of 6 setae along ventral margin, group of 4 setae located anterodorsally and 1 row of 4 setae on carpus surface close to ventral margin. Propodite as long as wide, with 5 groups of 3 setae on ventral margin, 4 setae on dorsal margin, 1 mesial seta on lateral surface, 8 anteroapical setae, one group of 5 setae on lateral surface close to ventral margin, and 3 setae close to palmar corner. 1 strong palmar spine, 1 supporting spine and 2 denticulate spines present in palmar corner. Dactylopodite with claw 28% of total dactylopodite length and 1 seta along outer margin.

Pereopods

Pereopod III (Fig. 16A): coxal plate in shape of rectangular, with width larger than depth, width : depth ratio 0.7. Propodite : dactylus length ratio 1.0 : 0.45. Dactylus, with nail measuring half of total length of dactylus, 1 dorsal seta with plumose tip, and 1 seta at nail base. Pereopod III nearly equal to pereopod IV (pereopod III : pereopod IV length ratio 1.0 : 0.98).

Pereopod IV (Fig. 16B): relatively rectangular coxal plate, with concavity on posterior margin, width : depth ratio 1.0 : 0.7. Propodite : dactylus length ratio 1.0 : 0.54. Robust dactylus, with nail half of total length of dactylus; 1 dorsal seta with plumose tip and 1 seta at nail base.

Pereopod V (Fig. 17A): coxal plate of irregular shape, with deep concavity on ventral side, 4 anterior setae and 1 posterior seta. Basis rectangular, length : width ratio 1.0 : 0.57, 4 setae on anterior margin, 9 setae on posterior margin, 3 anteroapical setae of different lengths. Dactylus with 1 dorsal seta with plumose tip, 1 seta at nail base, which represents 45% of total dactylus length. Propodite length : dactylus length ratio 1.0 : 0.36.

Pereopod VI (Fig. 17B): coxal plate smaller than that of pereopod V, with concavity on ventral side less deep than that of pereopod V, and 1 posterior seta. Basis rectangular, length : width ratio 1.0 : 0.55, 4 setae on anterior margin, 8 setae on posterior margin, 2 anteroapical setae. Dactylus with 1 plumose seta on

outer margin and 2 setae of different lengths near nail base. Nail 36% of total dactylus length. Ratio propodite : dactylus length 1.0 : 0.33.

Pereopod VII (Fig. 17C): longest leg (3.22 mm) of inspected paratype male. Coxal plate trapezoidal, with 1 seta on posterior margin. Basis rectangular, ratio length : width 1.0 : 0.5, 3 setae on anterior margin, 14 setae on posterior margin and 2 small anteroapical setae. Dactylus with 1 plumose seta on outer margin and 2 setae near nail base. Nail length 31% of total dactylus length. Ratio propodite : dactylus length 1.0 : 0.3.

Pereopods V : VI : VII ratio 1.0 : 1.35 : 1.42.

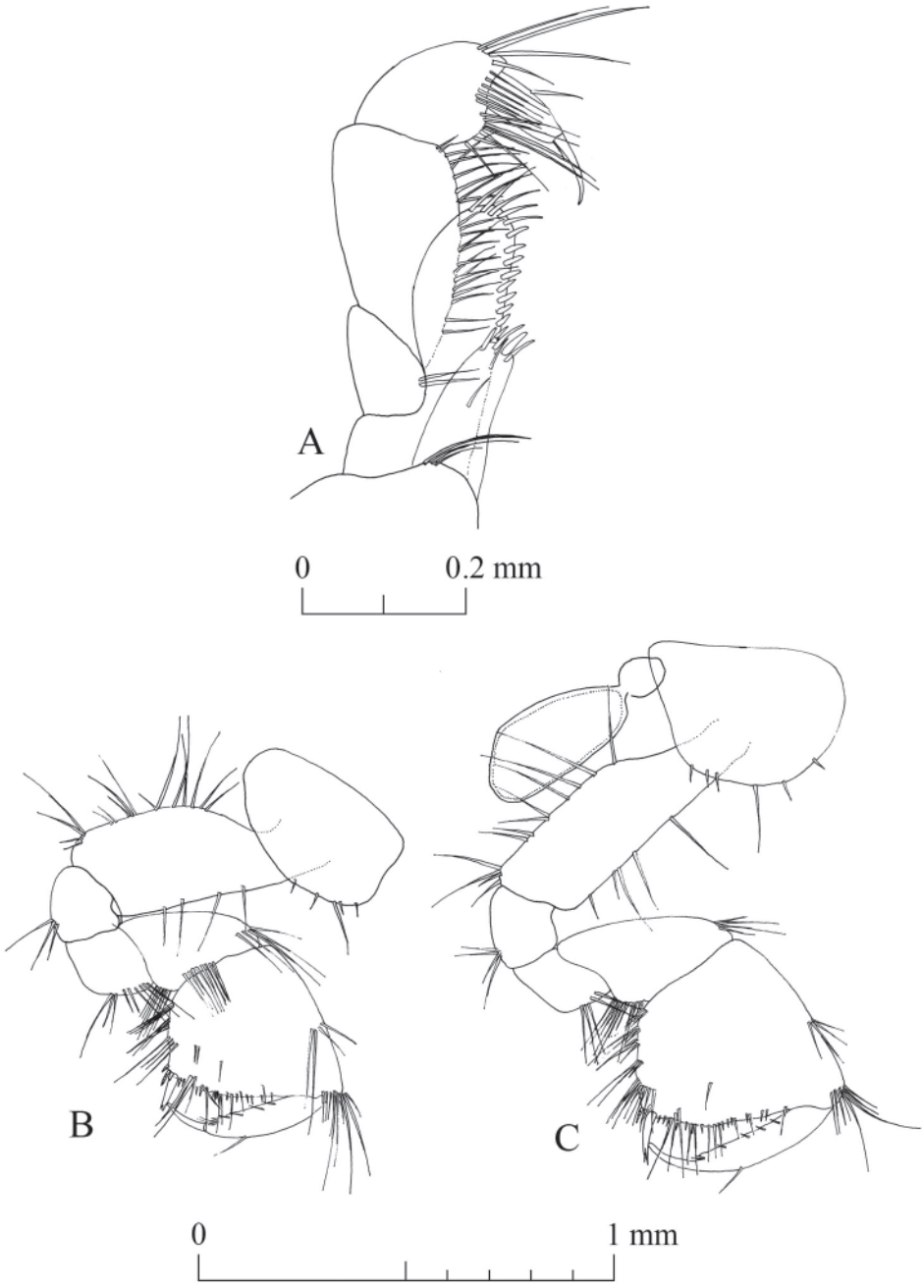

Fig. 15. *Niphargus palatinensis* Weber & Brad sp. nov., paratype, ♂ (ISER DW161214-01). **A**. Maxilliped. **B**. Gnathopod I. **C**. Gnathopod II.

Pleopods

Pleopods. Similar (pleopod III depicted in Fig. 18A), with unequal rami and 3 hooks on retinaculum.

Epimeral plates (Fig. 18B)

Epimeral plate I with right postero-ventral angle, relatively straight ventral margin, convex posterior margin with 6 setae. Epimeral plate II with right postero-ventral angle, convex ventral margin with 3 spines, convex posterior margin with 6 setae. Epimeral plate III with right posteroventral angle, convex ventral margin with 3 spines, convex posterior margin with 6 setae.

Uropods

Uropod I (Fig. 19A): with two dorso-lateral rows of 6–8 spines on peduncle. Exopodite slightly longer than endopodite, ratio exopodite : endopodite lengths> plural correct? 1.0 : 0.82. 1 strong spine at base of uropod I.

Uropod II (Fig. 19B): with 5 dorsal spines and 1 apical spine on peduncle. Endopodite slightly longer than exopodite, endopodite : exopodite length ratio 1.0 : 0.88, both rami provided with 4–6 dorsal and 4 apical spines.

Uropod III (Fig. 19C): sexually differentiated, longer in males. Peduncle with 5 apical, 3 anterior and 1 posterior setae. Endopodite 62% of length of peduncle, with 3 apical setae, 1 subapical and 1 lateral

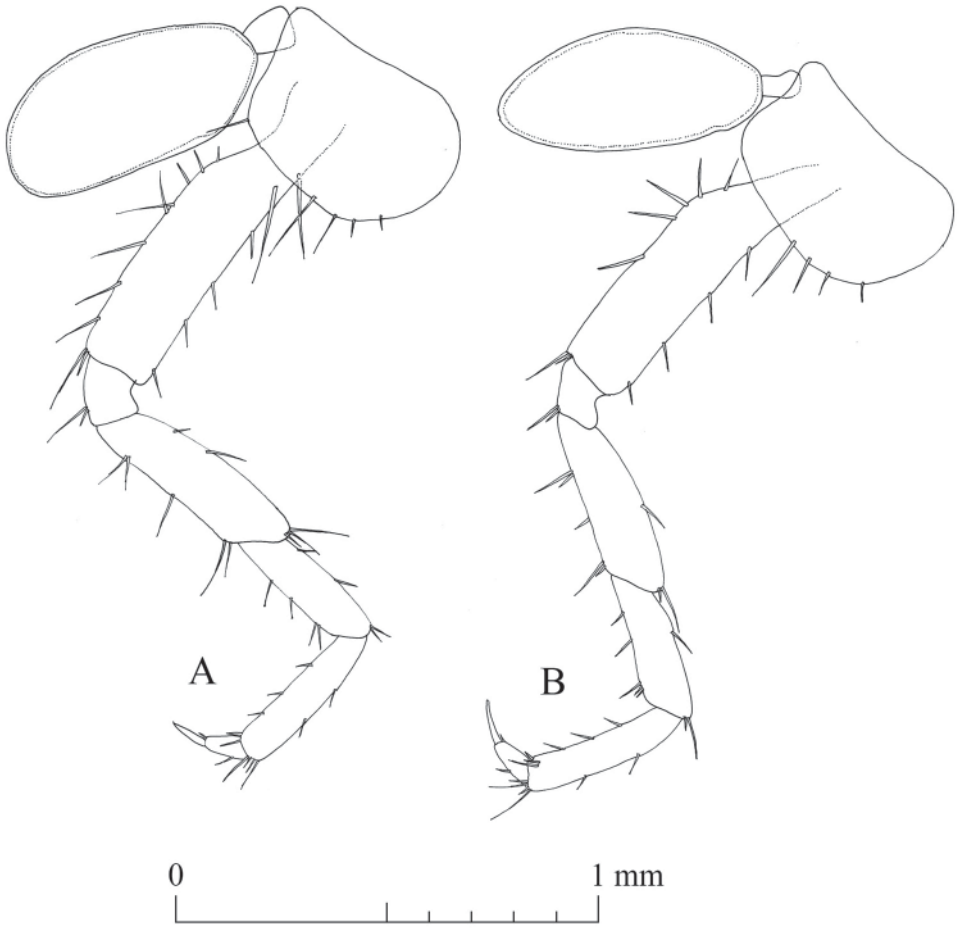

Fig. 16. *Niphargus palatinensis* Weber & Brad sp. nov., paratype, ♂ (ISER DW161214-01). **A**. Pereopod III. **B**. Pereopod IV.

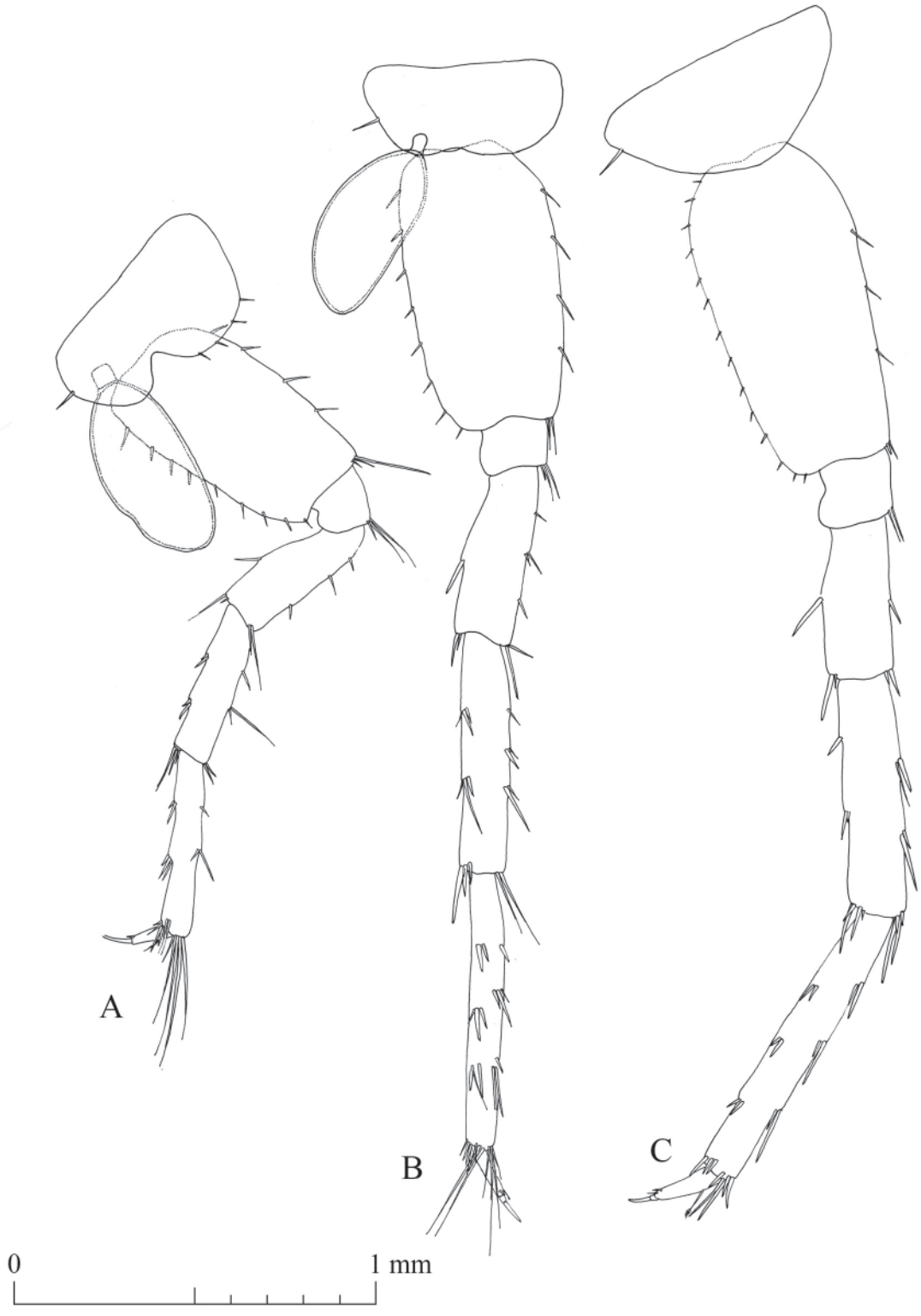

Fig. 17. *Niphargus palatinensis* Weber & Brad sp. nov., paratype, ♂ (ISER DW161214-01). **A**. Pereopod V. **B**. Pereopod VI. **C**. Pereopod VII.

seta on ventral margin. Proximal segment of exopodite shorter than distal segment. Distal : proximal articles length ratio 1.0 : 0.93. Anterior margin of proximal segment of exopodite with 6 groups of 1–3 setae (including plumose setae); posterior margin of exopodite with 5 groups of 1–2 setae; 3 antero- and 3 posteroapical setae. Distal segment of exopodite with 4 groups of 2 setae on anterior margin, 4 setae on posterior margin, and 7 apical setae of different lengths.

Telson

Telson (Fig. 19E). Nearly as wide as long (length : width ratio 0.95), with 2 subapical and 4 apical spines of different lengths on each lobe. Longest spine 60% of telson length. 2 thin setae of different lengths and plumose tip on each lobe, 1 seta medially on 1 lobe.

Sexual dimorphism

The examined male and female are highly similar. Besides the usual sexual dimorphism (e.g., slightly smaller gnathopods, presence of oostegites, and slightly deeper coxal plates I–VI in females), in *N. palatinensis* sp. nov., female uropod III (Fig. 19D) is shorter comparted to that of male. The telson of the inspected female paratype is provided apically with 4 setae on each lobe, and 2 subapical setae on one lobe only (Fig. 19F).

Type locality, ecology and distribution

The species is mainly distributed in the United Kingdom and Western Germany, although two sites from France and one from the Channel Islands (Guernsey) are known (Fig. 20). The type locality is the Felsenbrunnen in the Palatinate Forest (community of Waldleiningen, Rhineland-Palatinate, Germany)

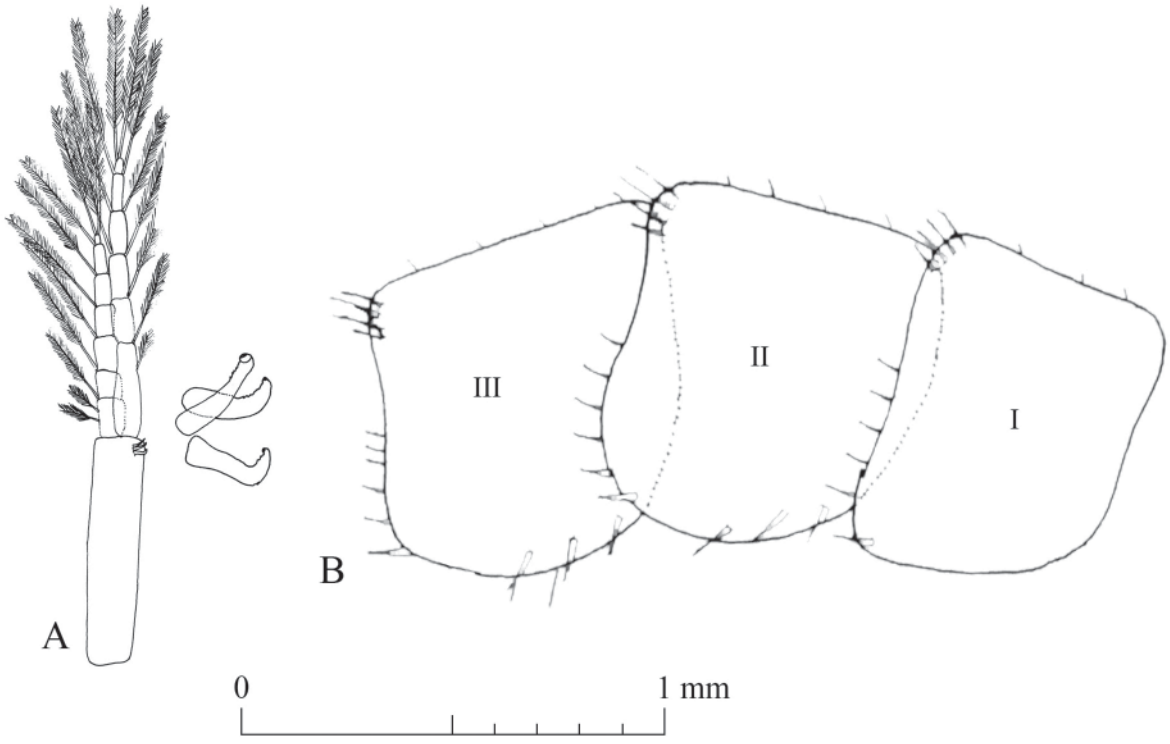

Fig. 18. *Niphargus palatinensis* Weber & Brad sp. nov., paratype, ♂ (ISER DW161214-01). **A**. Pleopod III, detail of the retinaculum. **B**. Detail of the epimeral plates.

in the Middle Buntsandstein at 49.2881° N, 7.8467° E (Supp. file 3.4). It is a natural rheocrene with a permanent moderate flow.

The bottom of the spring is covered with sand and rotting foliage above (Supp. file 3.5). With a hardness of 4°GH, the water is very soft. Other species of neither *Niphargus* nor gammarids were found in this spring. We confirm the permanent presence of this species in the type locality as it was found on

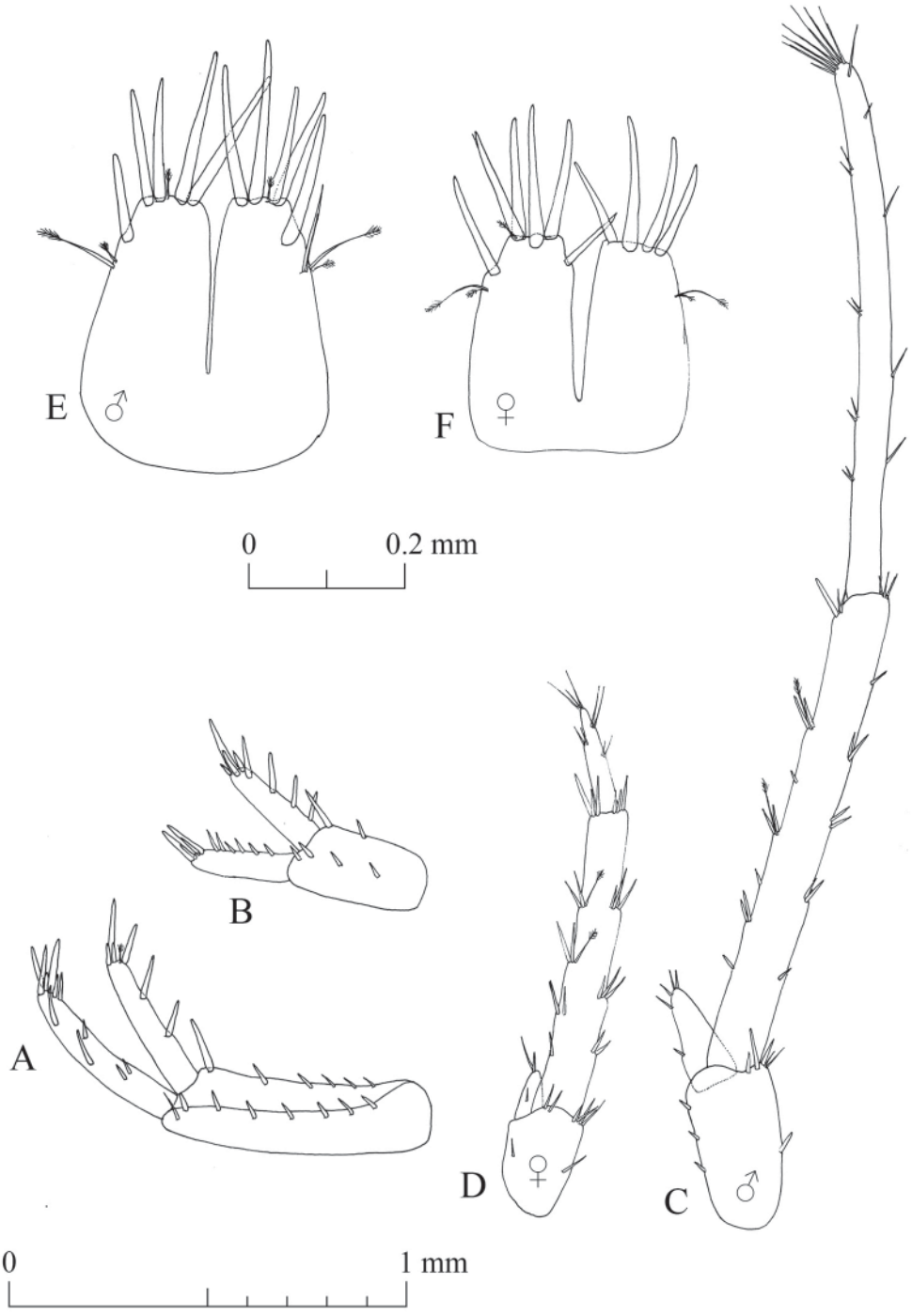

Fig. 19. *Niphargus palatinensis* Weber & Brad sp. nov., paratype, ♂ (ISER DW161214-01) and paratype, ♀ (ISER DW170808-13). **A**. Male uropod I. **B**. Male uropod II. **C**. Male uropod III. **D**. Female uropod III. **E**. Male telson. **F**. Female telson.

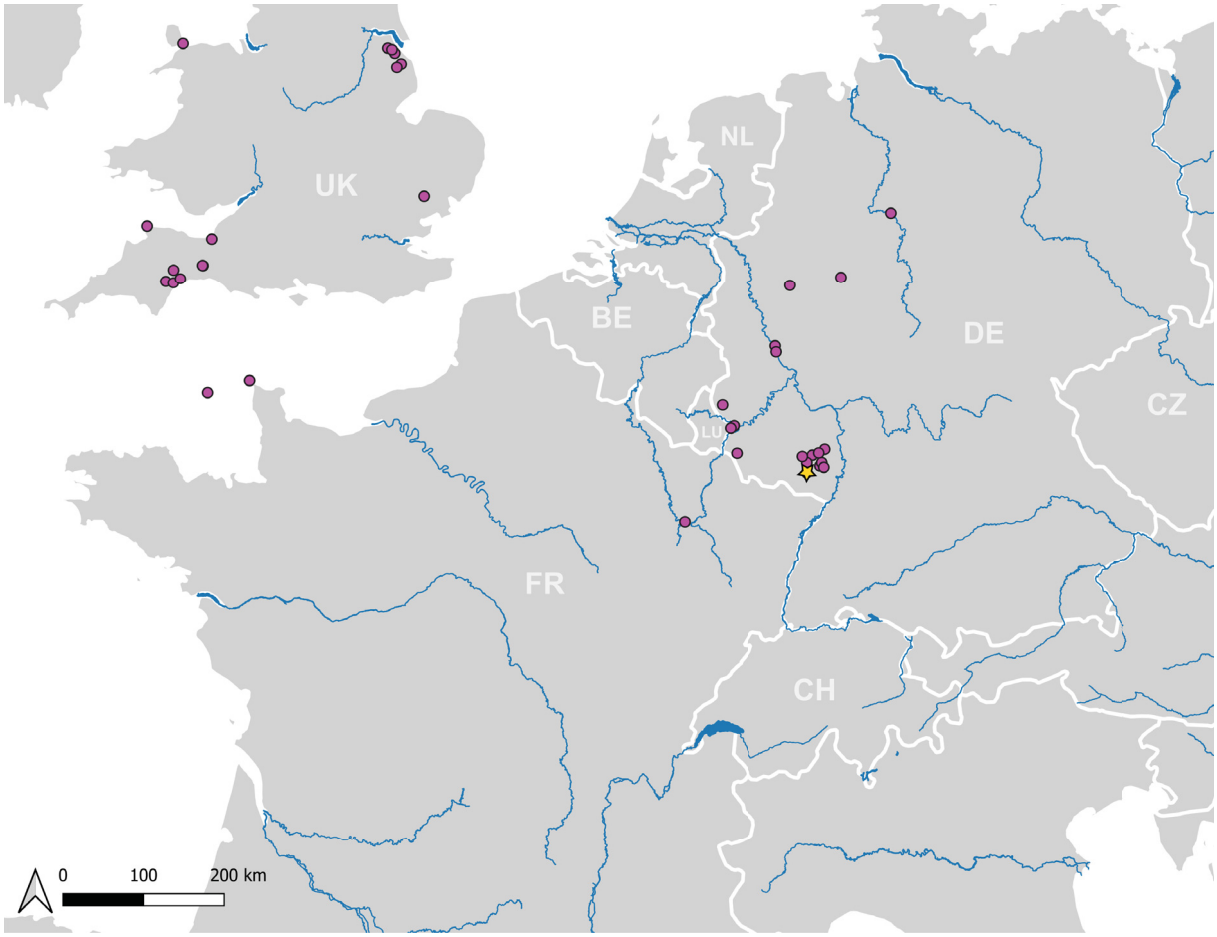

Fig. 20. Distribution of *Niphargus palatinensis* Weber & Brad sp. nov. confirmed by molecular data. The type locality at Felsenbrunnen (Germany) is marked by a yellow star, overlaying one site record. Very large freshwater bodies are indicated; country codes follow the ISO 3166 standard alpha-2 format.

14 December 2016 and 14 June 2019. The species was regularly found in all types of biotopes. Due to the small number of sampling sites, we withstand in providing a more detailed ecological interpretation (Supp. file 4.4).

Niphargus normandiensis Weber & Brad sp. nov.
urn:lsid:zoobank.org:act:DA362C5F-406A-4759-B64C-318A1A9E823E
Figs 21–29

Diagnosis

Medium-sized *Niphargus* species, poorly setose. Right postero-ventral angle of epimeral plates. Six spines of maxilla I outer lobe with 1 tooth each; 1 spine with several smaller teeth. Mandibular palp with small number (1–2) of B setae. Gnathopods with 1 seta along outer margin of dactylopodite. Pereiopod VII, the longest leg, slightly longer than half of total body length. Pleopods retinaculum with 5 hooks. Uropod I, longer exopodite. Uropod II, longer endopodite. Uropod III sexually dimorphic, exopodite elongated in males. Telson with 3 apical spines on each lobe. No pure diagnostic sites are present in the COI marker, but a single 28S rDNA allele as well as six COI barcodes are diagnostic.

Etymology

The species name derives from the French region of Normandy, where the type locality is located. In Weber *et al*. (2023), this species was treated as *N. aquilex* D, N.

Material examined

Holotype

FRANCE • ♂; Calvados, Carrière souterrain de Saint-Vaast-en-Auge, small lake in a subterranean quarry in sandstone outside the village Saint-Vaast-en-Auge; 49.2910° N, 0.0009° W; 26 May 2018; Dieter Weber leg.; kept intact in 96% ethanol; 180526-43a; MNHNL130577.

Paratypes

FRANCE • 1 ♂; same collection data as for holotype; 26 May 2018; dissected and appendages drawn; 180526-36; ISER microscope slide DW180526-36 • 1 ♀; same collection data as for holotype; 26 May 2018; dissected and appendages drawn; 180526-31; ISER microscope slide DW180526-31 • 1 ♀; same collection data as for holotype; 26 May 2018; ISER DW180526-32 • 1 ♀; same collection data as for holotype; 26 May 2018; ISER DW180526-33.

Molecular data

COI and 28S rDNA sequences of specimens belonging to *Niphargus normandiensis* sp. nov. were deposited in GenBank. COI and 28S rRNA accession numbers are present in Supp. file 6 and Supp. file 9, respectively.

Description (male paratype ISER DW180526-36)

Measurements

Total body length is 7.54 mm (Fig. 21).

Head

Head (Fig. 21) 7.3% of total body length. Eyes and rostrum absent.

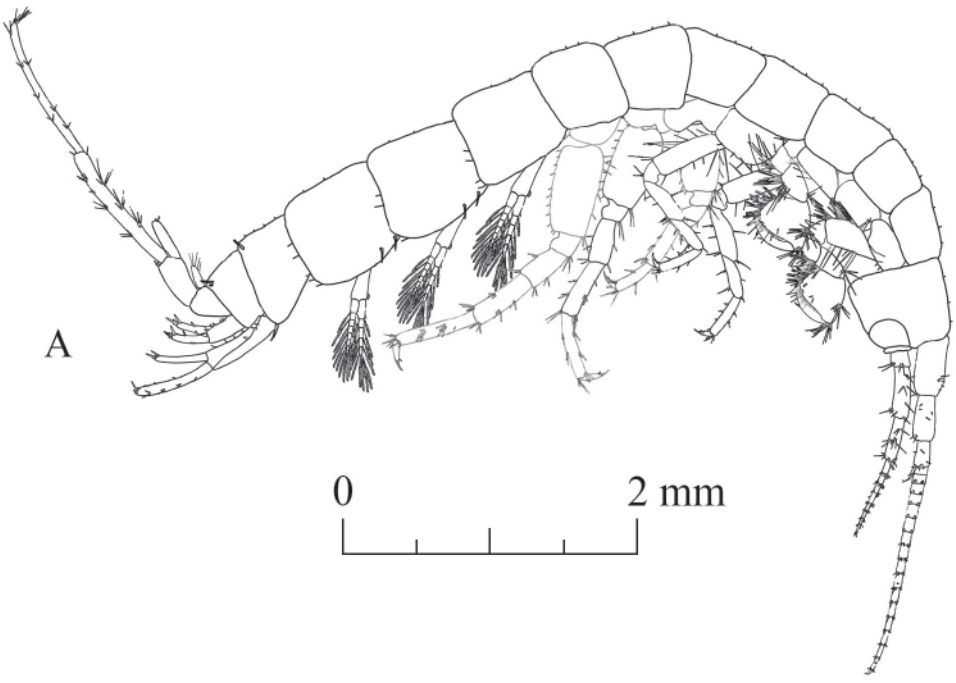

Fig. 21. *Niphargus normandiensis* Weber & Brad sp. nov., paratype, ♂ (ISER DW180526-36); general appearance.

Antennae

Antenna I (Fig. 22A): with main flagellum formed of 17 articles, representing 55% of total body length. Peduncle length 40% of total length of antenna I. Accessory flagellum (Fig. 22B) biarticulated; proximal article slightly longer than first article of main flagellum; distal article 28% of total length of accessory flagellum, with 3 apical setae of different lengths and 1 aesthetasc. Aesthetascs ⅓ of respective main flagellum articles (Fig. 22C).

Antenna II (Fig. 22D): flagellum formed of 8 articles and representing 42% of total length of antenna II. Most flagellum articles bear 1 aesthetasc, ¼ length of respective flagellum articles.

Mouthparts

Labrum (Fig. 23A): typical, subovoid shape. Labium (Fig. 23B). Large inner lobes with 1 row of fine setae on inner sides. Outer lobes with 1 row of fine setae subapically on inner sides.

Maxilla I (Fig. 23C): with 3 apical setae on distal article of palp. Six spines of outer lobe with 1 tooth each and 1 spine with several small teeth. Inner lobe with 1 apical seta.

Maxilla II (Fig. 23D): with inner lobe slightly shorter than outer lobe. 1 apical row of setae on each lobe.

Left mandible (Fig. 23E): 5 teeth on incisor process. 3 teeth on lacinia mobilis. 10 serrated setae between lacinia mobilis and molar process.

Right mandible (Fig. 23F): 4 teeth on incisor process. 2 teeth on lacinia mobilis. 5 serrated setae between lacinia mobilis and molar process. Long seta on molar process.

Mandibular palps (Fig. 23E–F): highly similar and of same length. 3 articles account for 18% (article 1), 36% (article 2) and 46% (article 3) of total length of palp. Proximal article without setae, median article with 6–7 ventral setae. Distal article of palp with one group of 5 A setae, four groups with 1 B setae each, 22–23D setae and 6 E setae.

Maxilliped (Fig. 24A): with palp formed of 4 articles. Article 1 asetose. Article 2 with 23 setae aligned along inner margin. Article 3 with 6 apical setae, one group of 6 dorsal setae and one group of 4 setae on inner margin. Article 4 with 1 seta located on outer margin and 2 setae at nail insertion. Outer lobe with 5 apical setae and 8 flattened setae on inner margin. Inner lobe provided apically with 5 setae and 1 flattened seta.

Gnathopods

Gnathopod I (Fig. 24B): coxal plate in shape of rectangular trapezoid, with depth larger than width (ratio depth : width 1.0 : 0.53). Basis length : width ratio 1.0 : 0.64. Ischiopodite with one posteroventral group of 8 setae. Basis : carpus length ratio 1.0 : 0.75. Carpus with row of 9 setae of various lengths along ventral margin, group of 3 setae located anterodorsally and one group of 2 setae on carpus surface close to ventral margin. Propodite nearly as long as wide, five groups of 3–4 setae on ventral margin, two groups of 2 setae each on dorsal margin, one group of 5 setae on propodite surface close to dorsal margin, one group of 10 anteroapical setae, 2 mesial setae on lateral surface, 2 setae on lateral surface close to ventral margin and one group of 3 setae close to palmar corner. 1 strong palmar spine, 1 supporting spine and 2 denticulate spines present in palmar corner. Dactylopodite with claw 30% of total dactylopodite length and 1 seta along outer margin.

Gnathopod II (Fig. 24C): slightly larger than gnathopod I, with coxal plate in shape of trapezoid; coxal plate wider than deep (ratio width : depth 1.0 : 0.7). Ovoid gill and of same length as coxal plate width. Basis length : width ratio 1.0 : 0.38. Ischiopodite with one posteroventral group of 6 setae. Basis : carpus

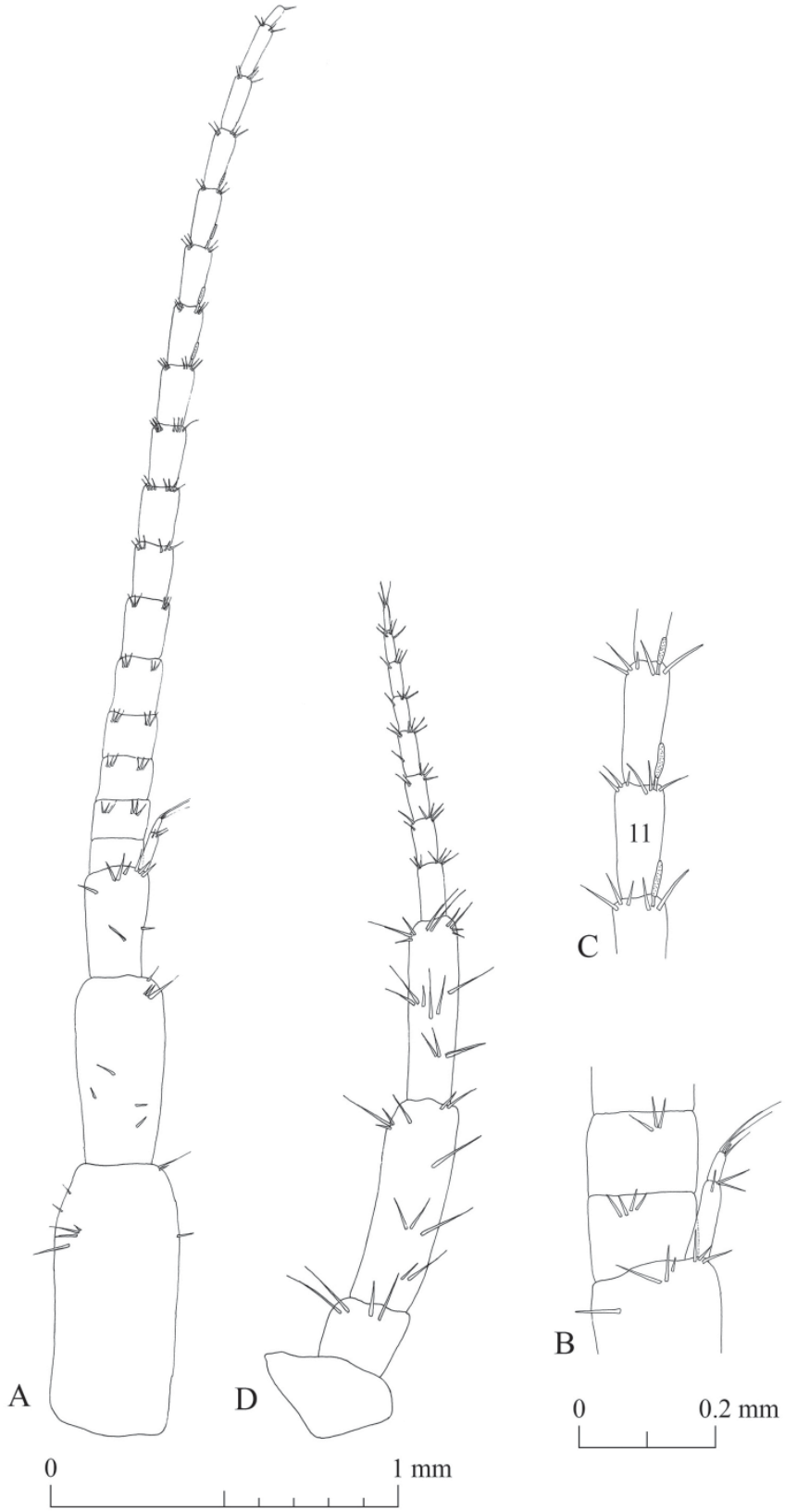

Fig. 22. *Niphargus normandiensis* Weber & Brad sp. nov., paratype, ♂ (ISER DW180526-36). **A**. Antenna I. **B**. Antenna I, details of the accessory flagellum. **C**. Antenna I, details of the aesthetascs. **D**. Antenna II.

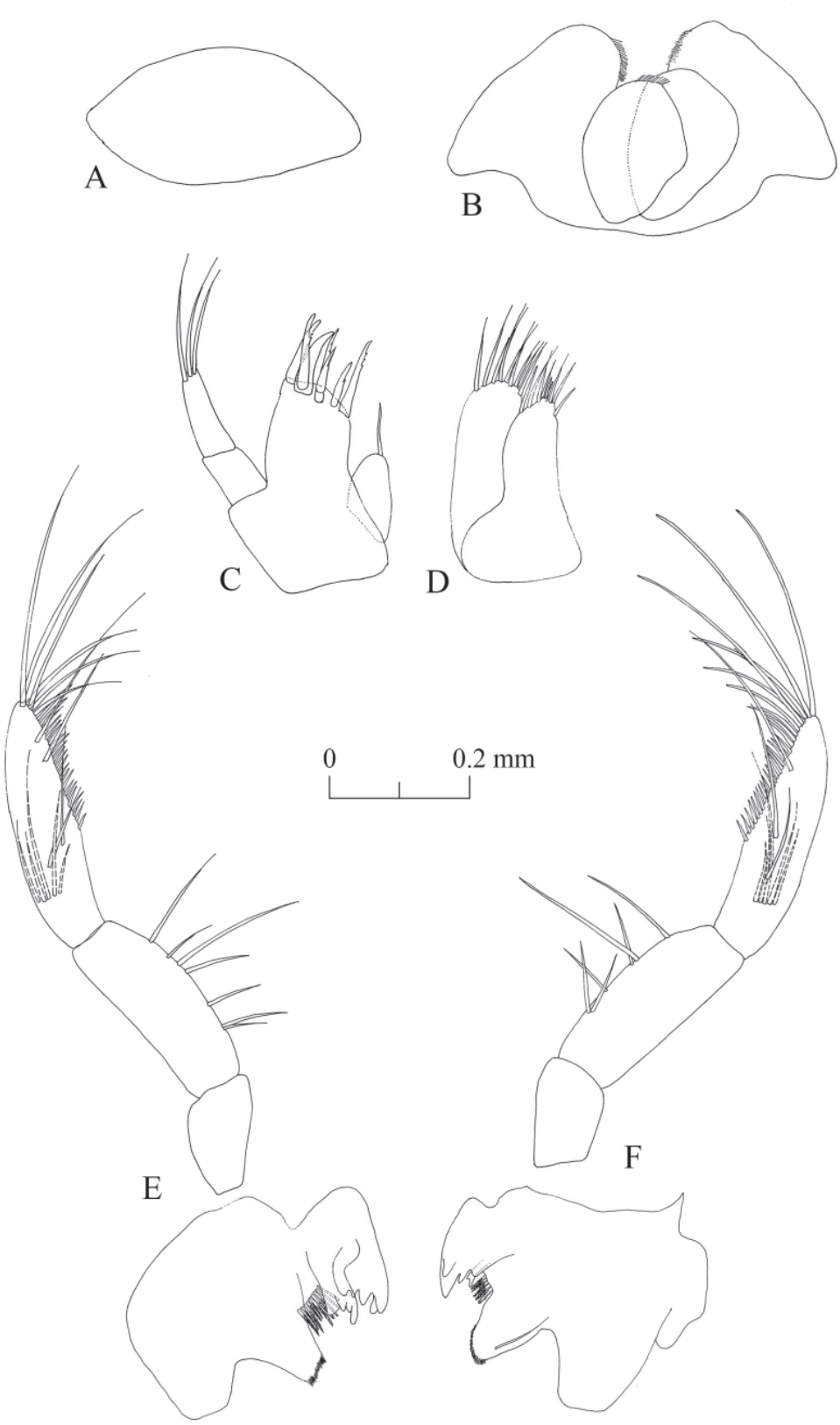

Fig. 23. *Niphargus normandiensis* Weber & Brad sp. nov., paratype, ♂ (ISER DW180526-36). **A**. Labrum. **B**. Labium. **C**. Maxilla I. **D**. Maxilla II. **E**. Left mandible. **F**. Right mandible.

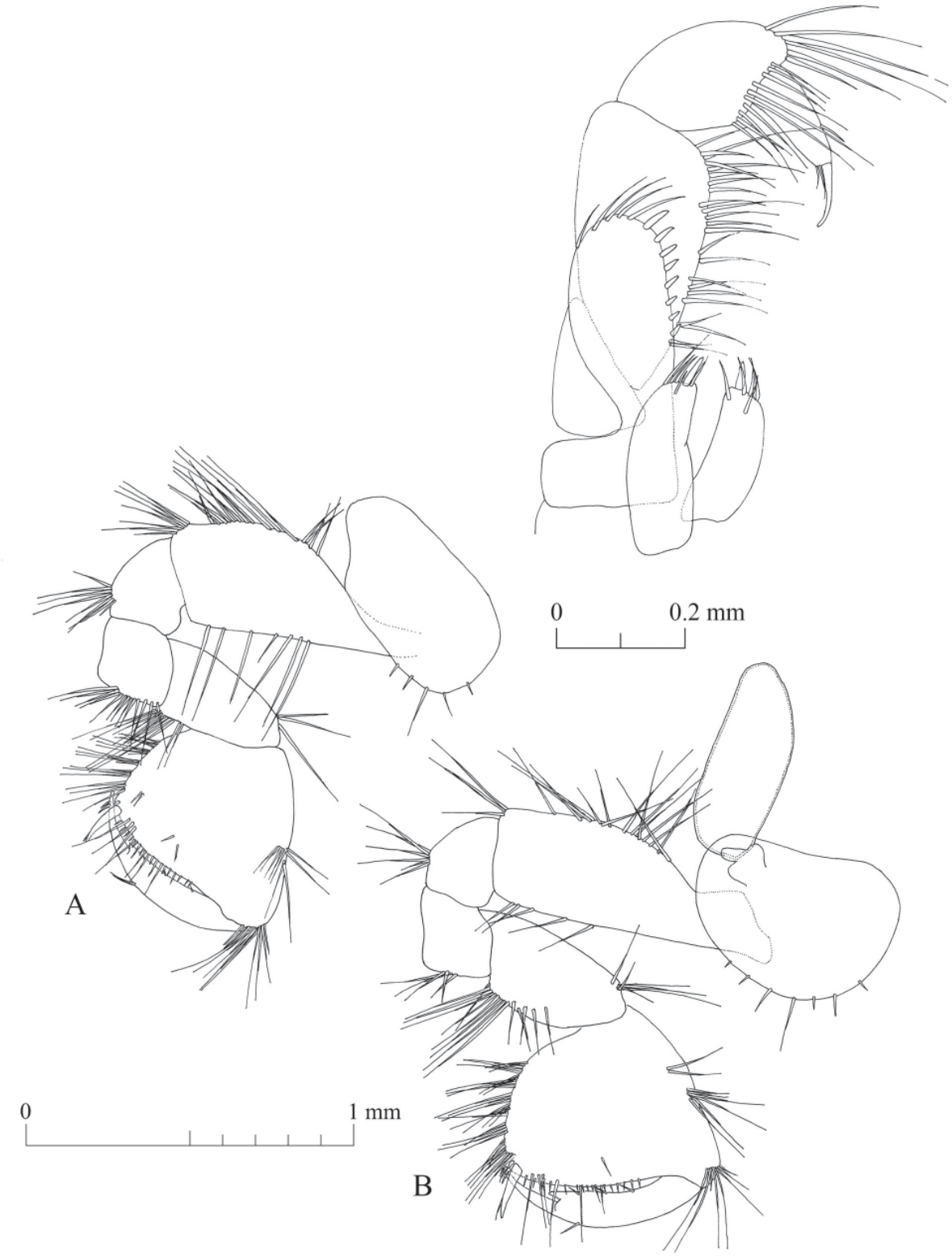

Fig. 24. *Niphargus normandiensis* Weber & Brad sp. nov., paratype, ♂ (ISER DW180526-36). **A**. Maxilliped. **B**. Gnathopod I. **C**. Gnathopod II.

length ratio 1.0 : 0.57. Carpus with row of 9 setae of various lengths along ventral margin, group of 6 setae located anterodorsally and 1 row of 5 setae on carpus surface close to ventral margin. Propodite width larger than length (ratio width : length 1.0 : 0.94), with 7 groups of 3–5 setae on ventral margin, one group of 6 setae on dorsal margin, one group of 2 setae on lateral surface close to dorsal margin, 1 mesial seta on lateral surface, one anterodorsal group of 8 setae, and one group of 3 long setae in vicinity of palmar corner. 1 strong palmar spine, 1 supporting spine and 3 denticulate spines present in palmar corner. Dactylopodite with claw 30% of total dactylopodite length and 1 seta along outer margin.

Pereopods

Pereopod III (Fig. 25A): coxal plate in shape of rectangular trapezoid, wider than deep (ratio width : depth 1.0 : 0.75). Propodite : dactylus length ratio 1.0 : 0.4. Dactylus, with nail measuring half of total length of dactylus, 1 dorsal seta with plumose tip, and 2 setae at nail base. Pereopod III slightly longer than pereopod IV (pereopod III : pereopod IV length ratio 1.0 : 0.95).

Pereopod IV (Fig. 25B): coxal plate in shape of rectangular trapezoid, width : depth ratio 1.0 : 0.68. Propodite : dactylus length ratio 1.0 : 0.4. Robust dactylus, with nail measuring almost half of total length of dactylus; 1 dorsal seta with plumose tip and 2 setae of different lengths at nail base.

Pereopod V (Fig. 26A). Shortest leg (2.64 mm) of inspected male paratype. Coxal plate of irregular shape, with deep concavity on ventral side, and 2 anterior setae. Basis rectangular, length : width ratio 1.0 : 0.62, 3 setae on anterior margin, 6 setae on posterior margin, 3 anteroapical setae of different lengths. Dactylus with 1 dorsal seta with plumose tip, 2 setae of different lengths at nail base, which representing 42% of total dactylus length. Propodite length : dactylus length ratio 1.0 : 0.49.

Pereopod VI (Fig. 26B): coxal plate relatively similar to that of pereopod V, with 1 posterior seta. Basis rectangular, length : width ratio 1.0 : 0.58, 4 setae on anterior margin, 10 setae on posterior margin, 3 anteroapical setae of different lengths. Dactylus with 1 plumose seta on outer margin and 2 setae of different lengths near nail base. Nail ⅓ of total dactylus length. Propodite : dactylus length ratio 1.0 : 0.42.

Pereopod VII (Fig. 26C): longest leg (3.90 mm) of inspected paratype male. Coxal plate trapezoidal, with 1 seta on posterior margin. Basis rectangular, ratio length : width 1.0 : 0.52, 5 setae on anterior margin, 11 setae on posterior margin and 2 anteroapical setae of different lengths. Dactylus with 1 plumose seta on outer margin and 1 seta near nail base. Nail length 35% of total dactylus length. Ratio propodite : dactylus length 1.0 : 0.38.

Pereopods V : VI : VII ratio 1.0 : 1.31 : 1.47.

Pleopods

Pleopods similar (pleopod III depicted in Fig. 27A), with unequal rami and 5 hooks on retinaculum. One of pleopods III laterally with 2 additional hooks on retinaculum.

Epimeral plates (Fig. 27B)

Epimeral plate I with right postero-ventral angle, straight ventral margin, relatively straight posterior margin with 4 setae. Epimeral plate II with right postero-ventral angle, convex ventral margin with 2 spines, convex posterior margin with 3 spines. Epimeral plate III with right posteroventral angle, straight ventral margin with 2 spines, convex posterior margin with 5 spines.

Uropods

Uropod I (Fig. 28A): with two dorso-lateral rows of 3–4 spines on peduncle. Exopodite longer than endopodite, exopodite : endopodite length ratio 1.0 : 0.66. 1 strong spine at base of uropod I.

Uropod II (Fig. 28B): with 4 dorsal and 2 apical spines on peduncle. Endopodite longer than exopodite, endopodite : exopodite length ratio 1.0 : 0.84, both rami provided with 1–2 dorsal and 5 apical spines.

Uropod III (Fig. 28C) sexually differentiated, longer in males. Peduncle with 4 posteroapical setae. Endopodite 67% of length of peduncle, with 4 small apical setae. Distal segment of exopodite slightly longer than proximal segment (ratio 1.0 : 0.95). Anterior margin of proximal segment of exopodite with

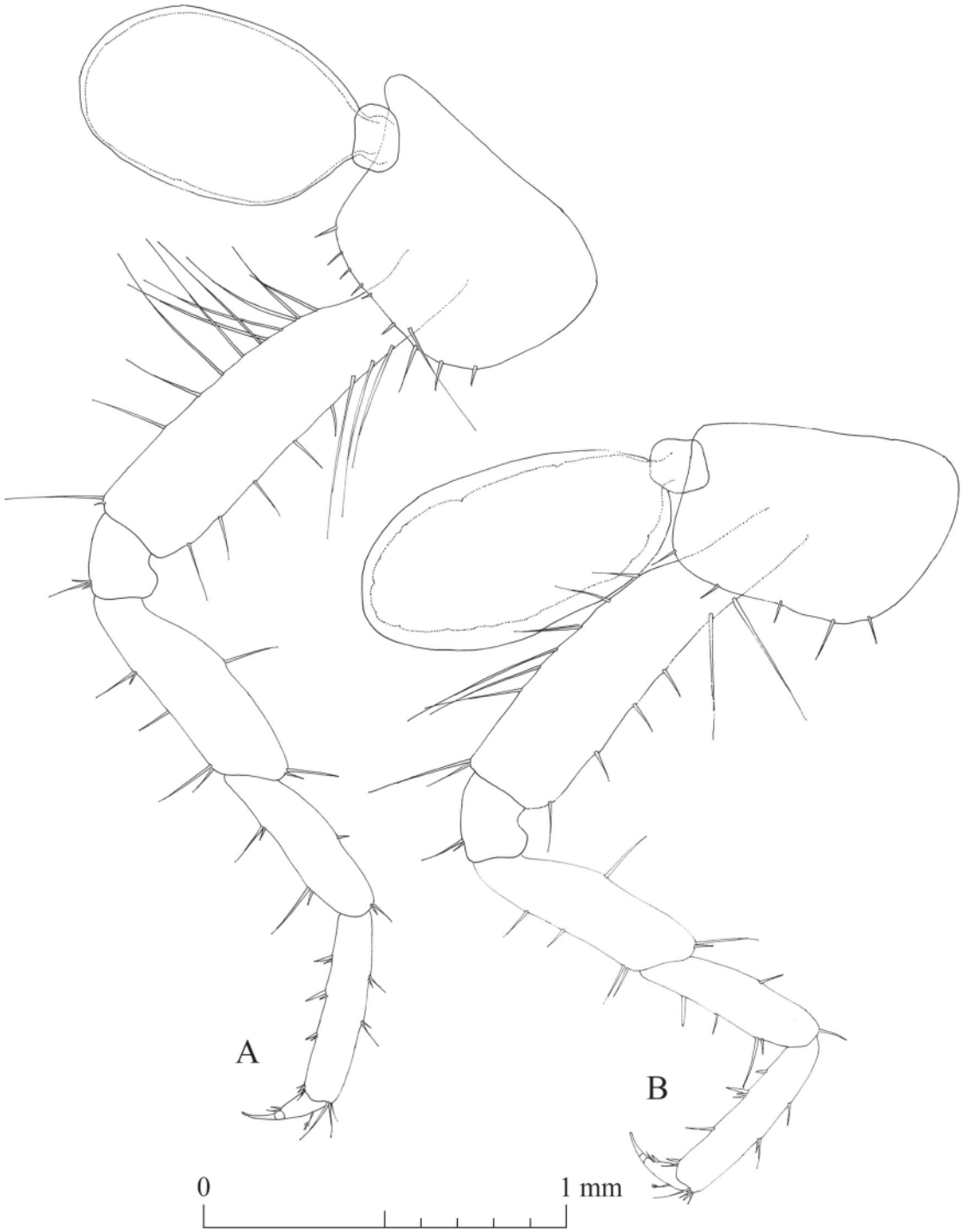

Fig. 25. *Niphargus normandiensis* Weber & Brad sp. nov., paratype, ♂ (ISER DW 180526-36). **A**. Pereopod III. **B**. Pereopod IV.

3 groups of 3–4 setae; posterior margin of exopodite with 4 groups of 2–4 setae; 1 antero- and 1 postero-apical seta. Distal segment of exopodite with 3 groups of 2 setae on anterior margin, 4 groups of 2 setae on posterior margin, and 8 apical setae of different lengths.

Telson

Telson (Fig. 28E) wide (width : length ratio 1.0 : 0.76), with 3 long apical spines, 2 spines and 2 thin setae with plumose tip located medially on each lobe. Longest spine 78% of telson length.

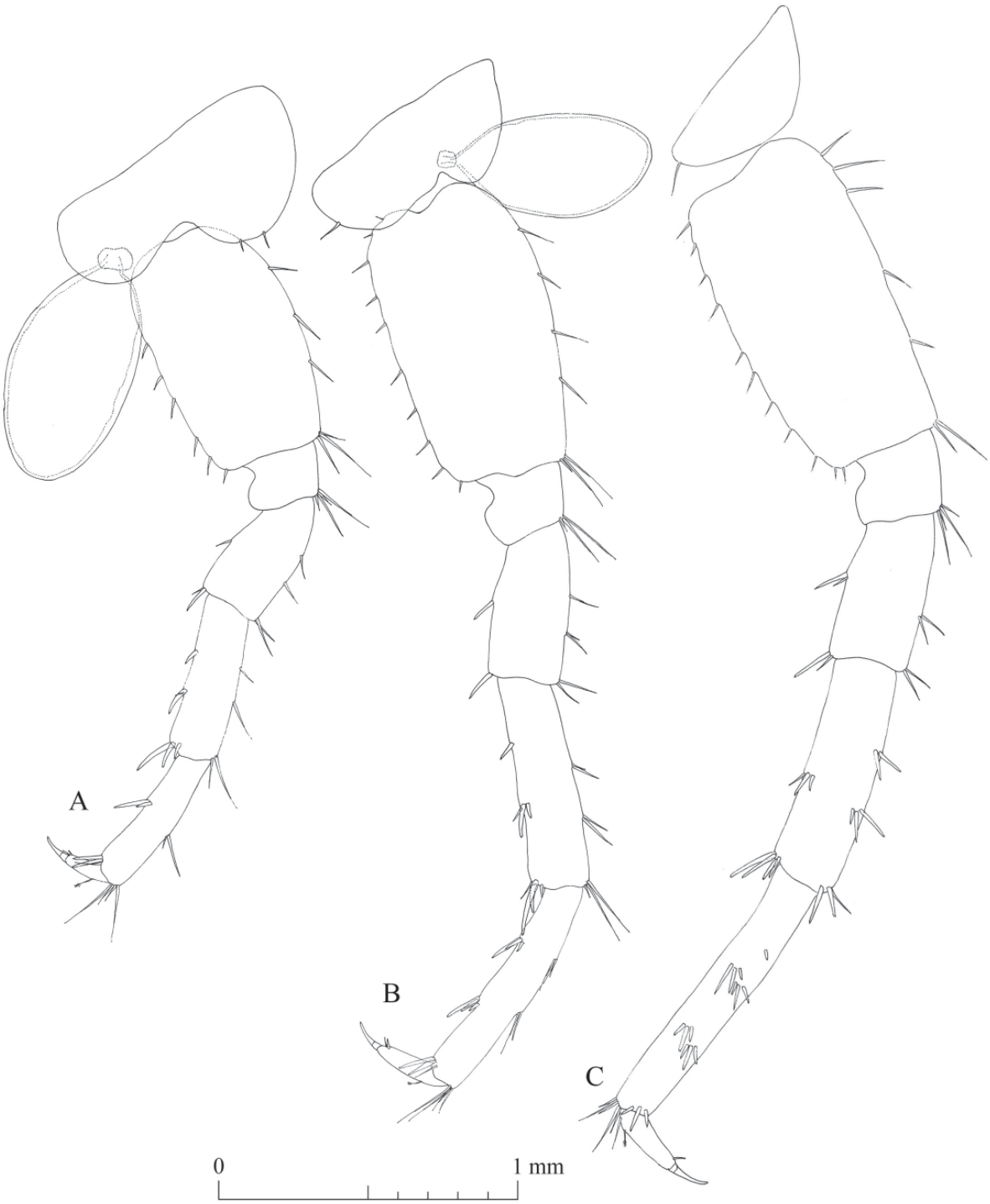

Fig. 26. *Niphargus normandiensis* Weber & Brad sp. nov., paratype, ♂ (ISER DW180526-36). **A**. Pereopod V. **B**. Pereopod VI. **C**. Pereopod VII.

Sexual dimorphism

The examined male and female are highly similar. Besides the usual sexual dimorphism (e.g., slightly smaller gnathopods, presence of oostegites, and slightly deeper coxal plates I–VI in females), in *N. normandiensis* sp. nov., the female uropod III is shorter comparted to that of the male (Fig. 28D). The female telson is highly similar to that of the male, but smaller (Fig. 28F).

Type locality, ecology and distribution

The species comprises three distinct genetic clades (clade N, D and non-annotated) which are distributed in the Normandy (France), with further scattered records on the Channel Islands (Guernsey, Jersey), on two islands off the Brittany Coast of France and in more Central France (Fig. 29). Thereby, clade D is restricted to Normandy (France), whereas both other clades occur on islands in the Atlantic Ocean and in more Central France. The type locality is the Carrière souterrain de Saint-Vaast-en-Auge, Calvados, France at 49.2910° N, 0.00090° W, a subterranean quarry in sandstone outside the village (Supp. file 3.6). The 50 m long cavity is completely dry with a small lake with stagnant water at 40–45 m distance from the entrance, behind a collapsed mine gallery. The water level varies seasonally from 20–70 cm. Specimens of *N. normandiensis* sp. nov. were found swimming on the clayey bottom of this lake. We confirm the permanent presence of this species in the type locality as it was found on 26 May 2018 as well as on 20 May 2019. We found this species in several springs and in one subterranean quarry. Ecological details are not inferred due to the small number of sampling sites.

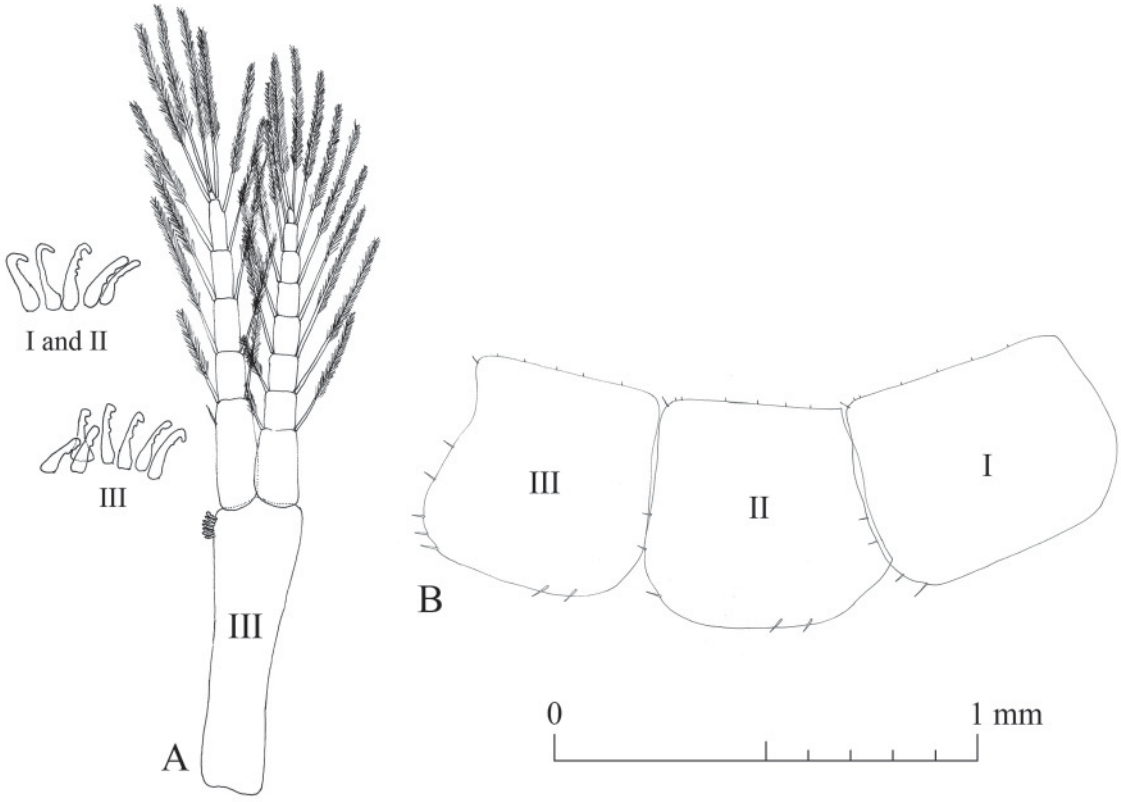

Fig. 27. *Niphargus normandiensis* Weber & Brad sp. nov., paratype, ♂ (ISER DW180526-36). **A**. Pleopod III, detail of the retinaculum. **B**. Detail of the epimeral plates.

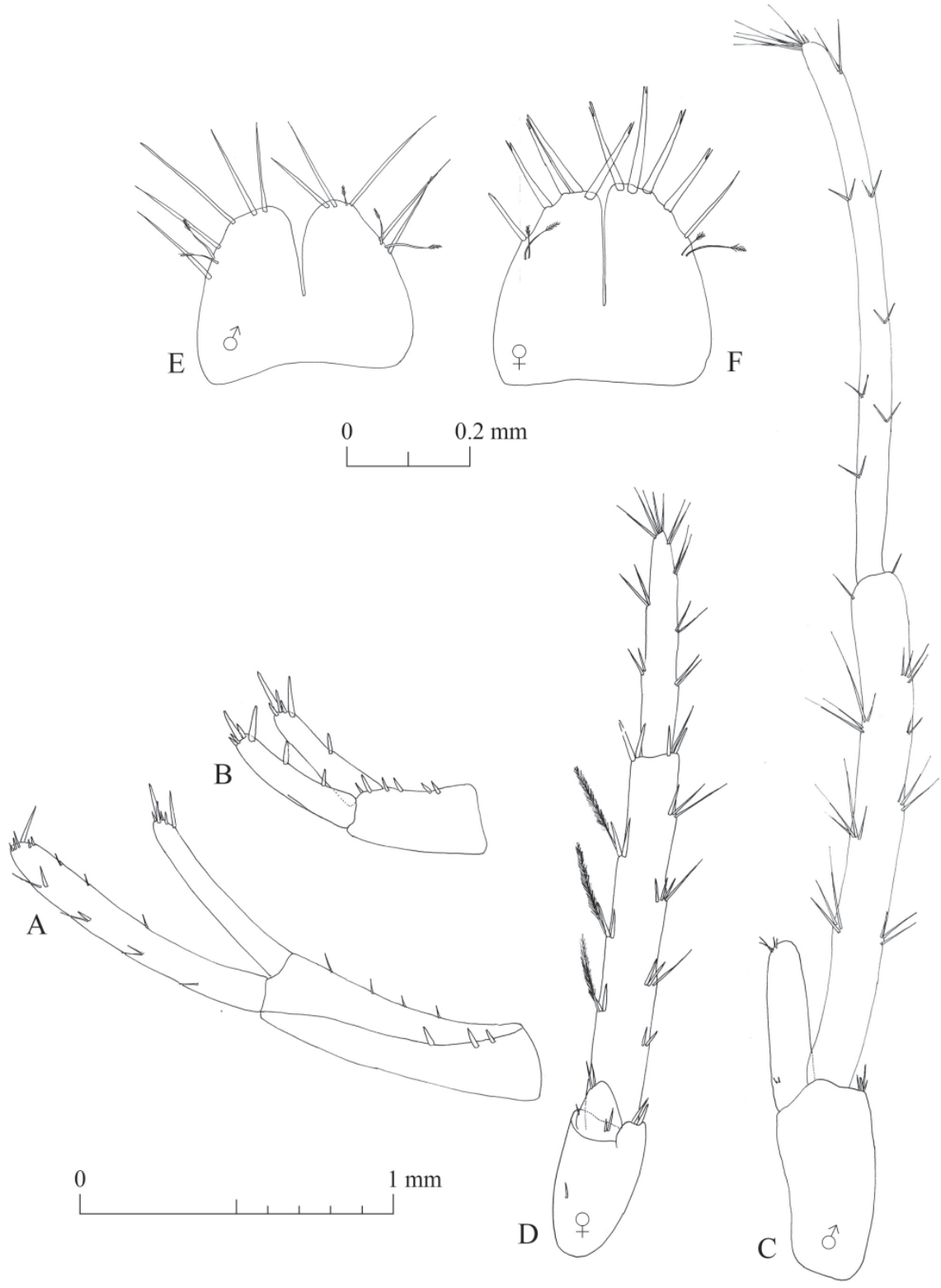

Fig. 28. *Niphargus normandiensis* Weber & Brad sp. nov., paratype, ♂ (ISER DW180526-36) and paratype, ♀ (ISER DW180526-31). **A**. Male uropod I. **B**. Male uropod II. **C**. Male uropod III. **D**. Female uropod III. **E**. Male telson. **F**. Female telson.

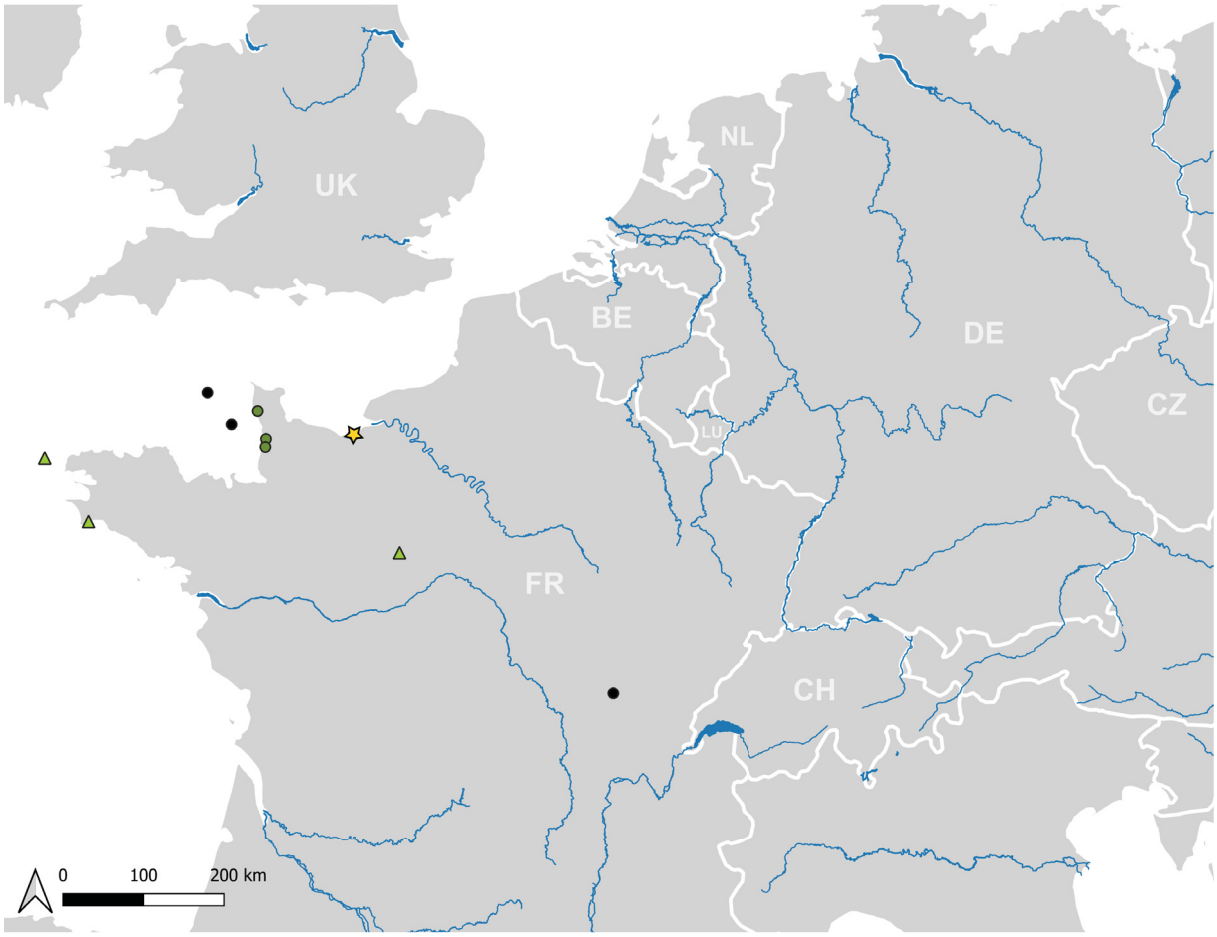

Fig. 29. Distribution of *Niphargus normandiensis* Weber & Brad sp. nov. confirmed by molecular data. Clade D is marked by green circles; clade N is marked by light-green triangles; a so far non-annotated clade is marked by black circles. The type locality at the Carrière souterrain de Saint-Vaast-en-Auge (France) is marked by a yellow star, overlaying one site record (clade D). Very large freshwater bodies are indicated; country codes follow the ISO 3166 standard alpha-2 format.

Niphargus wasgauensis Weber & Brad sp. nov.
urn:lsid:zoobank.org:act:E36BC687-B276-47E9-B685-24FC0718F3DA
Figs 30–38

Diagnosis

Medium-sized *Niphargus* species, poorly setose. Right postero-ventral angle of epimeral plates. 6 spines of maxilla I outer lobe with 1–3 teeth each; 1 spine with several smaller teeth. Mandibular palp with small number (1–2) of B setae. Gnathopods with 2 setae along outer margin of dactylopodite. Pereiopod VII, the longest leg, almost half of total body length. Pleopods retinaculum with 2–3 hooks. Uropod I, longer exopodite. Uropod II, longer endopodite. Uropod III sexually dimorphic, exopodite elongated in males. Telson with 5 apical spines on each lobe. The COI marker shows a single pure diagnostic site at position 586 (C). Two 28S rDNA alleles are diagnostic (with 1 heterozygous specimen) as well as 12 COI barcodes.

Etymology

The species name derives from the Wasgau uplands, which are formed by the Palatinate Forest (Germany) in the North and the Vosges Mountains (France) in the South. In Weber *et al*. (2023), this species was treated as *N. aquilex* I.

Material examined

Holotype

GERMANY • ♂; Rhineland-Palatinate, Sülzlochquelle 2 in the community of Godramstein; rheocrene spring; 49.2152° N, 8.0842° E; 1 Jan. 2017; Dieter Weber leg.; kept intact in 96% ethanol; 170101-25; MNHNL130578.

Paratypes

GERMANY • 1 ♂; same collection data as for holotype; 1 Jan. 2017; dissected and appendages drawn; 170101-22; ISER microscope slide DW170101-22 • 1 ♀; Rhineland-Palatinate, Breitenborntal-Brunnen 3 at Schweigen-Rechtenbach; 49.0643° N, 7.9406° E; 16 Jul. 2016; Dieter Weber leg.; dissected and appendages drawn; 160716-25; ISER microscope slide DW160716-25.

Molecular data

COI and 28S rDNA sequences of specimens belonging to *Niphargus wasgauensis* sp. nov. were deposited in GenBank. COI and 28S rRNA accession numbers are present in Supp. file 6 and Supp. file 9, respectively.

Description (male paratype ISER DW170101-22)

Measurements

Total body length is 6.22 mm (Fig. 30).

Head

Head (Fig. 30) 9.6% of total body length. Eyes and rostrum absent.

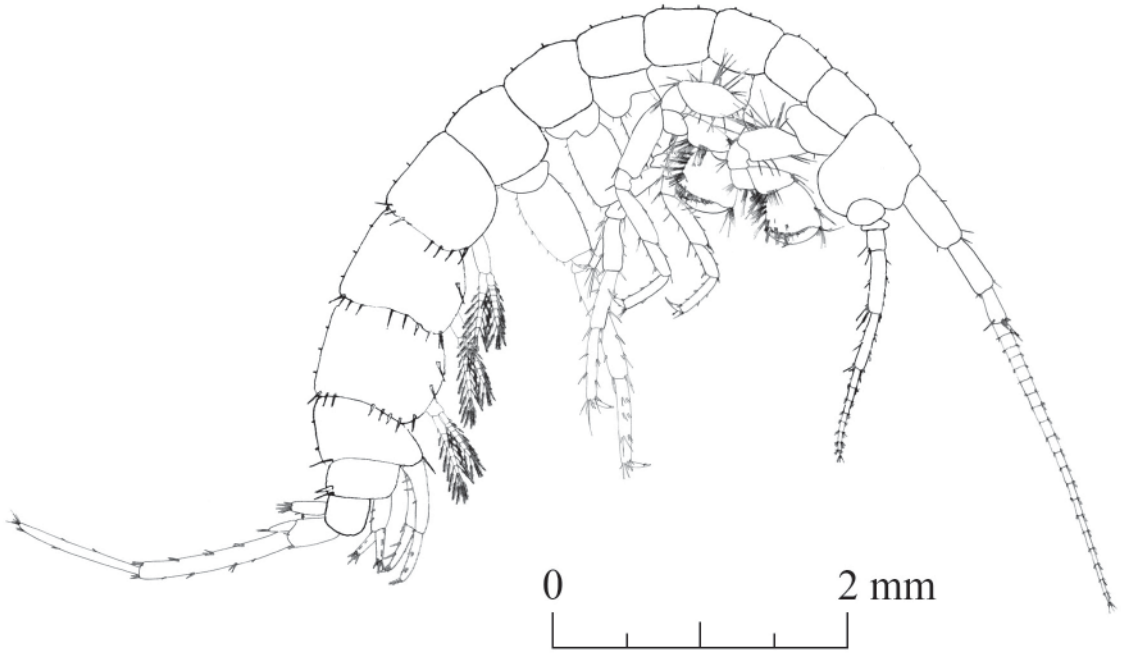

Fig. 30. *Niphargus wasgauensis* Weber & Brad sp. nov., paratype, ♂ (ISER DW170101-22); general appearance.

Antennae

Antenna I (Fig. 31A): with main flagellum formed of 20 articles, representing 52% of total body length. Peduncle length 36% of total length of antenna I. Accessory flagellum (Fig. 31B) biarticulated; proximal article shorter than first article of main flagellum; distal article 25% of total length of accessory flagellum,

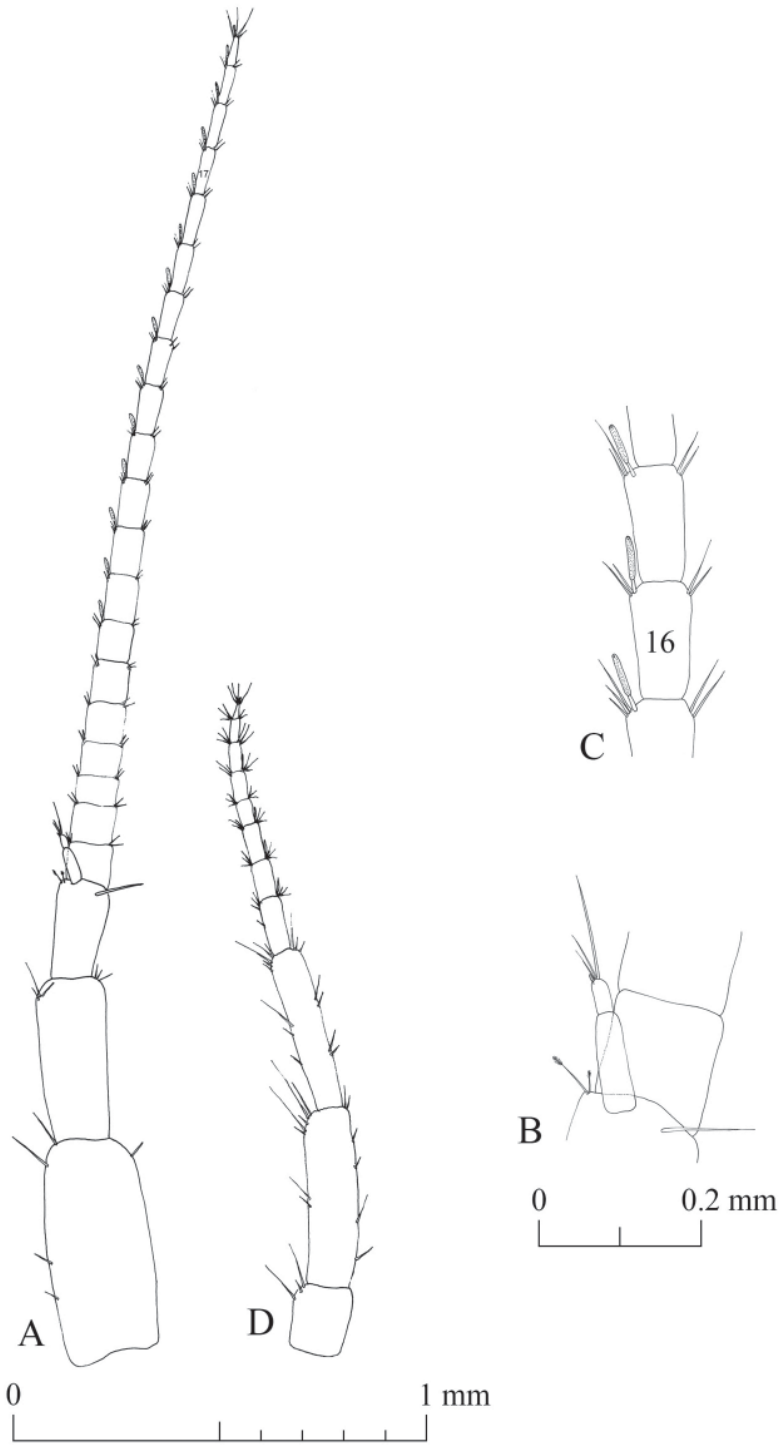

Fig. 31. *Niphargus wasgauensis* Weber & Brad sp. nov., paratype, ♂ (ISER DW170101-22). **A**. Antenna I. **B**. Antenna I, details of accessory flagellum. **C**. Antenna I, details of aesthetascs. **D**. Antenna II.

with 3 apical setae of different lengths and 1 aesthetasc. Aesthetascs half of respective main flagellum articles (Fig. 31C).

Antenna II (Fig. 31D): flagellum formed of 8 articles and representing 39% of total length of antenna II. Most flagellum articles bear 1 aesthetasc, half the length of respective flagellum articles.

Mouthparts

Labrum (Fig. 32A): typical, subovoid shape. Labium (Fig. 32B). Large inner lobes with 1 row of fine setae on inner sides. Outer lobes with 1 row of fine setae subapically on inner sides.

Maxilla I (Fig. 32C): with 4 apical setae on distal article of palp. Six spines of outer lobe with 1–4 teeth each and 1 spine with several small teeth. Inner lobe with 1 apical seta.

Maxilla II (Fig. 32D): with inner lobe slightly shorter than outer lobe. 1 apical and 1 subapical row of setae on each lobe. 1 row of fine setae on outer margin of outer lobe.

Left mandible (Fig. 32E): 4 teeth on incisor process. 4 teeth on lacinia mobilis. 4 serrate and 1 trifid seta between lacinia mobilis and molar process.

Right mandible (Fig. 32F): 4 teeth on incisor process. Several small denticles on lacinia mobilis. 4 serrate and 4 trifid setae between lacinia mobilis and molar process. Long seta at base of molar process.

Mandibular palps (Fig. 32E–F): highly similar and of same length. 3 articles account for 19% (article 1), 37% (article 2) and 44% (article 3) of total length of palp. Proximal article without setae, median article with 9–10 ventral setae. Distal article of palp with one group of 4 A setae, three groups with 1 B setae each, 9–13 D setae and 6 E setae.

Maxilliped (Fig. 33A): with palp formed of 4 articles. Article 1 with 2 setae on inner margin. Article 2 with 24 setae aligned along inner margin. Article 3 with 3 apical setae, one group of 5 dorsal setae and one group of 7 setae on inner margin. Article 4 with 1 seta located on outer margin and 2 setae at nail insertion. The outer lobe with 3 apical setae and 9 flattened setae on inner margin. Inner lobe provided apically with 7 setae and 1 flattened seta.

Gnathopods

Gnathopod I (Fig. 33B): coxal plate with irregular shape, with depth larger than width (ratio depth : width 1.0 : 0.64). Basis length : width ratio 1.0 : 0.44. Ischiopodite with one posteroventral group of 3 setae. Basis : carpus length ratio 1.0 : 0.6. Carpus with row of 11 setae of various lengths along ventral margin, group of 3 setae located anterodorsally and one group of 5 setae on carpus surface close to ventral margin. Propodite as long as wide, 4 groups of 1–4 setae on ventral margin, one anterodorsal group of 3 setae, one group of 7 anteroapical setae, 2 mesial setae on lateral surface, 2 setae on lateral surface close to ventral margin, and one group of 3 setae close to palmar corner. 1 strong palmar spine, 1 supporting spine and 2 denticulate spines present in palmar corner. Dactylopodite with claw 35% of total dactylopodite length and 2 setae along outer margin.

Gnathopod II (Fig. 33C): slightly larger than gnathopod I, with coxal plate in irregular shape (ratio width : depth 1.0 : 0.8). Ovoid gill and of same length as coxal plate width. Basis length : width ratio 1.0 : 0.35. Ischiopodite with one posteroventral group of 3 setae. Basis : carpus length ratio 1.0 : 0.51. Carpus with row of 11 setae of various lengths along ventral margin, group of 4 setae located anterodorsally and 1 row of 6 setae on carpus surface close to ventral margin. Propodite as long as wide, with 4 groups of 3–5 setae on ventral margin, one anterodorsal group of 5 setae, one anteroapical group of 7 setae, one group of 6 setae on lateral surface close to ventral margin, and one group of 3 long setae in vicinity of palmar corner. 1 strong palmar spine, 1 supporting spine and 2 denticulate spines present in palmar corner. Dactylopodite with claw 30% of total dactylopodite length and 2 setae along outer margin.

Pereopods

Pereopod III (Fig. 34A): coxal plate in shape of rectangular trapezoid, with width nearly equal to depth. Propodite : dactylus length ratio 1.0 : 0.43. Dactylus, with nail measuring half of total length of dactylus, 1 dorsal seta with plumose tip, and 1 seta at nail base. Pereopod III slightly longer than pereopod IV (pereopod III : pereopod IV length ratio 1.0 : 0.96).

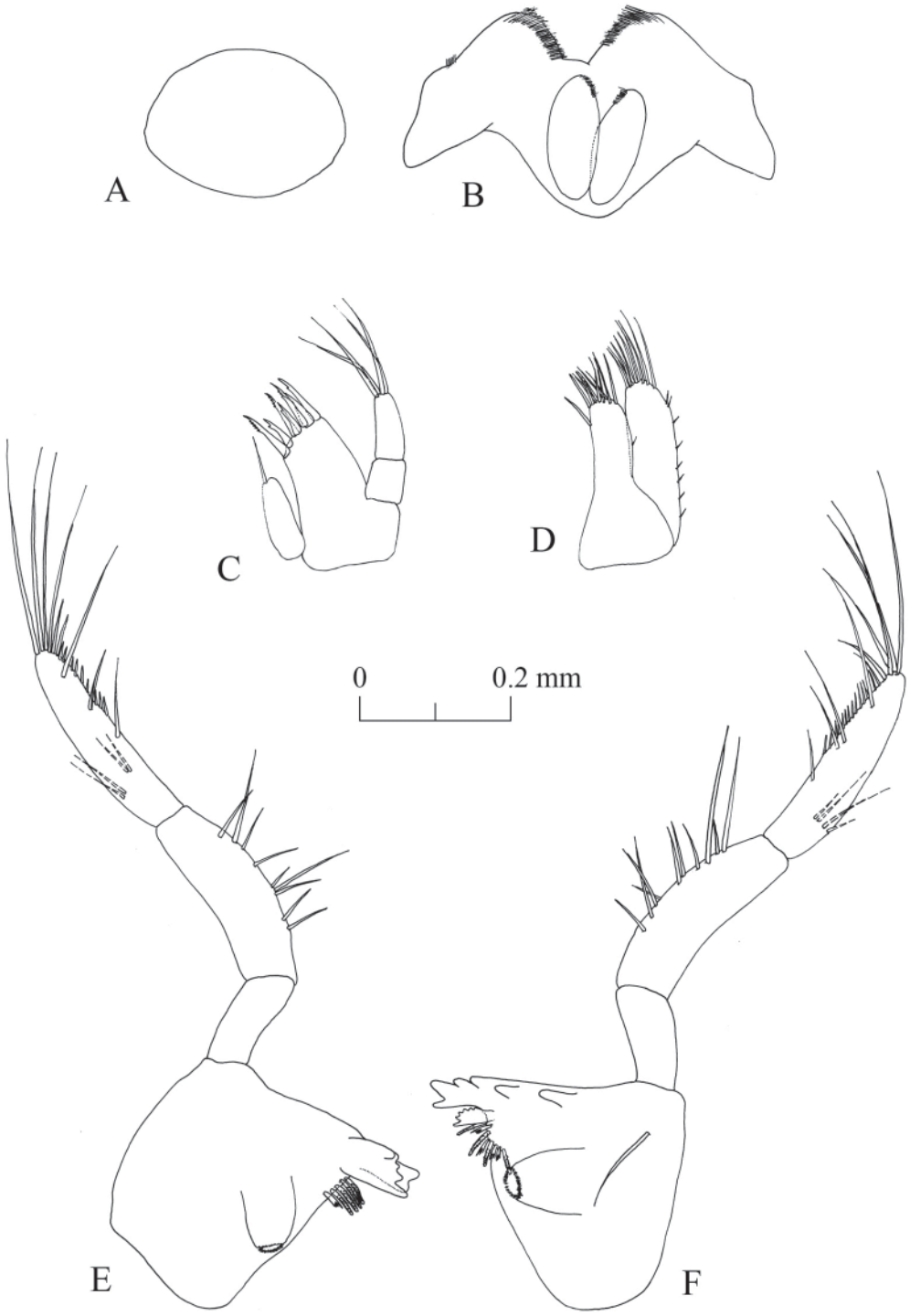

Fig. 32. *Niphargus wasgauensis* Weber & Brad sp. nov., paratype, ♂ (ISER DW170101-22). **A**. Labrum. **B**. Labium. **C**. Maxilla I. **D**. Maxilla II. **E**. Left mandible. **F**. Right mandible.

Pereopod IV (Fig. 34B): coxal plate in shape of rectangular, width : depth ratio 1.0 : 0.87. Propodite : dactylus length ratio 1.0 : 0.47. Robust dactylus, with nail measuring half of total length of dactylus; 1 dorsal seta with plumose tip and 1 seta at nail base.

Pereopod V (Fig. 35A): shortest leg (2.00 mm) of inspected male paratype. Coxal plate of irregular shape, with deep concavity on ventral side, 1 anterior and 4 posterior setae. Basis rectangular, length : width ratio

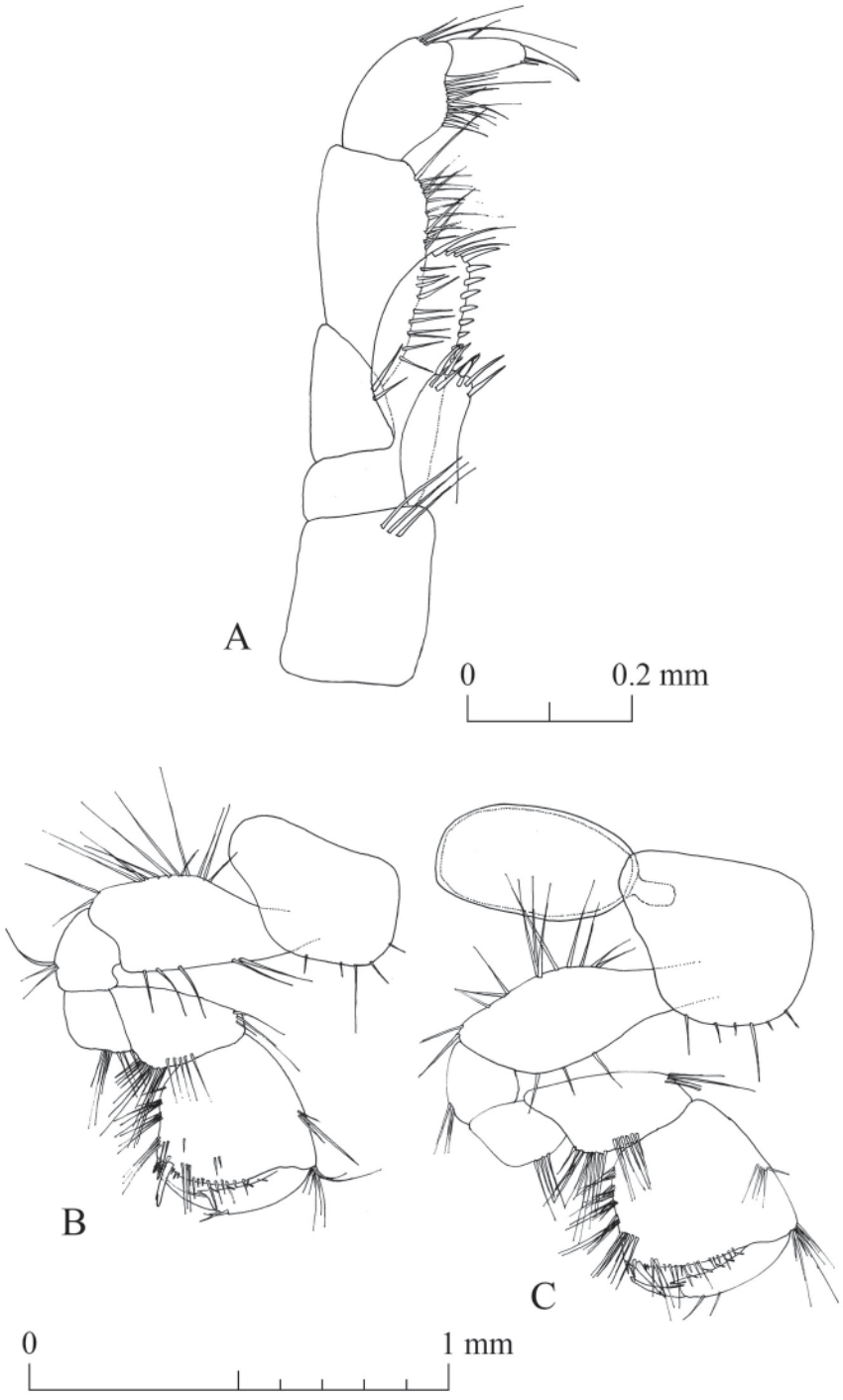

Fig. 33. *Niphargus wasgauensis* Weber & Brad sp. nov., paratype, ♂ (ISER DW170101-22). **A**. Maxilliped. **B**. Gnathopod I. **C**. Gnathopod II.

1.0 : 0.62, 4 setae on anterior margin, 7 setae on posterior margin, 2 anteroapical setae of different lengths. Dactylus with 1 dorsal seta with plumose tip, 2 setae of different lengths at nail base, which represents ⅓ of total dactylus length. Propodite length : dactylus length ratio 1.0 : 0.37.

Pereopod VI (Fig. 35B): coxal plate relatively similar to that of pereopod V, with 1 posterior seta. Basis rectangular, length : width ratio 1.0 : 0.58, 5 setae on anterior margin, 10 setae on posterior margin, 4 anteroapical setae of different lengths. Dactylus with 1 plumose seta on outer margin and 2 setae of different lengths near nail base. Nail 22% of total dactylus length. Propodite : dactylus length ratio 1.0 : 0.39.

Pereopod VII (Fig. 35C): longest leg (2.93 mm) of inspected paratype male. Coxal plate trapezoidal, with 1 seta on posterior margin. Basis rectangular, ratio length : width 1.0 : 0.6, 4 setae on anterior margin, 9 setae on posterior margin and 3 anteroapical setae of different lengths. Dactylus with 1 plumose seta on outer margin and 2 setae near nail base. Nail length 29% of total dactylus length. Ratio propodite : dactylus length 1.0 : 0.27.

Pereopods V : VI : VII ratio 1.0 : 1.40 : 1.47.

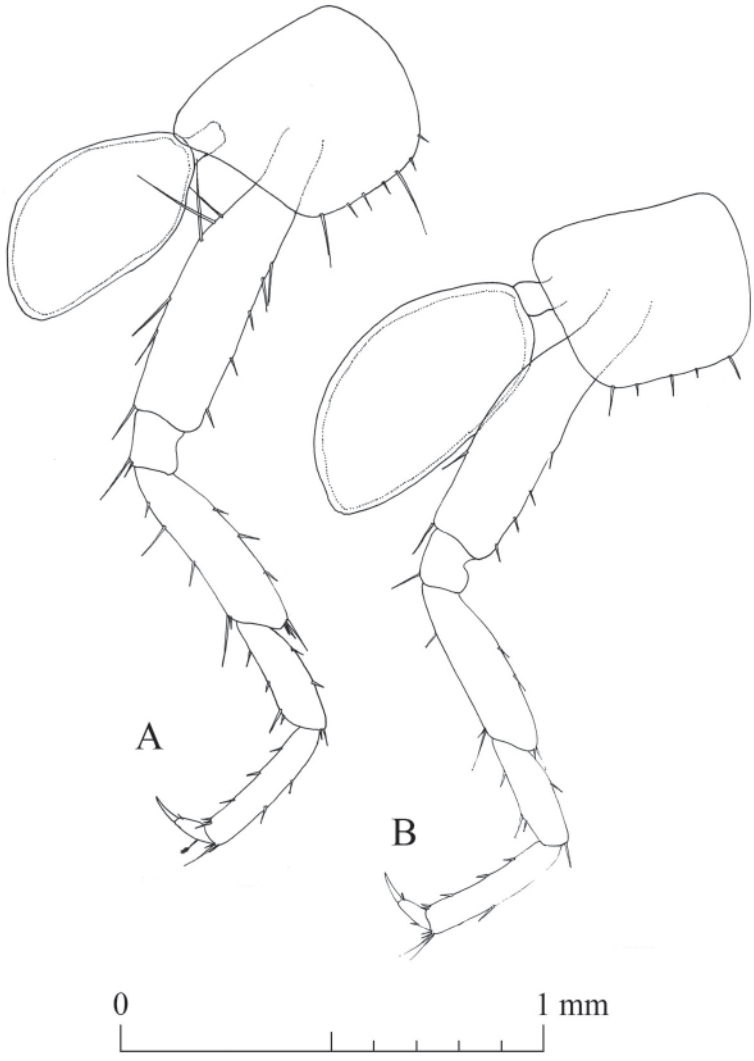

Fig. 34. *Niphargus wasgauensis* Weber & Brad sp. nov., paratype, ♂ (ISER DW170101-22). **A**. Pereopod III. **B**. Pereopod IV.

Pleopods

Pleopods I, II and III similar in shape (pleopod III, with 3 hooks on retinaculum, depicted in Fig. 36A), with unequal rami. Pleopods II and III with 2 hooks on retinaculum.

Epimeral plates (Fig. 36B)

Epimeral plate I with right postero-ventral angle, straight ventral margin, convex posterior margin with 4 setae. Epimeral plate II with right postero-ventral angle, convex ventral margin with 1 spine, convex posterior margin with 5 spines. Epimeral plate III with right posteroventral angle, convex ventral margin with 2 spines, convex posterior margin with 4 spines.

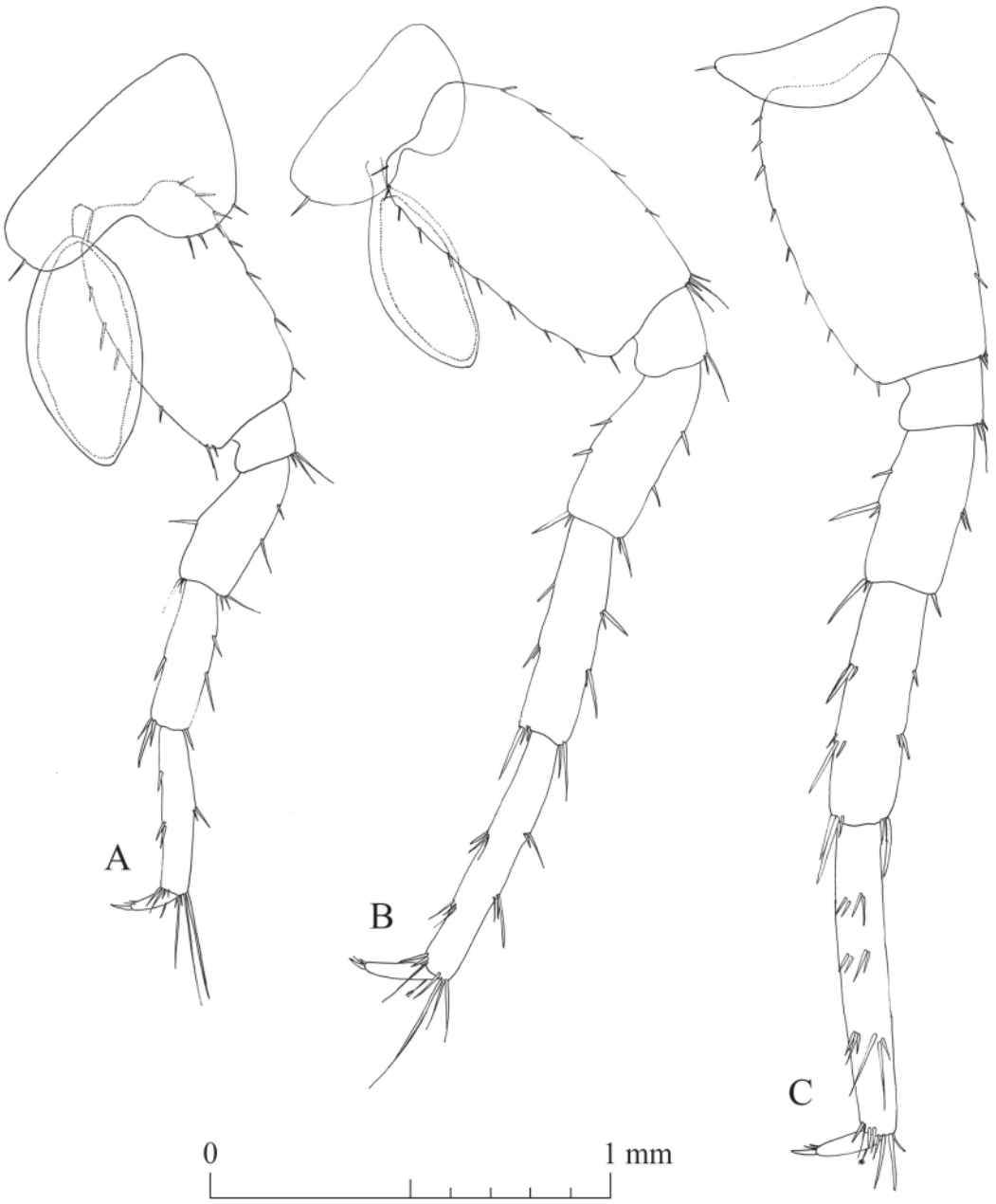

Fig. 35. *Niphargus wasgauensis* Weber & Brad sp. nov., paratype, ♂ (ISER DW170101-22). **A**. Pereopod V. **B**. Pereopod VI. **C**. Pereopod VII.

Uropods

Uropod I (Fig. 37A): with two dorsolateral rows of 2–4 spines on peduncle. Exopodite slightly longer than endopodite, exopodite : endopodite length ratio 1.0 : 0.91. 1 strong spine at base of uropod I.

Uropod II (Fig. 37B): with 3 dorsal and 3 apical spines on peduncle. Endopodite longer than exopodite, endopodite : exopodite length ratio 1.0 : 0.89, both rami provided with 2 dorsal and 5 apical spines of different lengths.

Uropod III (Fig. 37C): sexually differentiated, longer in males. Peduncle with 3 small apical setae. Short endopodite, 47% of length of peduncle, with 2 apical setae. Proximal segment of exopodite longer than distal segment (ratio 1.0 : 0.85). Anterior margin of proximal segment of exopodite with 3 groups of 2–3 setae; posterior margin of exopodite with 4 groups of 1–2 setae; 2 antero- and 2 postero-apical setae. Distal segment of exopodite with 2 setae on anterior margin, 1 seta on posterior margin, 2 subapical and 5 apical setae of different lengths.

Telson

Telson (Fig. 37E): wide (width : length ratio 1.0 : 0.9), with 5 long apical spines alongside small seta with plumose tip. Two thin setae with plumose tip on outer margin of 1 lobe. Longest spine 43% of telson length.

Sexual dimorphism

The examined male and female are highly similar. Besides the usual sexual dimorphism (e.g., slightly smaller gnathopods, presence of oostegites, and slightly deeper coxal plates I–VI in females), in *N. wasgauensis* sp. nov., the female uropod III is shorter than that of male (Fig. 37D). The telson of the

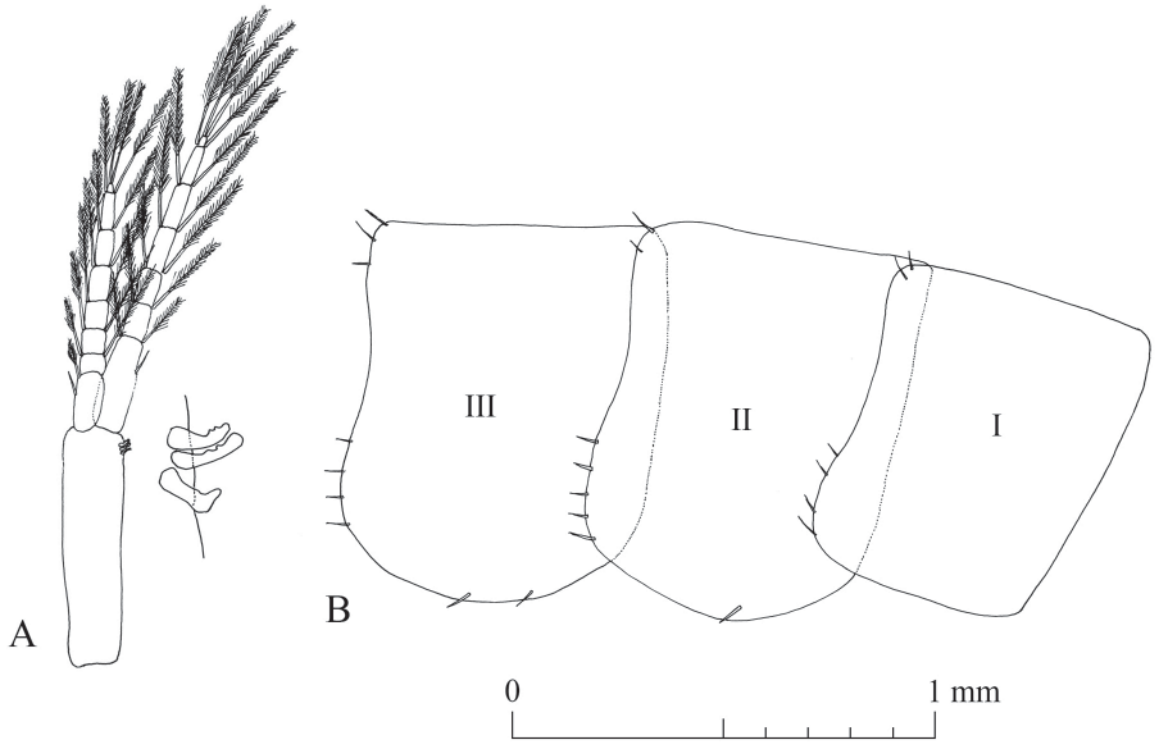

Fig. 36. *Niphargus wasgauensis* Weber & Brad sp. nov., paratype, ♂ (ISER DW170101-22). **A**. Pleopod III, detail of the retinaculum. **B**. Detail of the epimeral plates.

inspected female paratype (Fig. 37F) is smaller, with 6 spines on one lobe, and 2 fine setae with plumose tip on the outer margin of both lobes.

Type locality, ecology and distribution

The species shows a very narrow distribution limited to the Wasgau region, i.e., Franco-German uplands covering parts of the Federal State of Rhineland-Palatinate (Germany) and the Departments of Bas-Rhin and Moselle (both France) (Fig. 38). The type locality is the Sülzlochquelle 2 in the community of Godramstein (Rhineland-Palatinate, Germany) at 49.2152° N, 8.0842° E (Supp. file 3.7). It is a natural rheocrene spring with a permanent moderate flow, 21°GH hardness and 380 ppm TDS. No other species

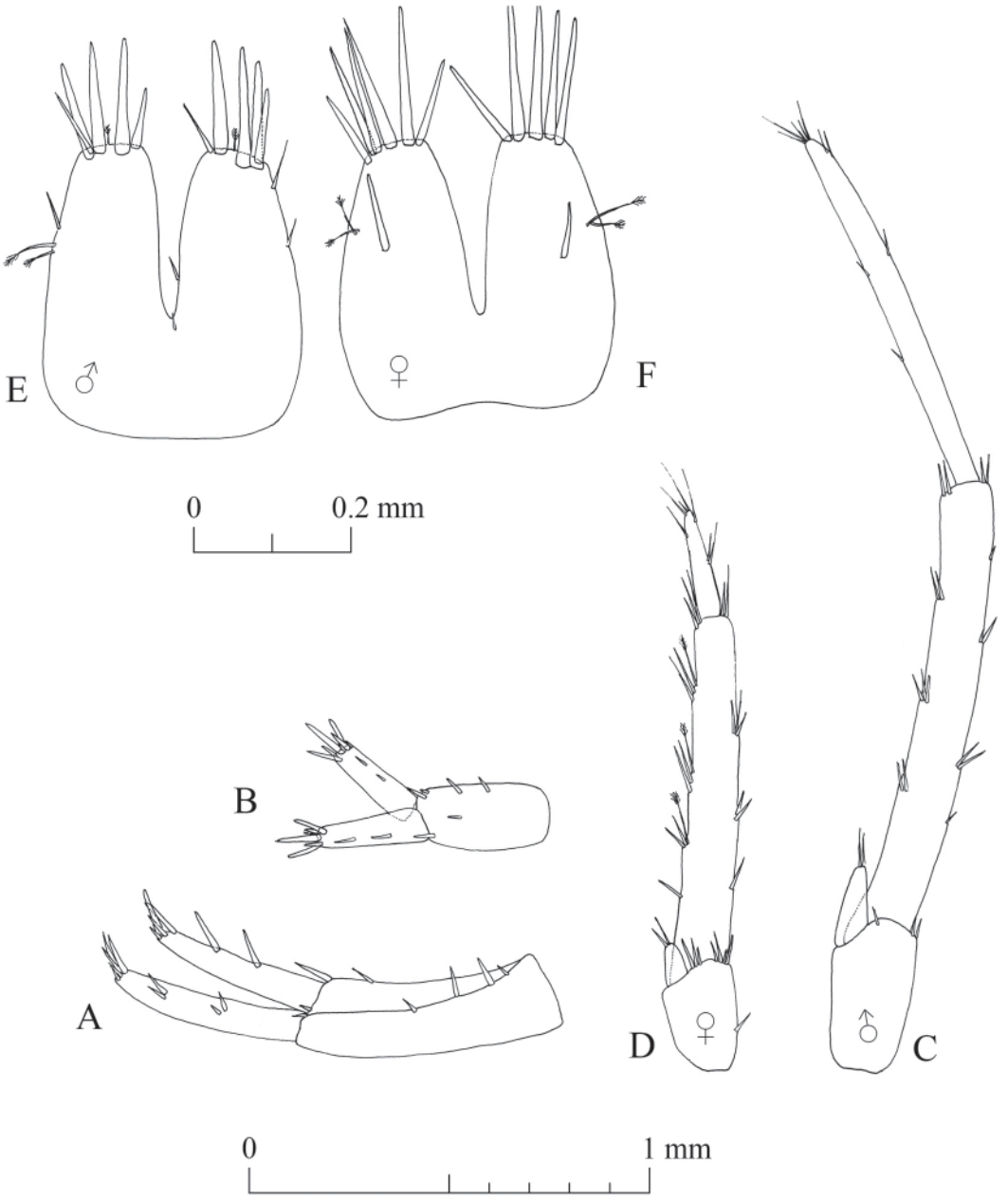

Fig. 37. *Niphargus wasgauensis* Weber & Brad sp. nov., paratype, ♂ (ISER DW170101-22) and paratype, ♀ (ISER DW160716-25). **A**. Male uropod I. **B**. Male uropod II. **C**. Male uropod III. **D**. Female uropod III. **E**. Male telson. **F**. Female telson.

of either *Niphargus* or gammarids (Amphipoda; Gammaridae) were found in this spring. Across its known distribution range, it was found in five springs, two abandoned mines and in one gallery of the Siegfried Line. The species seems to be absent in the interstitial environment. Previous published records from the Stollen am Sachsenstein (Germany), which referred to *N. aquilex aquilex* (Weber 1988, 1989), also belong to this species.

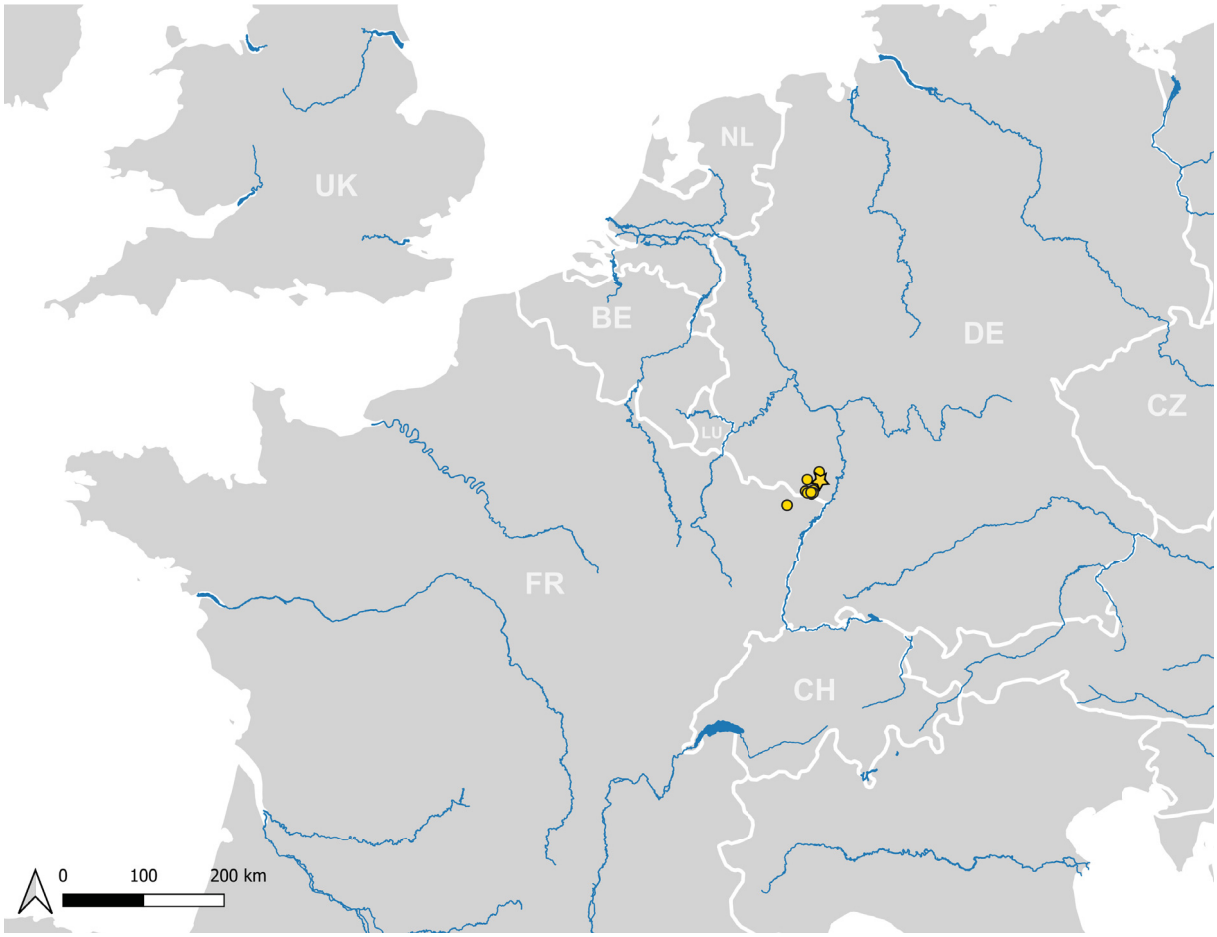

Fig. 38. Distribution of *Niphargus wasgauensis* Weber & Brad sp. nov. confirmed by molecular data. The type locality at Sülzlochquelle 2 (Germany) is marked by a yellow star, overlaying one site record. Very large freshwater bodies are indicated; country codes follow the ISO 3166 standard alpha-2 format.

Niphargus saraviensis Weber & Brad sp. nov.
urn:lsid:zoobank.org:act:C7E58FC7-564C-410B-ADBE-EE2AC9BA06AD
Figs 39–47

Diagnosis

Medium-sized *Niphargus* species, poorly setose. Right postero-ventral angle of epimeral plates. Six spines of maxilla I outer lobe with 1–2 teeth each; one spine with several smaller teeth. Mandibular palp with small number (1–2) of B setae. Gnathopods with 1 seta along outer margin of dactylopodite. Pereiopod VII, the longest leg, almost half of total body length. Pleopods retinaculum with 2 hooks. Uropod I, longer exopodite. Uropod II, longer endopodite. Uropod III sexually dimorphic, exopodite elongated in males. Telson with 4 apical spines on each lobe. The COI marker shows two single pure diagnostic sites at positions 94 (A) and 357 (A). Four 28S rDNA alleles are diagnostic (with 7 heterozygous specimens) as well as 23 COI barcodes.

Etymology

The species name derives from the German Federal State of Saarland, in which the type locality is located. In Weber *et al*. (2023), this species was treated as *N. aquilex* G.

Material examined

Holotype

GERMANY • ♂; Saarland, Zilla's Keller in Nunkirchen; 49.4826° N, 6.8317° E; 30 Dec. 2017; Dieter Weber leg.; kept intact in 96% ethanol; 171230-02; MNHNL130580.

Paratypes

GERMANY • 1 ♂; same collection data as for holotype; 30 Dec. 2017; dissected and appendages drawn; 171230-01; ISER microscope slide DW171230-01 • 1 ♀; same collection data as for preceding; dissected and appendages drawn; 171230-05; ISER microscope slide DW171230-05 • 1 ♂; same collection data as for holotype; 12 Mar. 2018; ISER DW180312-01 • 1 ♂; same collection data as for holotype; 12 Mar. 2018; ISER DW180312-06 • 1 ♀; same collection data as for holotype; 12 Mar. 2018; ISER DW180312-03 • 1 ♀; same collection data as for holotype; 30 Dec. 2017; ISER DW171230-07 • 1 ♂; same collection data as for holotype; 12 Mar. 2018; 180312-02; MNHNL130581 • 1 ♂; same collection data as for holotype; 12 Mar. 2018; 180312-04; MNHNL130582 • 1 ♀; same collection data as for holotype; 30 Dec. 2017; 171230-04; MNHNL130583 • 1 ♀; same collection data as for holotype; 30 Dec. 2017; 171230-06; MNHNL130584.

Molecular data

COI and 28S rDNA sequences of specimens belonging to *Niphargus saraviensis* sp. nov. were deposited in GenBank. COI and 28S rRNA accession numbers are present in Supp. file 6 and Supp. file 9, respectively.

Description (male paratype ISER DW171230-01)

The total body length is 7.91 mm (Fig. 39).

Head

Head (Fig. 39) 6.95% of total body length. Eyes and rostrum absent.

Antennae

Antenna I (Fig. 40A): with main flagellum formed of 18 articles, representing 50% of total body length. Peduncle length ⅓ of total length of antenna I. The accessory flagellum (Fig. 40B) biarticulated; proximal article almost twice as long as first article of main flagellum; distal article ¼ of total length of accessory

flagellum, with 2 apical setae of different lengths and one aesthetasc. Aesthetascs slightly more than half of respective flagellum articles (Fig. 40C).

Antenna II (Fig. 40D): flagellum formed of 6 articles and representing 40% of total length of antenna II. Most flagellum articles bear one short aesthetasc.

Mouthparts

Labrum (Fig. 41A): typical, subovoid shape. Labium (Fig. 41B). Relatively small inner lobes with 1 row of fine setae located subapically on inner sides. Outer lobes each with 1 row of fine setae on outer sides, 1 row of fine setae subapically on inner sides and 1 row of fine apical setae.

Maxilla I (Fig. 41C): with 4 apical setae on the distal article of palp. Six spines of outer lobe with 1–2 teeth each and one spine with several smaller teeth. Inner lobe with 1 apical seta.

Maxilla II (Fig. 41D): with inner lobe slightly shorter than outer lobe. 1 apical row of setae each lobe. Inner lobe with 2 subapical setae on inner margin. Outer lobe with 3 smaller setae on outer margin.

Left mandible (Fig. 41E): 5 teeth on incisor process. 3 teeth on lacinia mobilis. 6 serrated setae between lacinia mobilis and molar process.

Right mandible (Fig. 41F): 5 teeth on incisor process. 5 small teeth on lacinia mobilis. 4 serrated setae alternated with 4 trifid setae between lacinia mobilis and molar process. Long seta on molar process.

Mandibular palps (Fig. 41E–F): highly similar and of same length. 3 articles account for 21% (article 1), 37% (article 2) and 42% (article 3) of total length of palp. Proximal article with 1 apical seta. Median

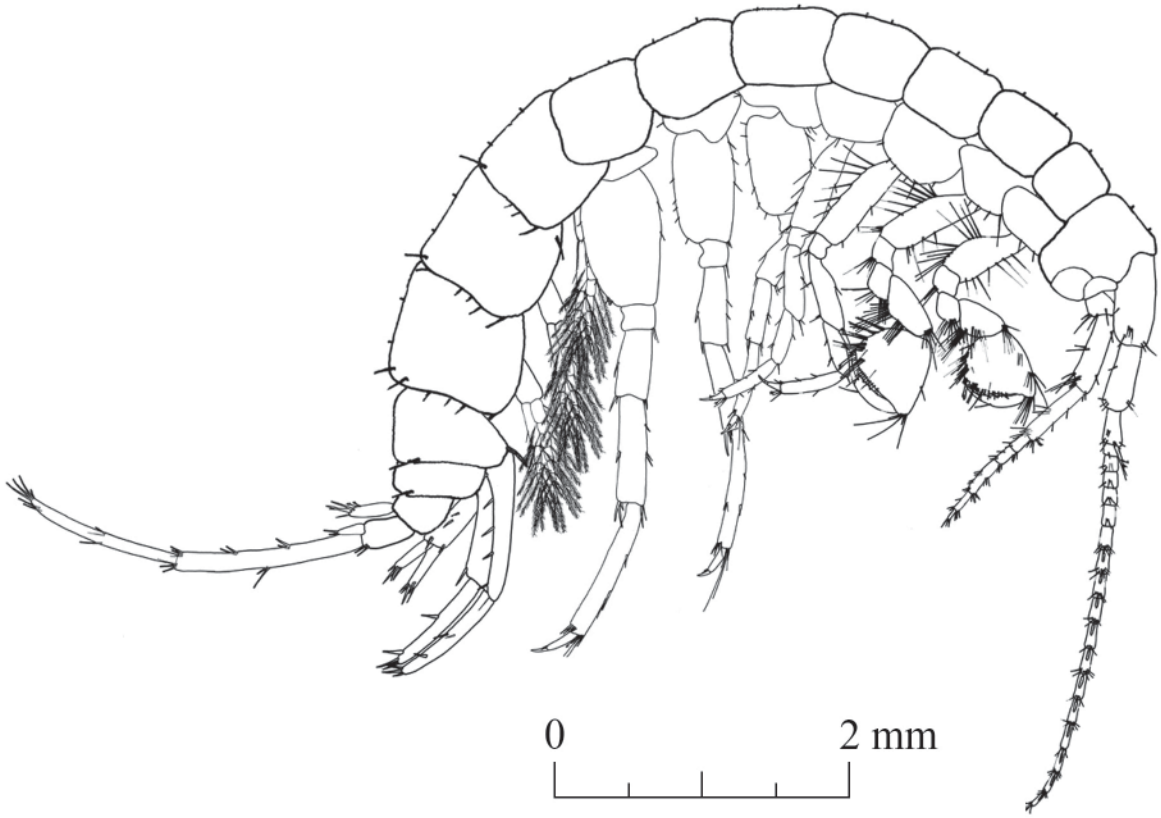

Fig. 39. *Niphargus saraviensis* Weber & Brad sp. nov., paratype, ♂ (ISER DW171230-01); general appearance.

article with 7 ventral setae. Distal article of palp with one group of 3 A setae, two groups with 1 B seta each, 23–24 D setae and 6–7 E setae.

Maxilliped (Fig. 42A): with palp formed of 4 articles. Article 1 asetose. Article 2 with 14 setae aligned along inner margin. Article 3 with 5 apical setae, one group of 4 dorsal setae and one group of 5 setae on inner margin. Article 4 with 1 seta located on outer margin and 2 setae at nail insertion. Outer lobe with 3 apical setae and 9 setae on inner margin, of which 7 flattened. Inner lobe provided apically with 1 flattened seta and 5 setae.

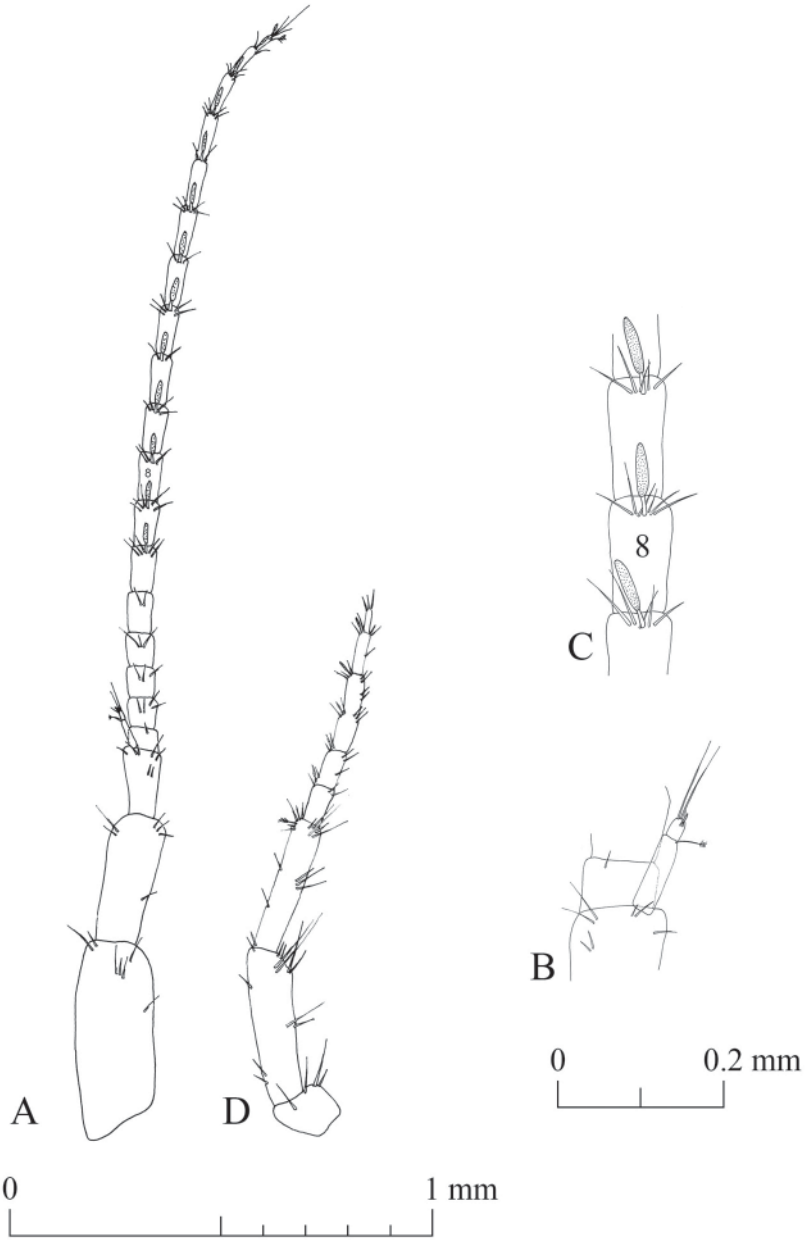

Fig. 40. *Niphargus saraviensis* Weber & Brad sp. nov., paratype, ♂ (ISER DW171230-01). **A**. Antenna I. **B**. Antenna I, details of accessory flagellum. **C**. Antenna I, details of aesthetascs. **D**. Antenna II.

Gnathopods

Gnathopod I (Fig. 42B): coxal plate in shape of rectangular trapezoid, with depth larger than width (ratio depth : width 1.0 : 0.62). Basis length : width ratio 1.0 : 0.40. Ischiopodite with one posteroventral group of 3 setae. Basis : carpus length ratio 1.0 : 0.56. Carpus with row of 6 setae along ventral margin, group of 5 setae located anterodorsally and two groups of 2–6 setae on carpus surface close to ventral margin. Propodite nearly as long as wide, 4 groups of 1–4 setae on ventral margin, one group of 3 setae on dorsal margin, one group of 5 anterodorsal setae, one group of 6 anteroapical setae, 1 mesial seta on lateral surface, 1 seta on lateral surface close to ventral margin and one group of 2 setae close to palmar corner.

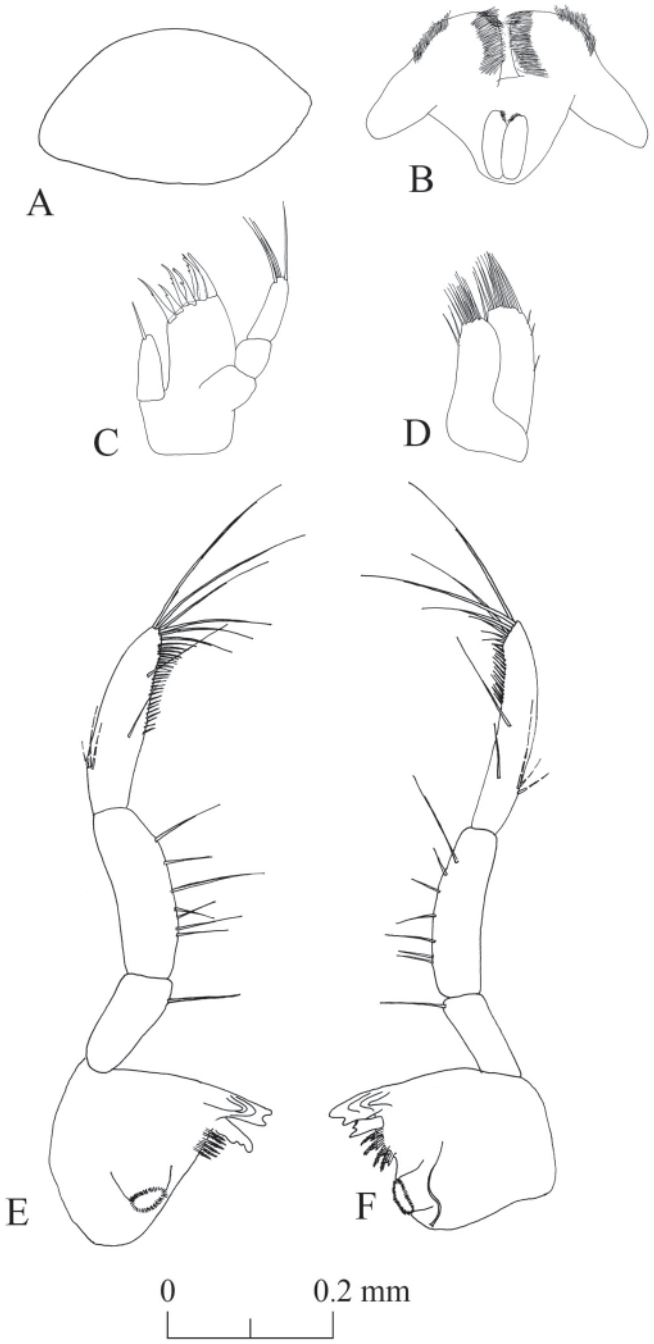

Fig. 41. *Niphargus saraviensis* Weber & Brad sp. nov., paratype, ♂ (ISER DW171230-01). **A**. Labrum. **B**. Labium. **C**. Maxilla I. **D**. Maxilla II. **E**. Left mandible. **F**. Right mandible.

One strong palmar spine, one supporting spine and two denticulate spines present in palmar corner. Dactylopodite with claw 33% of total dactylopodite length and 1 seta along outer margin.

Gnathopod II (Fig. 42C): slightly larger than gnathopod I, with coxal plate in shape of trapezoid; coxal plate slightly wider than long (ratio width : depth 1.0 : 0.80). Basis length : width ratio is 1.0 : 0.29. Ischiopodite with one posteroventral group of 4 setae. Basis : carpus length ratio 1.0 : 0.56. Carpus with

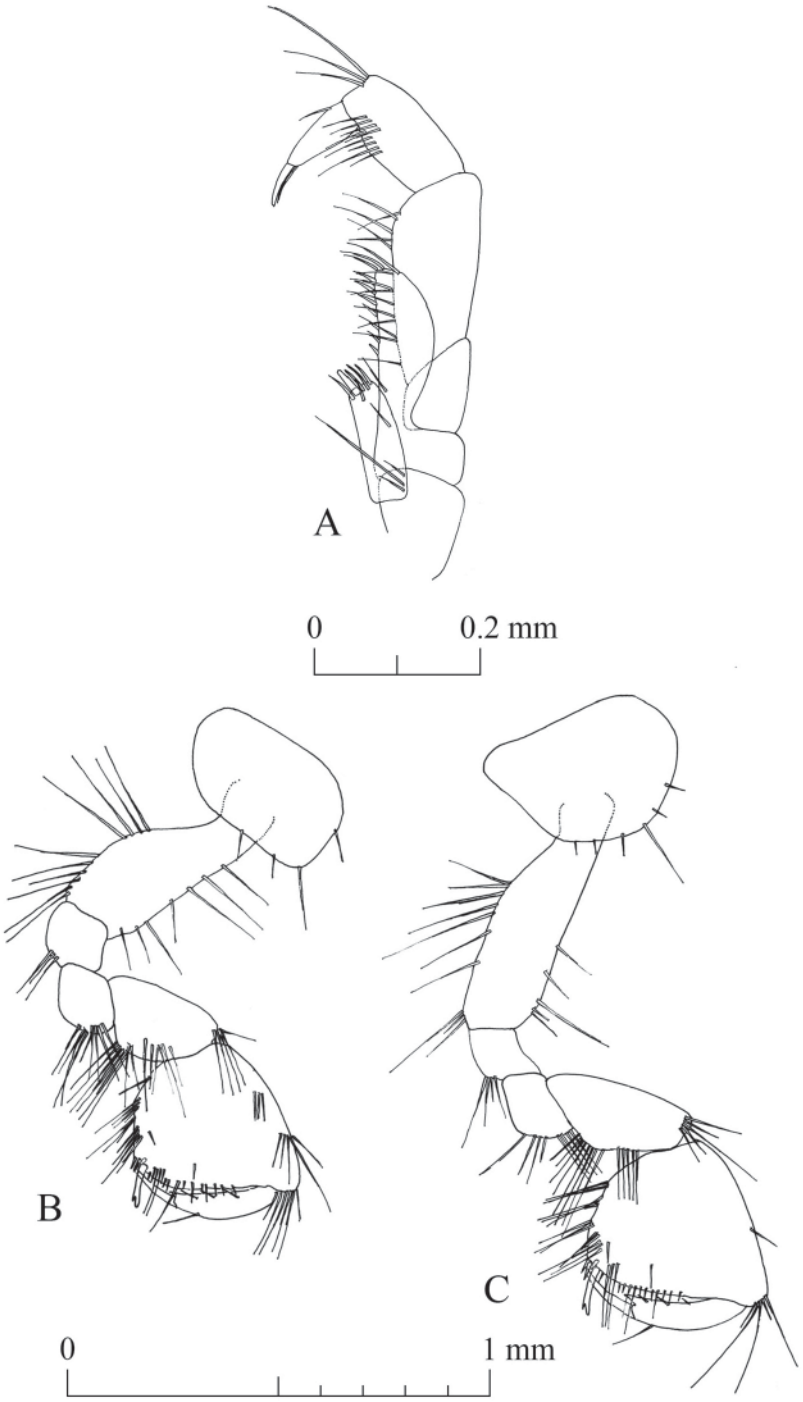

Fig. 42. *Niphargus saraviensis* Weber & Brad sp. nov., paratype, ♂ (ISER DW171230-01). **A**. Maxilliped. **B**. Gnathopod I. **C**. Gnathopod II.

row of 8 setae of various lengths along ventral margin, group of 5 setae located anterodorsally and one group of 5 setae on carpus surface close to ventral margin. Propodite almost as long as wide, 5 groups of 2–3 setae on ventral margin, 1 seta on dorsal margin, 1 seta on lateral surface close to ventral margin and 5 anteroapical setae of different lengths. 1 mesial seta on the lateral surface, 3 setae close to palmar corner. 1 strong palmar spine, 1 supporting spine and 2 denticulate spines present in palmar corner. Dactylopodite with claw 40% of total dactylopodite length and 1 seta along outer margin.

Pereopods

Pereopod III (Fig. 43A): coxal plate in shape of trapezoid, ratio width-depth 1.0 : 0.73. Propodite : dactylus length ratio 1.0 : 0.4. Dactylus with nail measuring half of total length of dactylus, 1 dorsal seta with plumose tip. Pereopod III equal slightly longer than pereopod IV (pereopod III : pereopod IV length ratio 1.0 : 0.95).

Pereopod IV (Fig. 43B): relatively rectangular coxal plate, width : depth ratio 1.0 : 0.75. Propodite : dactylus length ratio 1.0 : 0.41. Robust dactylus, with nail measuring half of total length of dactylus; 1 dorsal seta with plumose tip.

Pereopod V (Fig. 44A): coxal plate of irregular shape, with deep concavity on ventral side, 2 anterior setae and 1 posterior seta. Basis rectangular, length : width ratio 1.0 : 0.64, 6 setae on posterior margin, 3 setae on anterior margin, 2 anteroapical setae of different lengths. Dactylus with dorsal seta with plumose tip, 2 setae at nail base, which represents 44% of total dactylus length. Propodite length : dactylus length ratio 1.0 : 0.31.

Pereopod VI (Fig. 44B): coxal plate smaller than that of pereopod V, but similar in shape and 1 posterior seta. Basis rectangular, length : width ratio 1.0 : 0.55, 6 setae on posterior margin, 3 setae on anterior

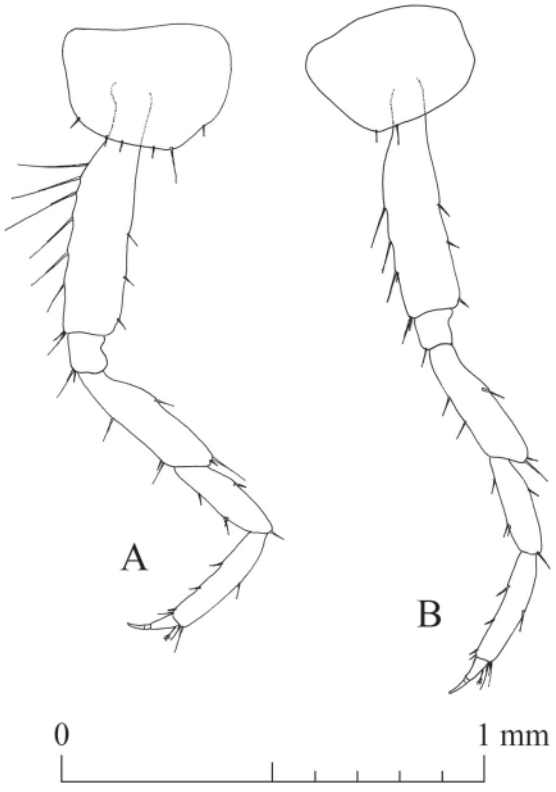

Fig. 43. *Niphargus saraviensis* Weber & Brad sp. nov., paratype, ♂ (ISER DW171230-01). **A**. Pereopod III. **B**. Pereopod IV.

margin and 2 anteroapical setae. Dactylus with 1 plumose seta on outer margin and 1 spine near nail base. Nail length ⅓ of te total dactylus length. Ratio propodite length : dactylus length 1.0 : 0.33.

Pereopod VII (Fig. 44C): longest leg (3.57 mm) of inspected paratype male. Coxal plate trapezoidal, with 1 posterior seta. Basis ovoid-trapezoidal, ratio length : width 1.0 : 0.6, 7 setae on posterior margin and 2 setae on anterior margin. Dactylus with 1 plumose seta on outer margin and 2 small setae near nail base. Nail length ⅓ of total dactylus length. Ratio propodite length : dactylus length 1.0 : 0.33.

Pereopods V : VI : VII ratio 1.0 : 1.38 : 1.57.

Pleopods

Pleopods. Similar (pleopod I depicted in Fig. 45A), with equal rami and 2 hooks on retinaculum.

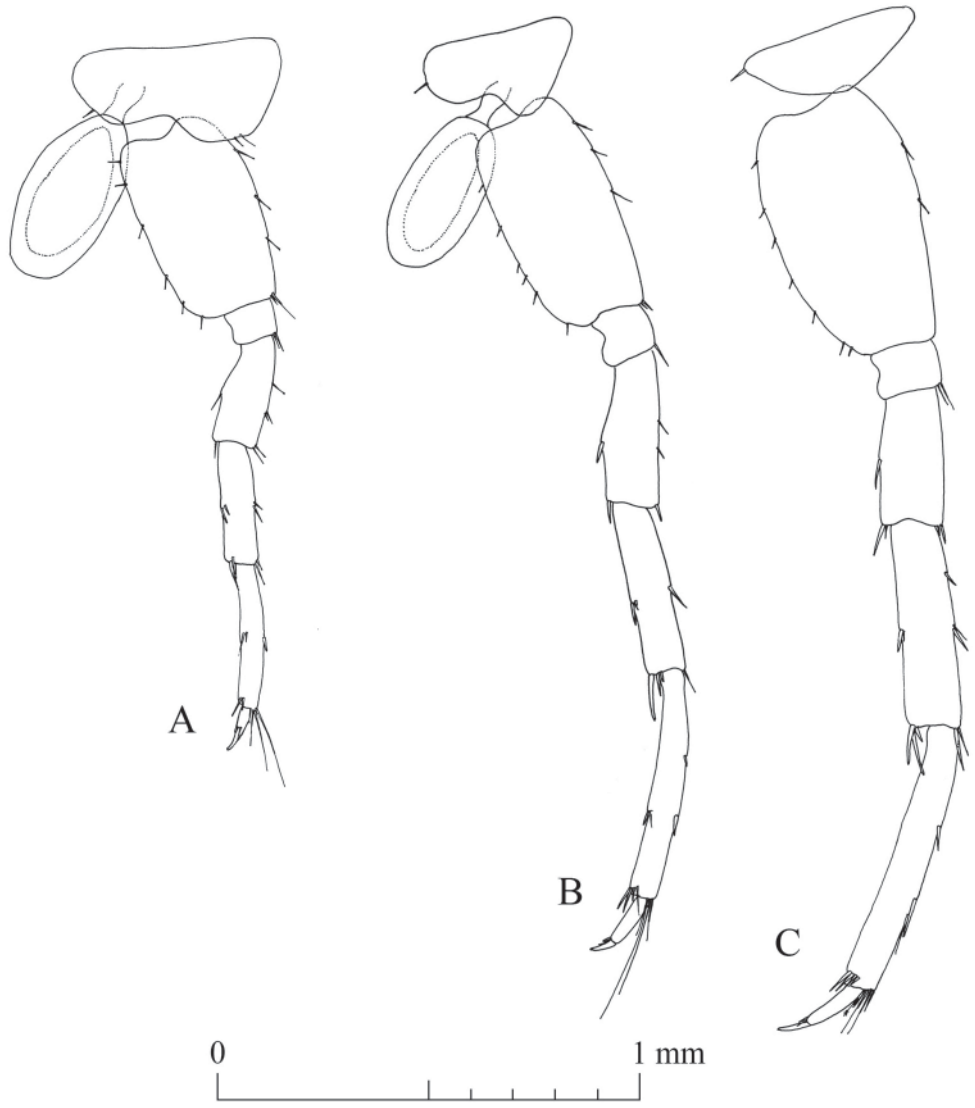

Fig. 44. *Niphargus saraviensis* Weber & Brad sp. nov., paratype, ♂ (ISER DW171230-01). **A**. Pereopod V. **B**. Pereopod VI. **C**. Pereopod VII.

Epimeral plates (Fig. 45B)
Epimeral plate I with right postero-ventral angle, straight ventral margin, relatively straight posterior margin with 2 postero-ventral setae. Epimeral plate II with right postero-ventral angle, relatively straight ventral margin with 1 antero-ventral spine, straight posterior margin with 4 setae. Epimeral plate III with right postero-ventral angle, relative convex ventral margin with 1 antero-ventral spine, straight posterior margin with 4 spines.

Uropods
Uropod I (Fig. 46A): with one dorso-lateral rows of 6 spines on peduncle. Exopodite slightly longer than endopodite (ratio 1.0 : 0.93). One strong spine at the base of the uropod I.

Uropod II (Fig. 46B): with 2 dorsal spine and 3 apical spines. Endopodite longer than exopodite, endopodite length : exopodite length ratio 1.0 : 0.83, both rami with 4–5 apical spines.

Uropod III (Fig. 46C): sexually differentiated, longer in males. Peduncle with 2 apical setae. Short endopodite about half length of peduncle, with 2 apical setae. Proximal segment of exopodite longer than distal segment (ratio 1.0 : 0.84). Anterior margin of proximal segment of exopodite with 2 groups of 2 setae; posterior margin of exopodite with one group of 2 setae; two groups of 3 apical setae. Distal segment of exopodite with one group of 2 setae on anterior margin, 2 groups of 1–2 setae on posterior margin and 4 apical setae of different lengths.

Telson
Telson (Fig. 46E): as wide as long, with 4 apical spines of different lengths on each lobe. Longest spine slightly longer than half of telson length. 2 thin setae of different lengths and plumose tip on 1 lobe, while other lobe provided with 1 such seta only.

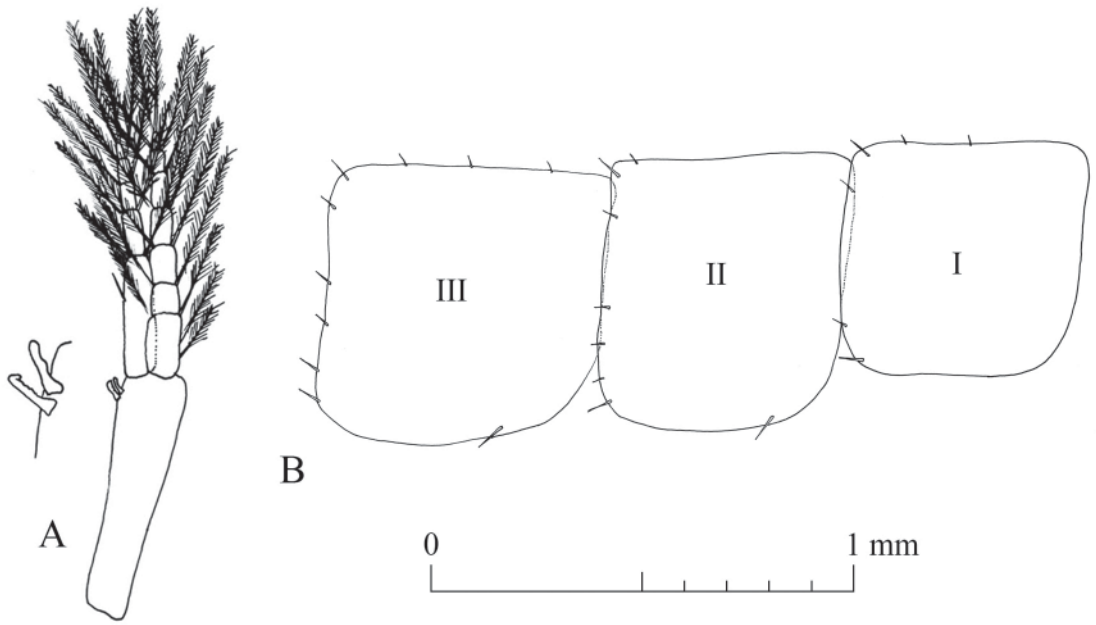

Fig. 45. *Niphargus saraviensis* Weber & Brad sp. nov., paratype, ♂ (ISER DW171230-01). **A**. Pleopod I, detail of the retinaculum. **B**. Detail of the epimeral plates.

Sexual dimorphism

The examined male and female are highly similar. Besides the usual sexual dimorphism (e.g., slightly smaller gnathopods, presence of oostegites, and slightly deeper coxal plates I–VI in females), in *N. saraviensis* sp. nov., the female uropod III (Fig. 46D) is shorter comparted to that of the male. The telson of the inspected female paratype (Fig. 46F) is with only 3 apical spines on 1 lobe and without the median plumose setae.

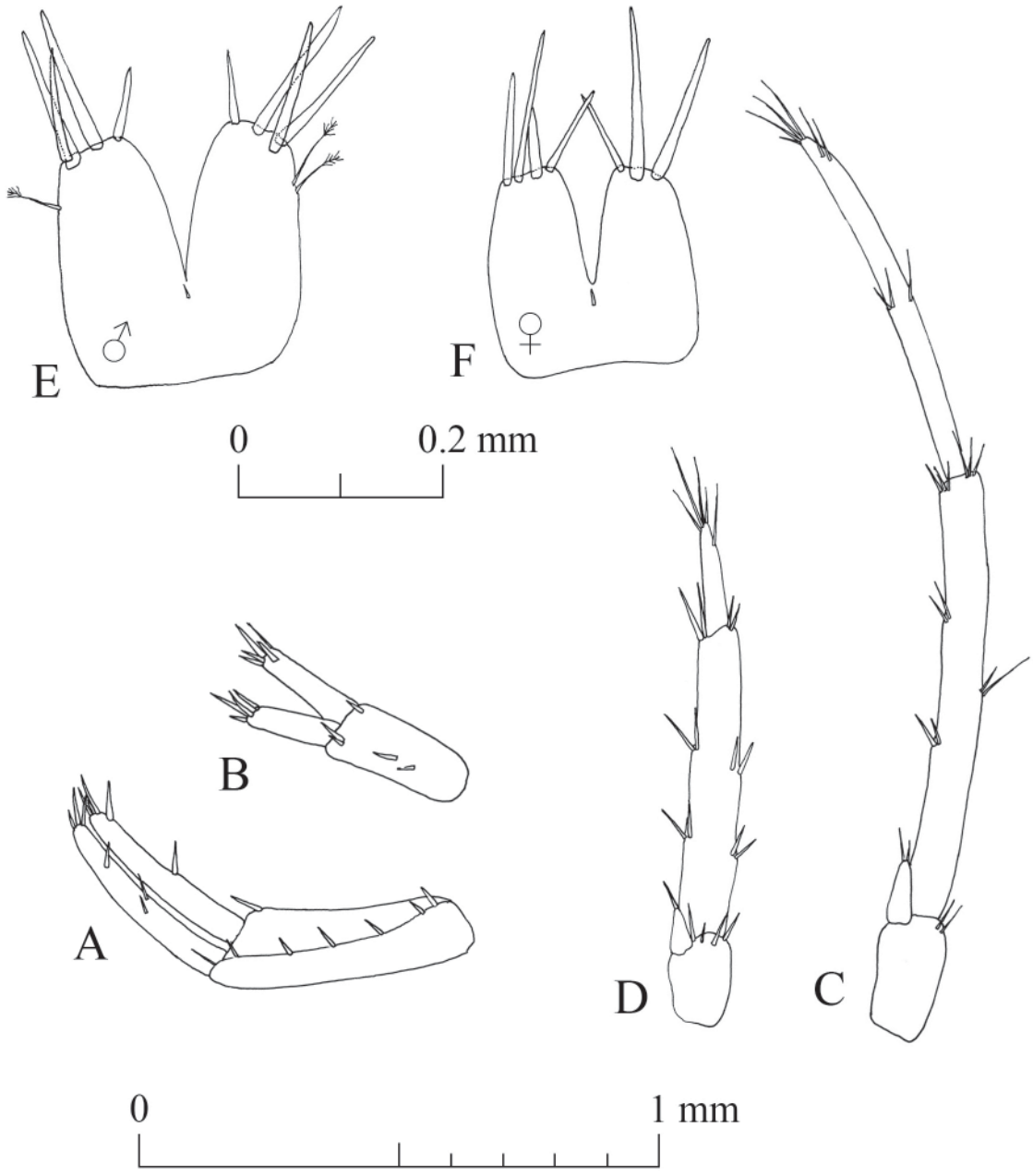

Fig. 46. *Niphargus saraviensis* Weber & Brad sp. nov., paratype, ♂ (ISER DW171230-01) and paratype, ♀ (ISER DW171230-05). **A**. Male uropod I. **B**. Male uropod II. **C**. Male uropod III. **D**. Female uropod III. **E**. Male telson. **F**. Female telson.

Type locality, ecology and distribution

The species distribution range is very large, with records originating from Central to Southern Germany, Luxembourg, the Czech Republic and Southern France (Fig. 47). The high frequency of records in Western and Southwestern Germany can most likely be attributed to a high sampling effort in those two regions. The type locality is Zilla's Keller in Nunkirchen (Saarland, Germany) at 49.4826° N, 6.8317° E, which is an old subterranean beer cellar dug in a Early–Middle Triassic sandstone formation (Supp. file 3.8). It is nowadays unused and locked. The cellar was bought by the Naturlandstiftung (Werno & Weber 2008) to keep it protected. Specimens were collected in a small spring (yield < 1l/min) at the end of this artificial cavern where it subsists on wood that it regularly renewed (Supp. file 3.9). In a water basin (capacity 100 l) 5 m from this spring, *N. saraviensis* sp. nov. was not detected. We confirm the permanent presence of this species at the type locality as it was found on 5 January 2013, 10 January 2015, 5 November 2017, 30 December 2017, and 9 October 2018. *Niphargus saraviensis* seems to be a subterranean-ubiquist (Supp. file 4.5). Previously published records from the Schillerhöhle (Germany), which referred to *N. aquilex aquilex* (Dobat 1968), also belong to this species.

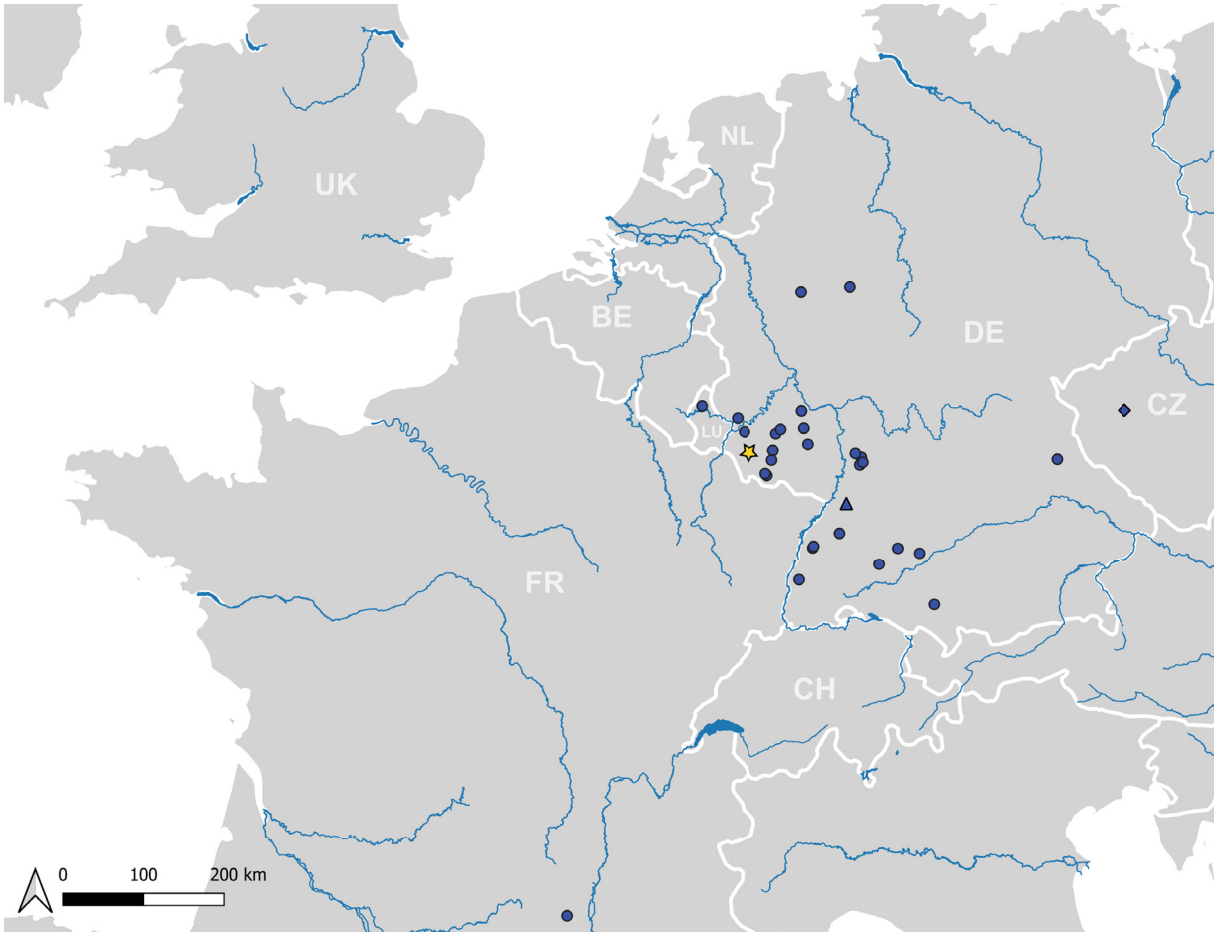

Fig. 47. Distribution of *Niphargus saraviensis* Weber & Brad sp. nov. confirmed by molecular data. The type locality at Zilla's Keller (Germany) is marked by a yellow star, overlaying one site record. The triangle and diamond refer to two clades which were delineated as distinct entities in subordinated ASAP partitions. Very large freshwater bodies are indicated; country codes follow the ISO 3166 standard alpha-2 format.

Niphargus lotharingiensis Weber & Brad sp. nov.
urn:lsid:zoobank.org:act:68DF3742-B5CA-4A8A-8B60-2410AD24708D
Figs 48–56

Diagnosis

Medium-sized *Niphargus* species, poorly setose. Right postero-ventral angle of epimeral plates. Six spines of maxilla I outer lobe with 1 tooth each; 1 spine with several smaller teeth. Mandibular palp with small number (1–2) of B setae. Gnathopods with 3 setae along outer margin of dactylopodite. Pereiopod VII, the longest leg, almost three quarters of total body length. Pleopods retinaculum with 3–4 hooks. Uropod I, longer exopodite. Uropod II, longer endopodite. Uropod III sexually dimorphic, exopodite elongated in males. Telson with 5 apical spines on each lobe. No pure diagnostic sites present in COI marker. A single 28S rDNA allele is diagnostic as well as 19 COI barcodes.

Etymology

The species name derives from the Latin name of Lorraine (Lotharingia), where the type locality is situated. In Weber *et al*. (2023), this species was treated as *N. schellenbergi* R, R*.

Material examined

Holotype

FRANCE • ♂; Tunnel du Col des Croix (connecting Vosges and Haute-Saône); 47.8632° N, 6.7464° E; 16 Apr. 2018; Dieter Weber leg.; kept intact in 96% ethanol; 180416-17; MNHNL130585.

Paratypes

FRANCE • 1 ♂; same collection data as for holotype; 3 Jul. 2016; dissected and appendages drawn; 160703-02; ISER microscope slide DW160703-02 • 1 ♀; same collection data as for preceding; dissected and appendages drawn; 160703-01; ISER microscope slide DW160703-01 • 1 ♂; same collection data as for holotype; 3 Jul. 2016; ISER DW160703-11 • 1 ♀; same collection data as for holotype; 3 Jul. 2016; ISER DW160703-07 • 1 ♀; same collection data as for holotype; 3 Jul. 2016; ISER DW160703-03 • 1 ♂; same collection data as for holotype; 3 Jul. 2016; 160703-09; MNHNL130586 • 1 ♀; same collection data as for holotype; 3 Jul. 2016; 160703-01; MNHNL130587.

Molecular data

COI and 28S rDNA sequences of specimens belonging to *Niphargus lotharingiensis* sp. nov. were deposited in GenBank. COI and 28S rRNA accession numbers are present in Supp. file 6 and Supp. file 9, respectively.

Description (male DW160703-02)

Measurements

Total body length is 7.80 mm (Fig. 48).

Head

Head (Fig. 48) 7.5% of total body length. Eyes and rostrum absent.

Antennae

Antenna I (Fig. 49A): with main flagellum formed of 16 articles, representing 60% of total body length. Peduncle length in 43% of total length of antenna I. Accessory flagellum (Fig. 49B) biarticulated; proximal article slightly longer than first article of main flagellum; distal article 15% of total length of accessory flagellum, with 2 apical setae of different lengths and one aesthetasc. Aesthetascs ¼ of respective main flagellum articles (Fig. 49C).

Antenna II (Fig. 49D): flagellum formed of 10 articles and representing 60% of total length of antenna II. Most flagellum articles bear one aesthetasc, half the length of respective flagellum articles.

Mouthparts

Labrum (Fig. 50A): typical, subovoid shape, with 2 rows of fine setae located, 1 apical and 1 subapical. Labium (Fig. 50B). Large inner lobes with 1 row of fine setae on inner sides. Outer lobes with 1 row of fine setae subapically on inner sides.

Maxilla I (Fig. 50C): with 4 apical setae on distal article of palp. 6 spines of outer lobe with 1 tooth each and 1 spine with several small teeth. Inner lobe with 1 apical seta and several smaller, subapical setae.

Maxilla II (Fig. 50D): with inner lobe slightly shorter than outer lobe. 1 apical row of setae and 1 subapical seta on outer lobe. Row of small setae on outer margin of outer lobe.

Left mandible (Fig. 50E): 4 teeth on incisor process. 3 teeth on lacinia mobilis. 14 serrated setae, and 6 setae, between lacinia mobilis and molar process.

Right mandible (Fig. 50F): 4 teeth on incisor process. 6 teeth on lacinia mobilis. 9 serrated setae between lacinia mobilis and molar process. Long seta on molar process.

Mandibular palps (Fig. 50E–F): highly similar and of same length. 3 articles account for 21% (article 1), 38% (article 2) and 41% (article 3) of total length of palp. Proximal article without setae, median article

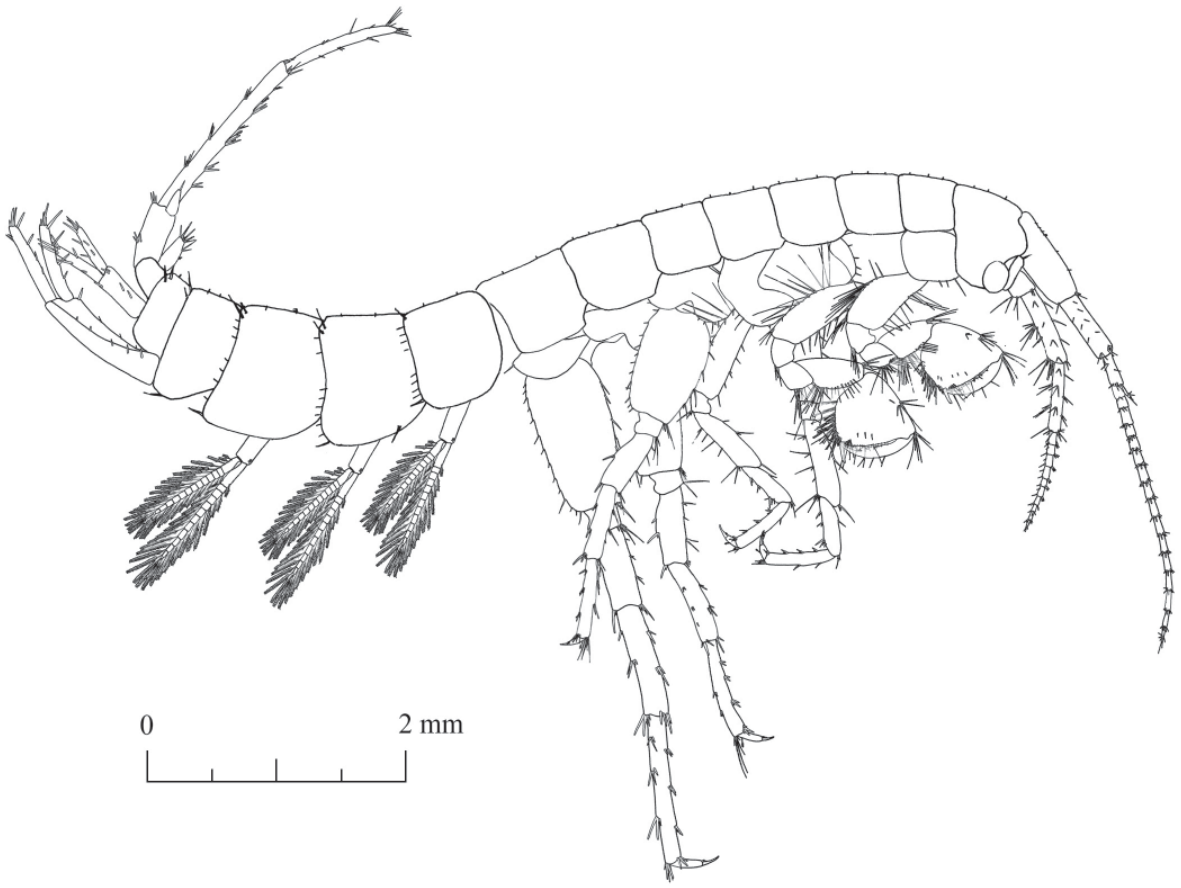

Fig. 48. *Niphargus lotharingiensis* Weber & Brad sp. nov., paratype, ♂ (ISER DW160703-02); general appearance.

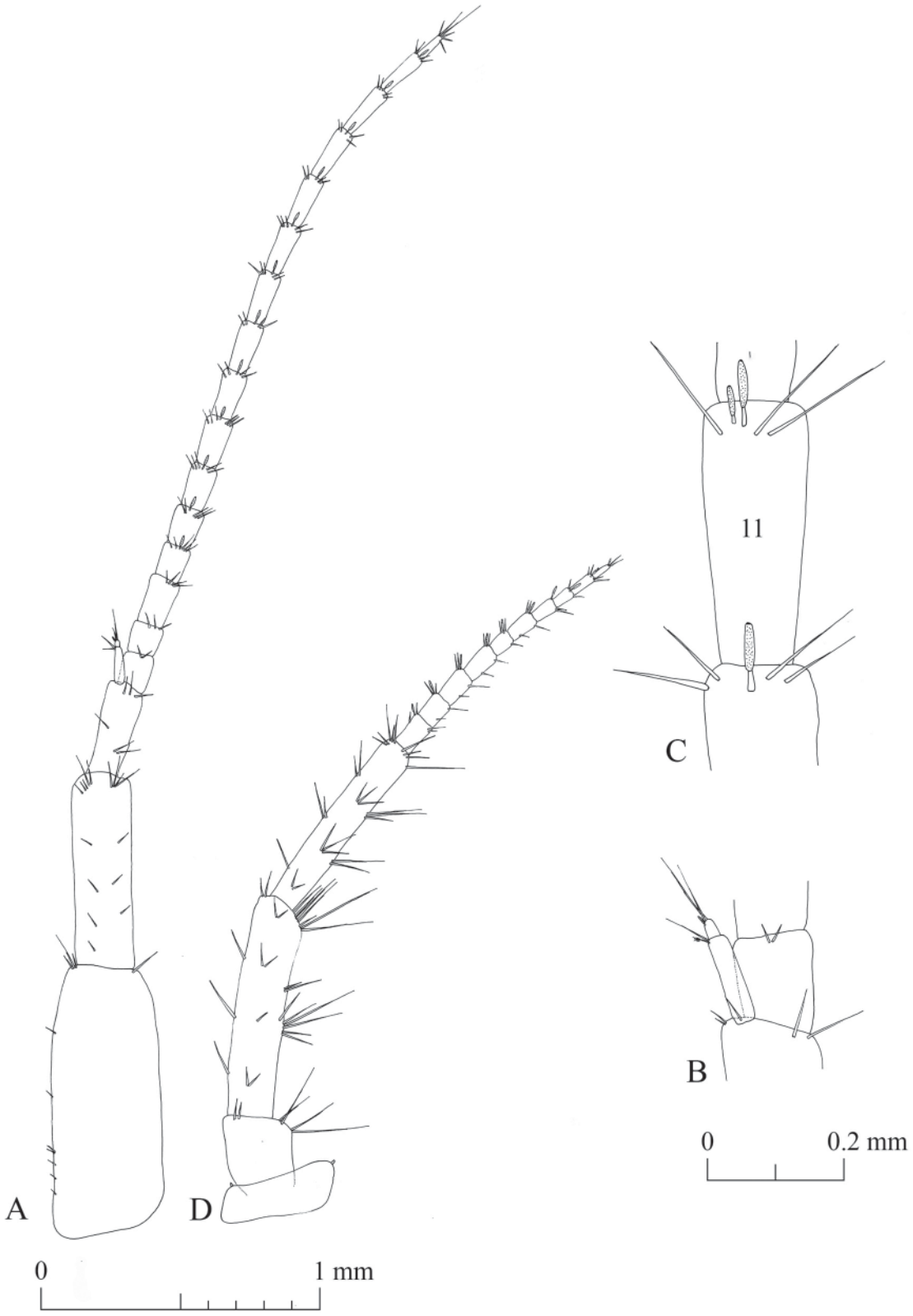

Fig. 49. *Niphargus lotharingiensis* Weber & Brad sp. nov., paratype, ♂ (ISER DW160703-02). **A**. Antenna I. **B**. Antenna I, details of accessory flagellum. **C**. Antenna I, details of aesthetascs. **D**. Antenna II.

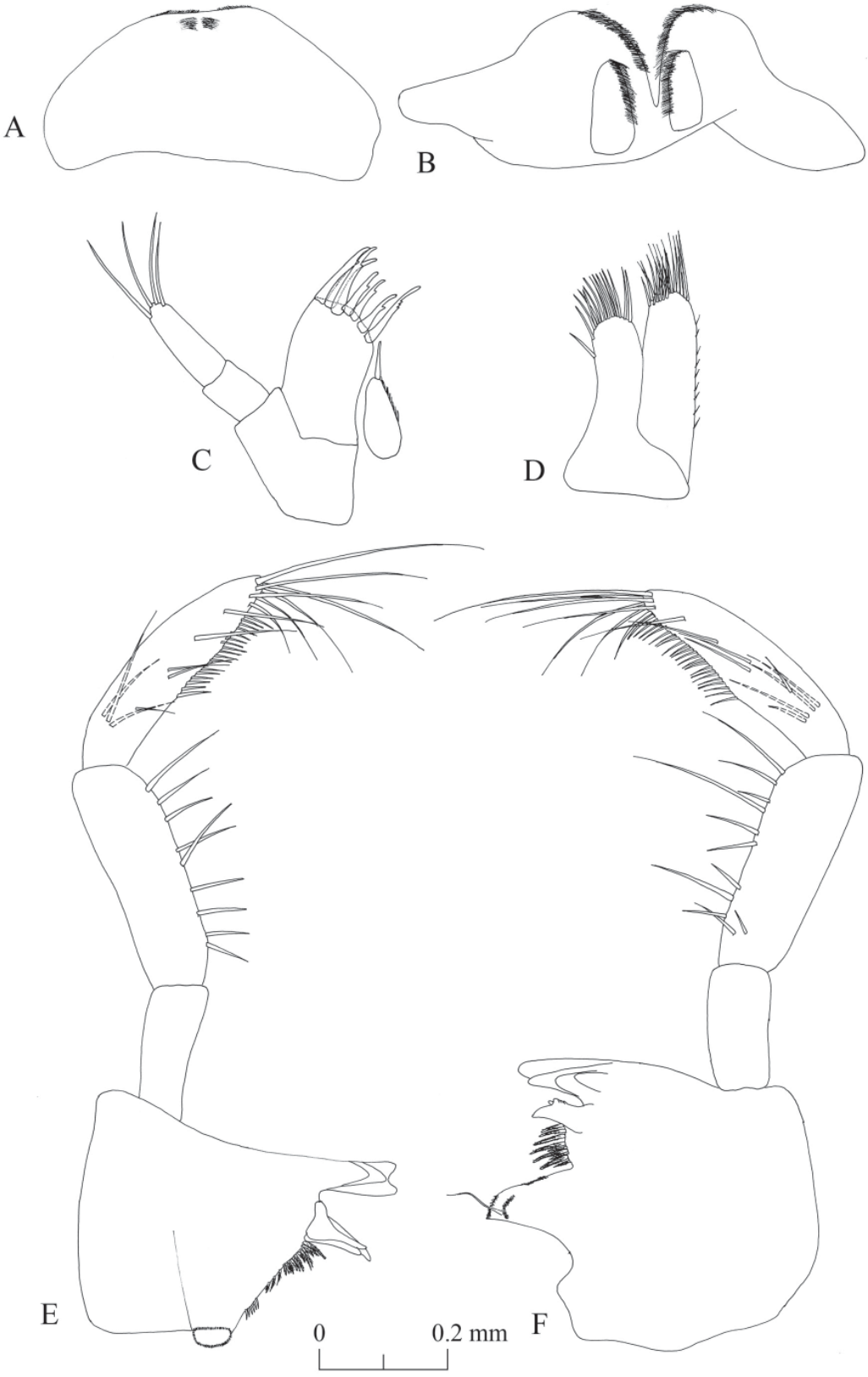

Fig. 50. *Niphargus lotharingiensis* Weber & Brad sp. nov., paratype, ♂ (ISER DW160703-02). **A**. Labrum. **B**. Labium. **C**. Maxilla I. **D**. Maxilla II. **E**. Left mandible. **F**. Right mandible.

with 9–11 ventral setae. Distal article of palp with one group of 4A setae, 4 groups with 1–2 B setae, 17–22 D setae and 7 E setae.

Maxilliped (Fig. 51A): with palp formed of 4 articles. Article 1 asetose. Article 2 with 31 setae aligned along inner margin. Article 3 with 6 apical setae, one group of 6 dorsal setae and one group of 9 setae on inner margin. Article 4 with 1 seta located on outer margin and 2 setae at nail insertion. Outer lobe with 4 apical setae and 15 flattened setae on inner margin. Inner lobe provided apically with 3 setae, 1 flattened seta and 2 plumose setae.

Gnathopods

Gnathopod I (Fig. 51B): coxal plate in shape of rectangular, with depth larger than width (ratio depth : width 1.0 : 0.8). Basis length : width ratio 1.0 : 0.41. Ischiopodite with one posteroventral group of 5 setae. Basis : carpus length ratio 1.0 : 0.56. Carpus with row of 14 setae of various lengths along ventral margin, group of 7 setae located anterodorsally and one group of 5 setae on carpus surface close to ventral margin. Propodite nearly as long as wide, seven groups of 2–5 setae on ventral margin, one group of 6 setae on dorsal margin, one group of 3 setae on propodite surface close to dorsal margin, one group of 5 anteroapical setae, 3 mesial setae on lateral surface, 2 setae on lateral surface close to ventral margin and one group of 4 setae close to palmar corner. One strong palmar spine, one supporting spine and two denticulate spines present in palmar corner. Dactylopodite with claw 26% of total dactylopodite length and 3 setae along outer margin.

Gnathopod II (Fig. 51C): slightly larger than gnathopod I, with coxal plate in th shape of rectangular trapezoid; coxal plate width equal to its depth (ratio width : depth 1.0 : 1.0). Ovoid gill and of same length as basis. Basis length : width ratio 1.0 : 0.27. Ischiopodite with one posteroventral group of 3 setae. Basis : carpus length ratio 1.0 : 0.54. Carpus with row of 12 setae of various lengths along ventral margin, group of 4 setae located anterodorsally and 1 row of 10 setae on carpus surface close to ventral margin. Propodite as long as wide, with 8 groups of 1–5 setae on ventral margin, 5 setae on dorsal margin, 3 mesial setae on lateral surface, 1 seta on lateral surface close to dorsal margin, 6 anteroapical setae and 4 setae close to palmar corner. 1 strong palmar spine, 1 supporting spine and 2 denticulate spines present in palmar corner. Dactylopodite with claw 33% of total dactylopodite length and 3 setae along outer margin.

Pereopods

Pereopod III (Fig. 52A): coxal plate in shape of rectangular trapezoid, as deep as wide. Propodite : dactylus length ratio 1.0 : 0.44. Dactylus, with nail measuring half of total length of dactylus, 1 dorsal seta with plumose tip, and 1 seta at nail base. Pereopod III slightly longer than pereopod IV (pereopod III : pereopod IV length ratio 1.0 : 0.92).

Pereopod IV (Fig. 52B): relatively rectangular coxal plate, with concavity on posterior margin, width : depth ratio 1.0 : 0.94. Propodite length : dactylus length ratio 1.0 : 0.4. Robust dactylus, with nail measuring half of total length of dactylus; 1 dorsal seta with plumose tip and 2 setae of different lengths at nail base.

Pereopod V (Fig. 53A): coxal plate of irregular shape, with deep concavity on ventral side, 6 anterior setae and 2 posterior setae. Basis ovoid-rectangular shaped, length : width ratio 1.0 : 0.62, 5 groups of 1–2 setae on anterior margin, 12 setae on posterior margin, 4 anteroapical setae of different lengths. Dactylus with 1 dorsal seta with plumose tip, 2 setae of different lengths at nail base, which represents 40% of total dactylus length. Propodite length : dactylus length ratio 1.0 : 0.28.

Pereopod VI (Fig. 53B): coxal plate smaller than that of pereopod V, but highly similar in shape and 2 posterior setae. Basis ovoid-rectangular shaped, length : width ratio 1.0 : 0.51, 6 groups of 1–2 setae on anterior margin, 12 setae on posterior margin, 5 anteroapical setae of different lengths. Dactylus with 1

plumose seta on outer margin and 2 setae of different lengths near nail base. Nail 35% of total dactylus length. Ratio propodite : dactylus length 1.0 : 0.34.

Pereopod VII (Fig. 53C): longest leg (5.65 mm) of inspected paratype male. Coxal plate trapezoidal, with 1 seta on posterior margin. Basis ovoid-rectangular, ratio length : width 1.0 : 0.5, 5 groups of 1–2 setae

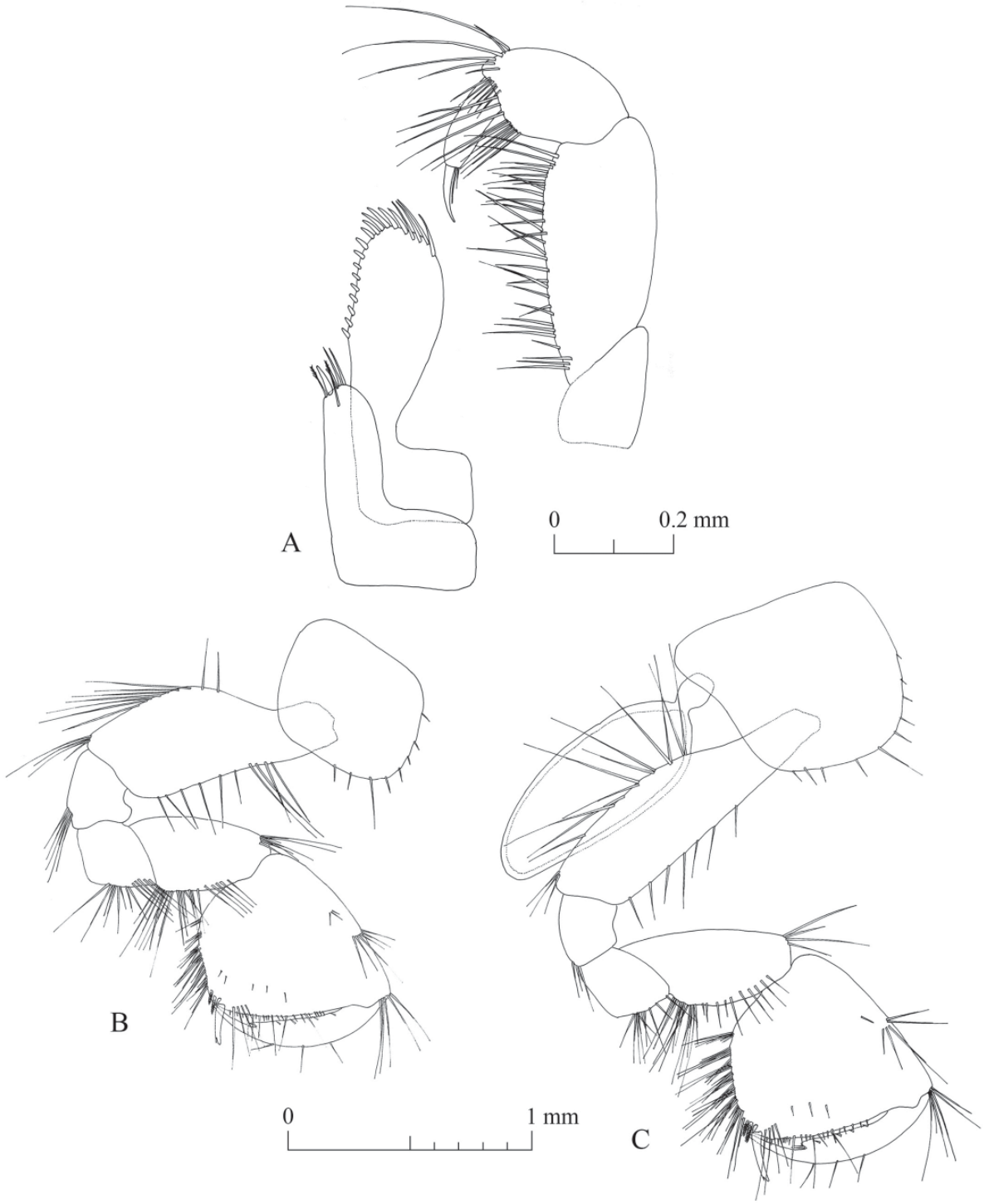

Fig. 51. *Niphargus lotharingiensis* Weber & Brad sp. nov., paratype, ♂ (ISER DW160703-02). **A**. Maxilliped. **B**. Gnathopod I. **C**. Gnathopod II.

on anterior margin, 14 setae on posterior margin and 4 anteroapical setae of different lengths. Dactylus with 1 plumose seta on outer margin and 2 setae of different lengths near nail base. Nail length 40% of total dactylus length. Ratio propodite : dactylus length 1.0 : 0.3.

Pereopods V : VI : VII ratio 1.0 : 1.22 : 1.52.

Pleopods

Pleopods: similar (pleopod I depicted in Fig. 54A), with unequal rami, 3 (pleopods I and II) and 4 (pleopods III) hooks on retinaculum.

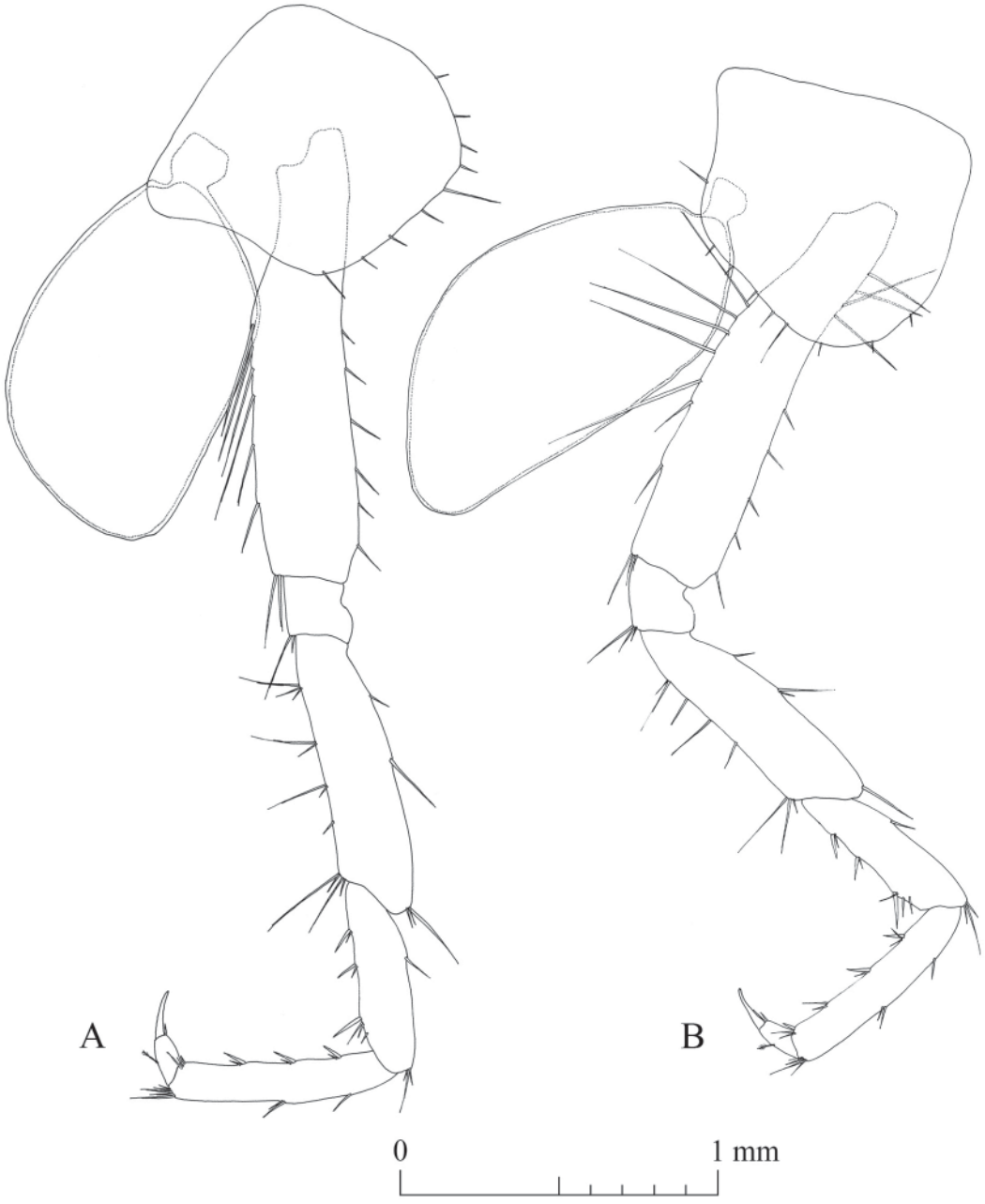

Fig. 52. *Niphargus lotharingiensis* Weber & Brad sp. nov., paratype, ♂ (ISER DW160703-02). **A**. Pereopod III. **B**. Pereopod IV.

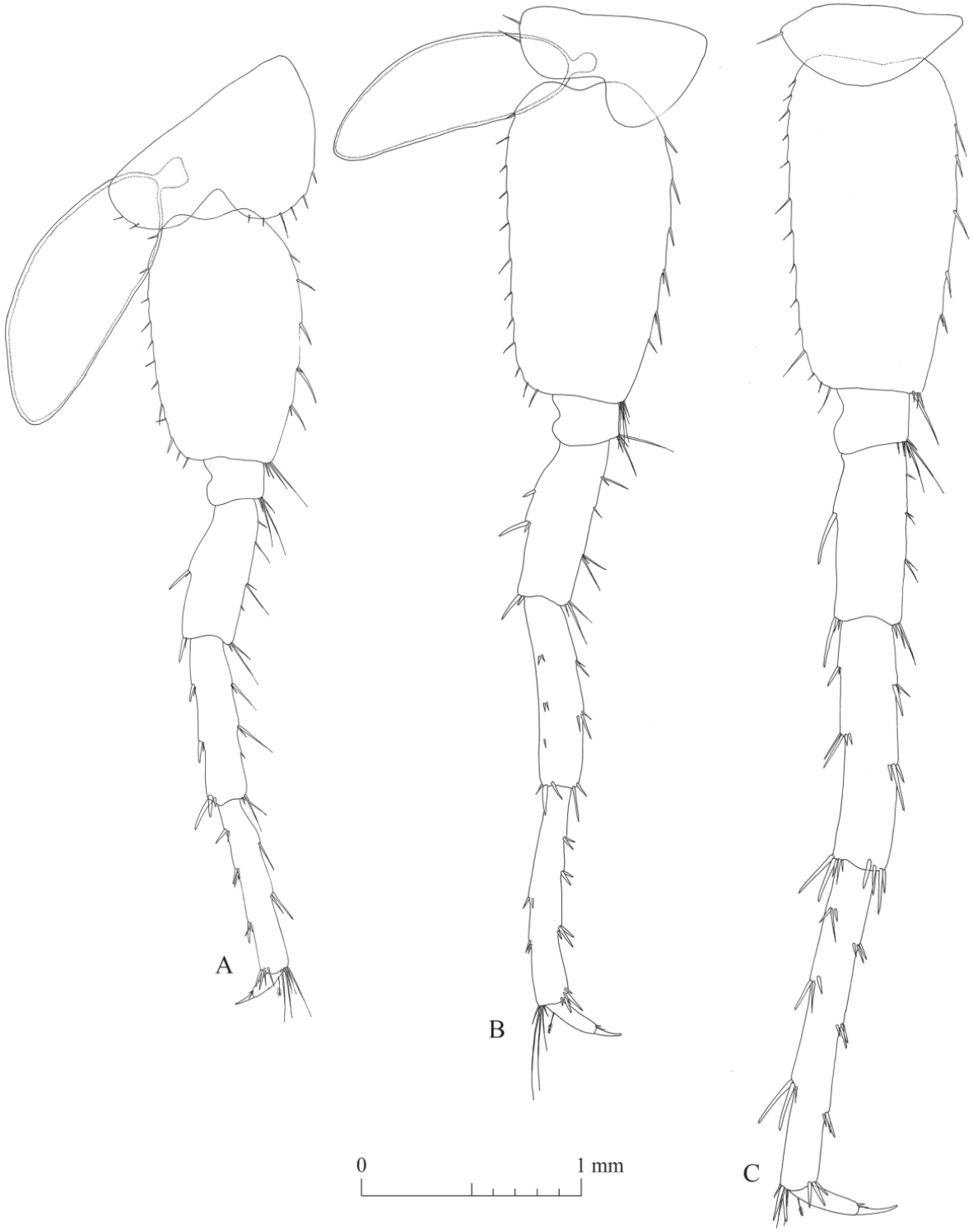

Fig. 53. *Niphargus lotharingiensis* Weber & Brad sp. nov., paratype, ♂ (ISER DW160703-02). **A**. Pereopod V. **B**. Pereopod VI. **C**. Pereopod VII.

Epimeral plates (Fig. 54B)
Epimeral plate I with right postero-ventral angle, relatively straight ventral margin, convex posterior margin with 2 setae. Epimeral plate II with right postero-ventral angle, convex ventral margin with 1 antero-ventral spine, convex posterior margin with 8 setae. Epimeral plate III with right posteroventral angle, relative straight ventral margin with 2 antero-ventral spines, straight posterior margin with 9 setae.

Uropods
Uropod I (Fig. 55A): with two dorso-lateral rows of 4–5 spines on peduncle. Exopodite slightly longer than endopodite, ratio exopodite : endopodite lengths 1.0 : 0.95. 1 strong spine at base of uropod I.

Uropod II (Fig. 55B): with 2 dorsal spine and 3 apical spines on peduncle. Endopodite slightly longer than exopodite, endopodite : exopodite length ratio 1.0 : 0.96, both rami provided with 3–4 dorsal and 5–6 apical spines.

Uropod III (Fig. 55C): sexually differentiated, longer in males. Peduncle with 3 apical and 3 posterior setae. Short endopodite, 40% of length of peduncle, with 1 apical seta. Proximal segment of exopodite longer than distal segment (ratio 1.0 : 0.7). Anterior margin of proximal segment of exopodite with 6 groups of 2–4 setae (including plumose setae); posterior margin of exopodite with 3 groups of 3–4 setae; 4 antero- and 4 postero-apical setae. Distal segment of exopodite with 3 groups of 1–2 setae on anterior margin, 3 groups of 1–2 setae on posterior margin, 4 apical and 4 subapical setae of different lengths.

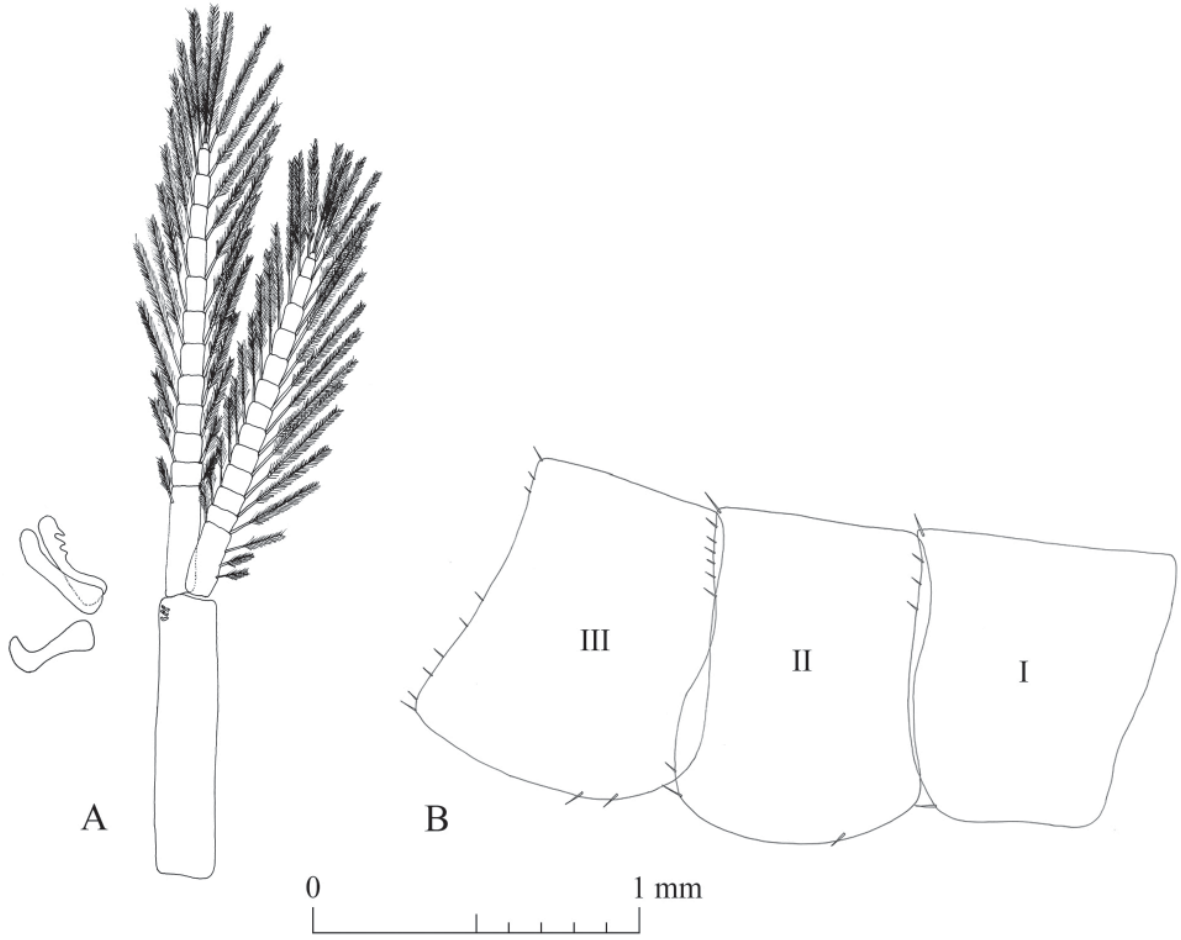

Fig. 54. *Niphargus lotharingiensis* Weber & Brad sp. nov., paratype, ♂ (ISER DW160703-02). **A**. Pleopod I, detail of the retinaculum. **B**. Detail of the epimeral plates.

Telson

Telson (Fig. 55E): nearly as wide as long (width : length ratio 0.95), with 2 subapical and 5 apical spines of different lengths on each lobe. Longest spine slightly longer than half of telson length. 2 thin setae of different lengths and plumose tip, 1 seta medially on 1 lobe.

Sexual dimorphism

The examined male and female are highly similar. Besides the usual sexual dimorphism (e.g., slightly smaller gnathopods, presence of oostegites, and slightly deeper coxal plates I–VI in females), in

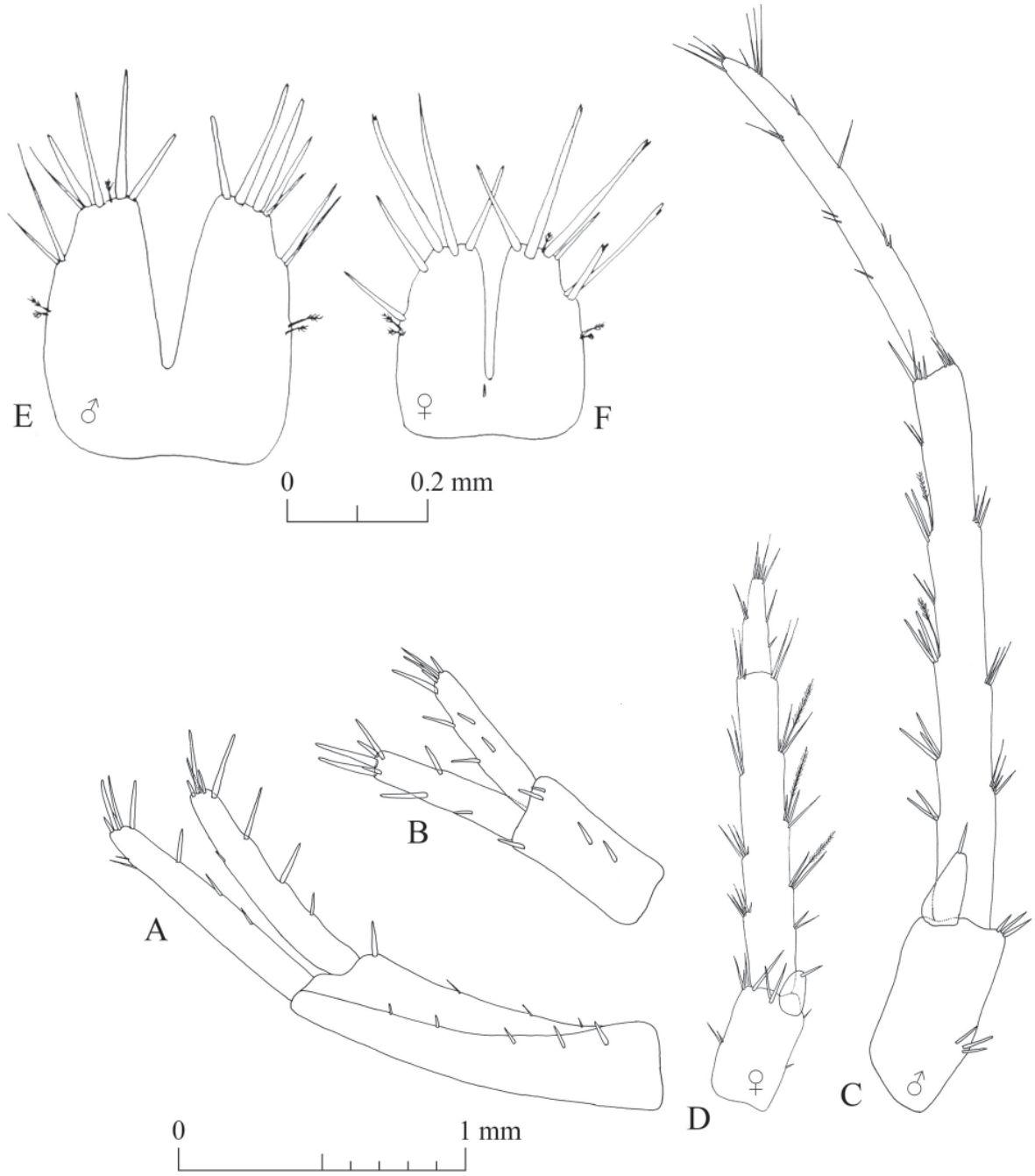

Fig. 55. *Niphargus lotharingiensis* Weber & Brad sp. nov., paratype, ♂ (ISER DW160703-02) and paratype, ♀ (ISER DW160703-01). **A**. Male uropod I. **B**. Male uropod II. **C**. Male uropod III. **D**. Female uropod III. **E**. Male telson. **F**. Female telson.

N. lotharingiensis sp. nov., the female uropod III (Fig. 55D) is shorter than that of the male, and the telson of the inspected female paratype is provided apically with 4 setae only on each lobe (Fig. 55F).

Type locality, ecology and distribution

The species is widely distributed in eastern France (Fig. 56), with a slight geographical overlap with its sister species *N. schellenbergi* sensu stricto in the northeastern margin of its distribution range (Fig. 2). It comprises two distinct genetic clades, of which one is very rare and currently only known from two sites in the eastern part of the species' range. The type locality is the Tunnel du Col des Croix (connecting Vosges and Haute-Saône, France) at 47.8632° N, 6.7464° E, in the very east of the species known distribution (Supp. file 3.10). It is a 1087 m long abandoned railway tunnel with a 1 m rail gage once connecting Lure (Haute-Saône, France) with Le Thillot (Vosges, France). After its closure in 1962, it was used for the supply of potable water and was therefore locked.

Niphargus lotharingiensis sp. nov. can be found in a variety of subterranean biotopes (Supp. file 4.6). However, the inferred absence in the interstitial environment is most likely due to the fact that the species does not occur in the area where the interstitial environment was intensively sampled.

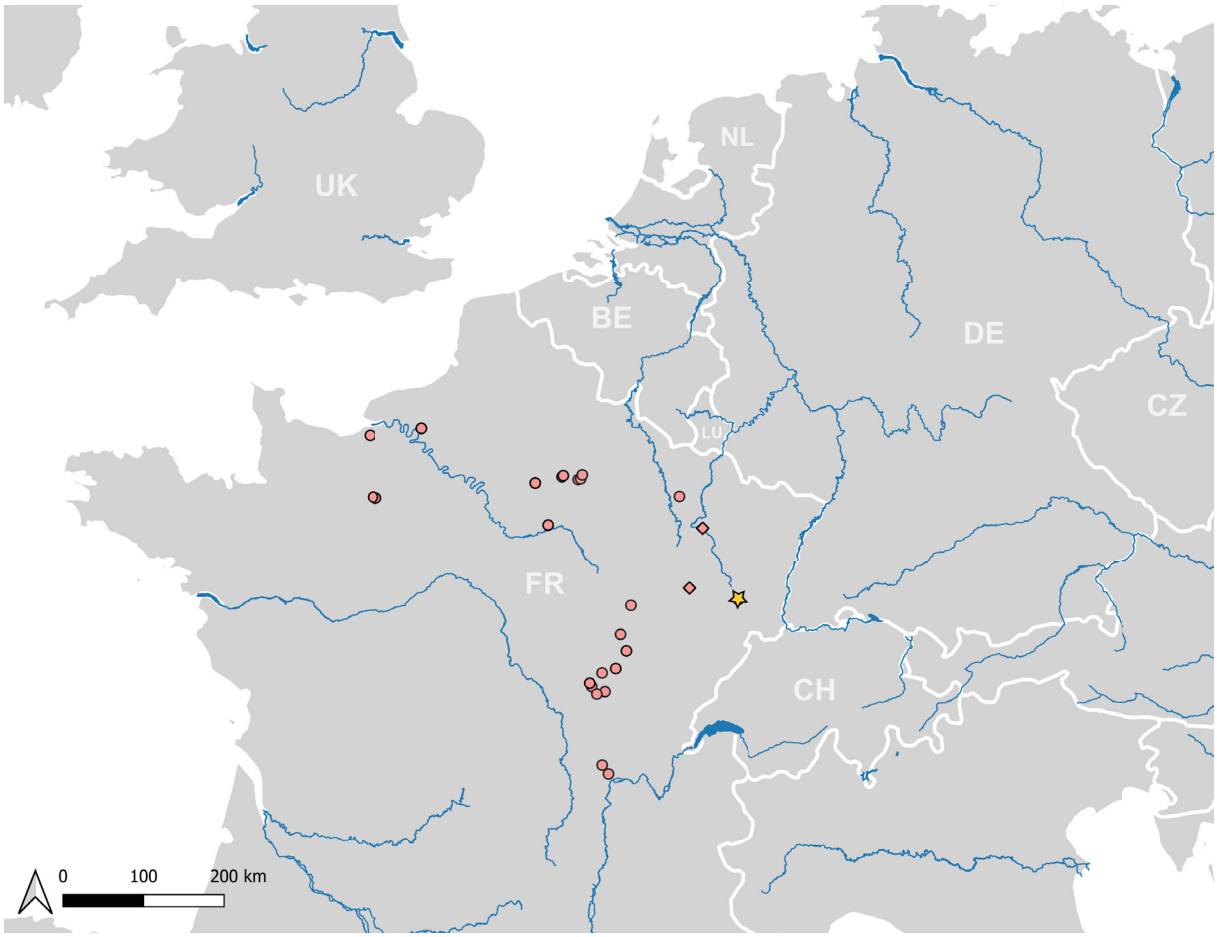

Fig. 56. Distribution of *Niphargus lotharingiensis* Weber & Brad sp. nov. confirmed by molecular data. The type locality at the Tunnel du Col des Croix (France) is marked by a yellow star, overlaying one site record. Circles and diamonds refer to two distinct genetic clades. Very large freshwater bodies are indicated; country codes follow the ISO 3166 standard alpha-2 format.

Discussion

Notes on crypsis and pseudocrypsis in the *N. aquilex* species complex

With the recent integration of DNA characters, Weber *et al.* (2023) provided the first solid molecular framework to shed further light on the complex taxonomic situation within the *N. aquilex* species complex. In the present work, by adding new molecular data as well as an in-depth morphological (re)investigation, we newly described six of the molecular entities delineated by Weber *et al.* (2023). Morphologically, the six species described herein can be considered pseudocryptic because several minor morphological differences were observed. In general, species are counted as cryptic if they cannot be distinguished by their morphology, that is, if the morphological variation within a species is that high (i.e., variable) or low (i.e., static) that it widely overlaps with its congeners. Cryptic species of *Niphargus* can only be distinguished by means of methods other than morphology, which are currently mainly molecular characters in their DNA. By incorporating other lines of evidence (e.g., DNA sequences) and morphologically re-examining the specimens at hand according to the proposed genetic clustering, it may become apparent that other morphological characters can serve as diagnostic traits to allow robust species delineations (Knowlton 1993; Luttikhuizen & Dekker 2010). The *N. aquilex* species complex is an excellent example of a combination of cryptic and pseudocryptic species pairs. The six species described herein can be best distinguished by the nucleotide sequences of their COI and 28S rDNA gene fragments, along with a few morphological differences. Pure diagnostic nucleotide positions in their COI barcodes – allowing the unambiguous identification of a single species from one or a few single nucleotide polymorphisms (SNPs) – were scarce or even non-existing for some species (*N. schellenbergi* sensu stricto, *N. normandiensis* sp. nov., *N. lotharingiensis* sp. nov.). A notable exception was *N. palatinensis* sp. nov., which showed six pure diagnostic nucleotide positions. The reduced number of informative (diagnostic) SNPs to identify single species can be best explained by the combination of the following aspects: a) COI comprises a rather fast-evolving protein-coding gene, with the degeneracy of the genetic code allowing codons to mutate more easily while still coding for an identical amino acid, b) nucleotide data has only four character states (A, T, G, C), and homoplastic characters can arise over time due to parallel mutations at homologous sites, c) the number of unique DNA sequence variants was high in several species (213 for *N. schellenbergi* sensu stricto, 79 for *N. luxemburgensis* sp. nov., and 51 for *N. aquilex* sensu stricto), and d) the analysis of sister species pairs within a hyperdiverse species complex with more similar genetic sequence variants when compared to more distantly related congeners. All these aspects reduce the likelihood of observing pure diagnostic SNPs for a single species.

Notes on molecular species delimitations

In a more comprehensive ASAP species delimitation approach, the new genetic data yielded between 16 and 21 potential species, while initially only 10 to 15 potential species were delineated (Weber *et al.* 2023). However, not all potential species groups were affected by ASAP analysis of our comprehensive molecular dataset. As such, the newly described species *N. palatinensis* sp. nov. (former species A sensu Weber *et al.* 2023) and *N. wasgauensis* sp. nov (former species I sensu Weber *et al.* 2023) always formed a single distinct molecular cluster (Table 1). The same situation holds true for the former species B sensu Weber *et al.* (2023), which, based on three specimens found in the stated area of the type locality (Crowborough, UK) (Karaman 1980), can be assigned to *N. aquilex* sensu stricto. This taxon has not been re-described here because a comprehensive re-description is available (Karaman 1980).

For the other taxa morphologically examined in the present study, the genetically enriched ASAP analysis provided a more complex situation. The two molecular lineages, S and R+R* sensu Weber *et al.* (2023), of the morphospecies *N. schellenbergi* were clearly separated by their 28S rDNA markers, but ASAP analysis failed to clearly separate them. This result, however, was reasonable given that ASAP is a genetic distance-based approach, and only two mutational steps are present between their nuclear 28S rDNA alleles. However, COI partitions also differed in their results. Partition 1 clustered both potential species

Table 1. Summary of molecular species delimitations. Numbers in columns 2-4 refer to the cluster names by ASAP in this study.

Species name	COI ASAP partition 1	COI ASAP partition 2	COI ASAP partition 3	28S rDNA ASAP (Weber *et al.* 2023)	Haplotype network (Weber *et al.* 2023)
Niphargus aquilex s. str.	5	4	5	B	B
Niphargus luxemburgensis sp. nov.	3	7	8	F’	F
Niphargus luxemburgensis sp. nov.	3	8	9	F	F
Niphargus normandiensis sp. nov.	9	15	17	missing	missing
Niphargus normandiensis sp. nov.	9	11	12	N	N
Niphargus normandiensis sp. nov.	9	18	20	missing	missing
Niphargus palatinensis sp. nov.	1	1	1	A	A
Niphargus saraviensis sp. nov.	4	3	3	G	G
Niphargus saraviensis sp. nov.	4	4	4	missing	missing
Niphargus saraviensis sp. nov.	4	16	18	missing	missing
Niphargus schellenbergi s. str.	2	2	2	S	S
Niphargus lotharingiensis sp. nov.	2	6	7	R	R
Niphargus lotharingiensis sp. nov.	2	6	16	R*	R
Niphargus wasgauensis sp. nov.	6	5	6	I	I
not described	10	12	13	K	K
not described	10	12	13	L	L
not described	11	13	14	H’	H
not described	7	9	10	H	H
not described	8	10	11	J	J
not described	12	14	15	missing	missing
not described	13	17	19	missing	missing
not described	14	19	21	missing	missing
not described	15	20	22	missing	missing
not described	16	21	23	missing	missing

as a single entity, while partition 2 delineated S and R+R*, and partition 3 even delineated S, R and R* into three entities (Table 1). As discussed more comprehensively by Weber *et al.* (2023), the hypothesis of a single species, S+R+R*, can be rejected with high confidence, even though a single specimen existed that had contradicting COI and 28S assignments. This was attributed to the evolutionary phenomenon of mitochondrial DNA capture, a common source of mitonuclear discordance (Weber *et al.* 2023). The delineated molecular lineage S thereby refers to *N. schellenbergi* sensu stricto, as it includes individuals from a locality very close to the type locality of this species. The molecular lineage R sensu Weber *et al.* (2023), which is widely distributed in France, was newly described as *N. lotharingiensis* sp. nov.

For *N. luxemburgensis* sp. nov., both genetic markers, COI and 28S rDNA, resulted in two distinct clades (F+F’). However, the 28S rDNA dataset comprises two heterozygous individuals that also bear COI haplotypes from both clades F and F’. Likewise, partition 1 of ASAP (but not partitions 2 and 3) supports the delineation of a single species based on genetic distances. Therefore, we described the former species F+F’ sensu Weber *et al.* (2023) as *N. luxemburgensis* sp. nov.

The distinctiveness of the newly described species *N. normandiensis* sp. nov. – referring to the former species D sensu Weber *et al.* (2023) – is supported by an identical 28S rDNA allele of all individuals, even though COI sequences were quite distinct. As a result, the partitions 2 and 3 of the ASAP analysis of the COI dataset suggested the presence of three putative species in total.

Acknowledgements

We thank Jochen Babist, Arne Beermann, Charles Bernard, Sandra Cervantes, Claire Chauveau, Serge Delaby, J. Diergarten, M. Diergarten-Ahlmer, Robert Dondelinger, Rolf Dorn, Jessica Durkota, Ute Fricke, Reinhard Gerecke, Hamon Goutorbe, Christine Harbusch, Christof Huber, Tim Johns, Peter Jordan, Sabine Kaufmann, Gregory Kirby, Lee Knight, Erich Knust, Dieter Kraus, Andreas Krause, Thomas Sebastian Lechner, Andy Lewington, Bernard Lips, Josiane Lips, Christa Locke, Hans-Martin Luz, Florian Malard, Stefan Meyer, Agnieszka Noculak, Patrice Notteghem, L. Ochs, Joep Orbons, Aneliya Pavlova, Christophe Prevot, Yves Quinif, Catalina Ramirez-Portilla, Alexander Ramm, Iris Rudolf, Alexandre Ruffioni, Axel Rüthrich, Stephan Schild, Rainer Sennewald, F. Seumer, Helmut Steiner, Fabio Stoch, Julia Streich, J. Subzow, Vid Svara, Ursula Swaelus, Udo Tauchert, Ann-Cathrin Thiery, Jens Trasberger, Klaus Tuschinsky, Markus Utesch, Stefan Voigt, Monika Weber, Verena Weber, Heinz-Werner Weber, Debbie White, Siegfried Wielert, Annette Zaenker, Christian Zaenker, and Stefan Zaenker for their assistance in collecting the samples. Collecting and access to the protected site Kossmannskaule was permitted by the city of Königswinter, Armin Krämer, Allgemeine Sicherheit und Ordnung, 53639 Königswinter, dated March 16th, 2017; Verschönerungsverein für das Siebengebirge, Naturpark Siebengebirge, Werner Stieber, Geschäftsführung, Königswinter, Forsthaus Lohrberg dated March 28th, 2017; Streve‘sche Liegenschaftsverwaltung, Josef Schliebusch dated May 2nd, 2017. Serge Delaby, UNESCO Global Geopark Famenne-Ardenne, permitted access to the Grotte d’Éprave and to the Grotte Lorette. Jochen Babist, and Gregory Kirby, Arbeitsgemeinschaft Altbergbau Odenwald, permitted the access to the Schwefelkiesbergwerk. Most of the sequences were generated in the laboratory of Jean-François Flot, Université libre de Bruxelles (Belgium) and in the laboratory of the Musée national d’histoire naturelle du Luxembourg. Bernd Haenfling provided his unpublished sequences from the UK and the Channel Islands. Marie Jo Olivier allowed using her unpublished data from France. Stefan Zaenker allowed using unpublished data from Hesse (Germany). Fabio Stoch greatly assisted in checking and correcting the morphological descriptions.

Funding

This research was funded by Biodiversa+, the European Biodiversity Partnership under the 2021–2022 BiodivProtect joint call for research proposals, co-funded by the European Commission (GA N°101052342) and with the funding organisations Ministry of Universities and Research (Italy), Agencia Estatal de Investigación – Fundación Biodiversidad (Spain), Fundo Regional para a Ciência e Tecnologia (Portugal), Suomen Akatemia – Ministry of the Environment (Finland), Belgian Science Policy Office (Belgium), Agence Nationale de la Recherche (France), Deutsche Forschungsgemeinschaft e.V. (Germany), Schweizerischer Nationalfonds (Grant N° 31BD30_209583, Switzerland), Fonds zur Förderung der Wissenschaftlichen Forschung (Austria), Ministry of Higher Education, Science and Innovation (Slovenia), the Executive Agency for Higher Education, Research, Development and Innovation Funding (Romania), and the Ministry of Environment, Climate and Biodiversity (Luxembourg).

References

Aparicio-Puerta E., Gómez-Martín C., Giannoukakos S., Medina J.M., Scheepbouwer C., García-Moreno A., ... & Hackenberg M. 2022. sRNAbench and sRNAtoolbox 2022 update: accurate miRNA and sncRNA profiling for model and non-model organisms. *Nucleic Acids Research* 50 (W1): W710–W717. https://doi.org/10.1093/nar/gkac363

Astrin J.J. & Stüben P.E. 2008. Phylogeny in cryptic weevils: molecules, morphology and new genera of western Palaearctic Cryptorhynchinae (Coleoptera: Curculionidae). *Invertebrate Systematics* 22 (5): 503–522. https://doi.org/10.1071/IS07057

Brad T., Fišer C., Flot J.-F. & Sarbu S.M. 2015. *Niphargus dancaui* sp. nov. (Amphipoda, Niphargidae) – a new species thriving in sulfidic groundwaters in southeastern Romania. *European Journal of Taxonomy* 164: 1–28. https://doi.org/10.5852/ejt.2015.164

Delić T., Trontelj P., Rendoš M. & Fišer C. 2017. The importance of naming cryptic species and the conservation of endemic subterranean amphipods. *Scientific Reports* 7: 3391. https://doi.org/10.1038/s41598-017-02938-z

Dobat K. 1968. Mitteilung über die aquatile Fauna einiger Höhlen der Schwäbischen Alb. *Mitteilungen des Verbandes der deutschen Höhlen- und Karstforscher e. V.* 14 (11): 31–33.

Dobreanu E., Manolache C. & Puscariu V. 1953. Noi specii de Amphipode freatice din R.P.R. *Bulletin Stiintific, Sectiunea de Stiinte Biologice, Agronomice, Geologice si Geografice* 5 (3): 603–616.

Eme D., Zagmajster M., Delić T., Fišer C., Flot J.-F., Konecny-Dupré L., Snaebjörn P., Stoch F., Zakšek V., Douady C.J. & Malard F. 2018. Do cryptic species matter in macroecology? Sequencing European groundwater crustaceans yields smaller ranges but does not challenge biodiversity determinants. *Ecography* 41 (2): 424–436. https://doi.org/10.1111/ecog.02683

Esmaeili-Rineh S., Sari A., Fišer C. & Bargrizaneh Z. 2017. Completion of molecular taxonomy: description of four amphipod species (Crustacea: Amphipoda: Niphargidae) from Iran and release of database for morphological taxonomy. *Zoologischer Anzeiger* 271: 57–79. https://doi.org/10.1016/j.jcz.2017.04.009

Fišer C. & Zagmajster M. 2009. Cryptic species from cryptic space: the case of *Niphargus fongi* sp. n. (Amphipoda, Niphargidae). *Crustaceana* 82 (5): 593–614. https://doi.org/10.1163/156854009X407704

Fišer C., Sket B., Turjak M. & Trontelj P. 2009a. Public online databases as a tool of collaborative taxonomy: a case study on subterranean amphipods. *Zootaxa* 2095 (1): 47–56. https://doi.org/10.11646/zootaxa.2095.1.5

Fišer C., Trontelj P., Luštrik R. & Sket B. 2009b. Towards a unified taxonomy of *Niphargus* (Crustacea: Amphipoda): a review of morphological variability. *Zootaxa* 2061 (1): 1–22. https://doi.org/10.11646/zootaxa.2061.1.1

Fišer C., Konec M., Alther R., Švara V. & Altermatt F. 2017. Taxonomic, phylogenetic and ecological diversity of *Niphargus* (Amphipoda: Crustacea) in the Hölloch cave system (Switzerland). *Systematics and Biodiversity* 15 (3) 218–237. https://doi.org/10.1080/14772000.2016.1249112

Fišer C., Alther R., Zakšek V., Borko Š., Fuchs A. & Altermatt F. 2018. Translating *Niphargus* barcodes from Switzerland into taxonomy with a description of two new species (Amphipoda, Niphargidae). *ZooKeys* 760: 113–141. https://doi.org/10.3897/zookeys.760.24978

Flot J.-F., Wörheide G. & Dattagupta S. 2010. Unsuspected diversity of *Niphargus* amphipods in the chemoautotrophic cave ecosystem of Frasassi, central Italy. *BMC Evolutionary Biology* 10: 171. https://doi.org/10/dbpkg8

Folmer O., Black M., Hoeh W., Lutz R. & Vrijenhoek R. 1994. DNA primers for amplification of mitochondrial cytochrome *c* oxidase subunit I from diverse metazoan invertebrates. *Molecular Marine Biology and Biotechnology* 3 (5): 294–299.

Gerecke R., Stoch F., Meisch C. & Schrankel I. 2005. *Die Fauna der Quellen und des hyporheischen Interstitials in Luxembourg.* Ferrantia 41. Museum of Natural History of Luxembourg, Luxembourg.

Horton T., De Broyer C., Bellan-Santini D., Coleman C.O., Copilaş-Ciocianu D., Corbari L., Daneliya M.E., Dauvin J.-C., Decock W., Fanini L., Fišer C., Gasca R., Grabowski M., Guerra-García J.M., Hendrycks E.A., Hughes L.E., Jaume D., Kim Y.-H., King R.A., Lo Brutto S., Lörz A.-N., Mamos T., Serejo C.S., Senna A.R., Souza-Filho J.F., Tandberg A.H.S., Thurston M.H., Vader W., Väinölä R., Valls Domedel G., Vandepitte L., Vanhoorne B., Vonk R., White K.N. & Zeidler W. 2023. The World Amphipoda Database: history and progress. *Records of the Australian Museum* 75 (4): 329–342. https://doi.org/10.3853/j.2201-4349.75.2023.1875

Husmann S. 1976. Studies on subterranean drift of stygobiont crustaceans (*Niphargus*, *Crangonyx*, *Graeteriella*). *International Journal of Speleology* 8: 81–92. https://doi.org/10.5038/1827-806X.8.1.7

Inkscape Project. 2017. Inkscape (Version 0.92) [Computer software].
Available from https://inkscape.org [accessed 14 Aug. 2025].

Jörger K.M. & Schrödl M. 2014. How to use CAOS software for taxonomy? A quick guide to extract diagnostic nucleotides or amino acids for species descriptions. *Spixiana* 37 (1): 21–26.

Karaman G.S. 1980. Contribution to the knowledge of the Amphipoda 113. Redescription of *Niphargus aquilex* Schiödte and its distribution in Great Britain. *Biosistematika* 6 (2): 175–185.

Karaman G.S. 1993. *Fauna d'Italia (31): Crustacea Amphipoda (d'aqua dolce)*. Edizioni Calderini, Bologna.

Karaman G.S. 2017. New data on two subterranean species of the family Niphargidae from Spain, *Niphargus gallicus* Schell., 1935 and *N. delamarei* Ruffo, 1954 (contribution to the knowledge of the Amphipoda 282). *Contributions, Section of Natural, Mathematical and Biotechnical Sciences* 36 (2): 105–120.

Karaman S. 1932. 5. Beitrag zur Kenntnis der Süsswasser-Amphipoden. *Prirodoslovne razprave* 2: 179–232.

Knowlton N. 1993. Sibling species in the sea. *Annual Review of Ecology and Systematics* 24 (1): 189–216. https://doi.org/10.1146/annurev.es.24.110193.001201

Kumar S., Stecher G., Li M., Knyaz C. & Tamura K. 2018. MEGA X: molecular evolutionary genetics analysis across computing platforms. *Molecular Biology and Evolution* 35 (6): 1547–1549.
https://doi.org/10.1093/molbev/msy096

Kureck A. 1967. Über die tagesperiodische Ausdrift von *Niphargus aquilex schellenbergi* KARAMAN aus Quellen. *Zeitschrift für Morphologie und Ökologie der Tiere* 58: 247–262.
https://doi.org/10.1007/BF00407379

Luttikhuizen P.C. & Dekker R. 2010. Pseudo-cryptic species *Arenicola defodiens* and *Arenicola marina* (Polychaeta: Arenicolidae) in Wadden Sea, North Sea and Skagerrak: Morphological and molecular variation. *Journal of Sea Research* 63 (1): 17–23. https://doi.org/10.1016/j.seares.2009.09.001

McInerney C.E., Maurice L., Robertson A.L., Knight L.R.F.D., Arnscheidt J., Venditti C., Dooley J.S.G., Mathers T., Matthijs S., Erikkson K., Proudlove G.S. & Hänfling B. 2014. The ancient Britons: Groundwater fauna survived extreme climate changes over tens of millions of years across NW Europe. *Molecular Ecology* 23: 1153–1166. https://doi.org/10.1111/mec.12664

Puillandre N., Brouillet S. & Achaz G. 2020. ASAP: assemble species by automatic partitioning. *Molecular Ecology Resources* 21: 609–620. https://doi.org/10.1111/1755-0998.13281

QGIS Development Team. 2025. QGIS Geographic Information System (Version 3.x) [Computer software]. QGIS Association. Available from https://qgis.org [accessed 14 Aug. 2025].

Sayers E.W., Cavanaugh M., Clark K., Pruitt K.D., Schoch C.L., Sherry S.T. & Karsch-Mizrachi I. 2021. GenBank. *Nucleic Acids Research* 49: D92–D96. https://doi.org/10.1093/nar/gkaa1023

Schellenberg A. 1932. Deutsche subterrane Amphipoden. *Zoologischer Anzeiger* 99 (11/12): 311–323.

Schellenberg A. 1933. Weitere deutsche und ausländische Niphargiden. *Zoologischer Anzeiger* 102: 22–33.

Schiödte J.C. 1855. Om den i England opdagede art af hulekrebs-slægten *Niphargus*. *Oversigt over det Kongelige danske Videnskabernes Selskabs Forhandlinger og dets Medlemmers Arbeider i Aaret* 1855 (7–8): 349–351.

Sket B. 1999. *Niphargus aquilex dobati* ssp. n. (Crustacea) from the karst of Slovenia. *Mitteilungen des Verbandes der deutschen Höhlen- und Karstforscher* 45: 54–56.

Straškraba M. 1972. Les groupement des espèces du genre *Niphargus* (sensu lato). *In*: Ruffo S. (ed.) *Actes du premier colloque international sur le genre Niphargus*: 85–90. Museo Civico di Storia Naturale di Verona.

Thienemann A. 1922. Hydrobiologische Untersuchungen an Quellen. *Archiv für Hydrobiologie* 14: 151–190.

Verovnik R., Sket B. & Trontelj P. 2005. The colonization of Europe by the freshwater crustacean *Asellus aquaticus* (Crustacea: Isopoda) proceeded from ancient refugia and was directed by habitat connectivity. *Molecular Ecology* 14 (14): 4355–4369. https://doi.org/10.1111/j.1365-294X.2005.02745.x

Weber D. 1988. *Die Höhlenfauna und -flora des Höhlenkatastergebietes Rheinland-Pfalz/Saarland*. Abhandlungen zur Karst- und Höhlenkunde 22. Verband der deutschen Höhlen- und Karstforscher, München.

Weber D. 1989. *Die Höhlenfauna und -flora des Höhlenkatastergebietes Rheinland-Pfalz/Saarland, 2. Teil*. Abhandlungen zur Karst- und Höhlenkunde 23. Verband der deutschen Höhlen- und Karstforscher, München.

Weber D. & Weigand A.M. 2023. Groundwater amphipods of the hyporheic interstitial: a case study from Luxembourg and the greater region. *Diversity* 15 (3): 411. https://doi.org/10.3390/d15030411

Weber D., Flot J.-F., Frantz A.C. & Weigand A.M. 2022. Molecular analyses of groundwater amphipods (Crustacea: Niphargidae) from Luxembourg: new species reveal limitations of morphology-based checklists. *Zootaxa* 5222 (6): 501–533. https://doi.org/10.11646/zootaxa.5222.6.1

Weber D., Brad T., Weigand A. & Flot J.-F. 2023. Water diviners multiplied: cryptic diversity in the *Niphargus aquilex* species complex in Northern Europe. Preprint BioRxiv 2023.08.13.553147. https://doi.org/10.1101/2023.08.13.553147

Werno A. & Weber D. 2008. 'Zillas Felsenkeller' in Nunkirchen (Saarland), ein künstlicher Hohlraum mit herausragender Evertebratenfauna. *Abhandlungen der Delattinia* 34: 139–146.

Westwood J.O. 1853. Notice of the discovery in England of a new genus and species of Amphipodous Crustacea, the *Niphargus stygius* of Schiödte. *Proceedings of the Linnean Society of London* 2: 218–219.

Wrześniowski A. 1890. Über drei unterirdische Gammariden. *Zeitschrift für wissenschaftliche Zoologie* 50: 600–724.

Printed versions of all papers are deposited in the libraries of four of the institutes that are members of the *EJT* consortium: Muséum national d'Histoire naturelle, Paris, France; Meise Botanic Garden, Belgium; Royal Museum for Central Africa, Tervuren, Belgium; Royal Belgian Institute of Natural Sciences,

Brussels, Belgium. The other members of the consortium are: Natural History Museum of Denmark, Copenhagen, Denmark; Naturalis Biodiversity Center, Leiden, the Netherlands; Museo Nacional de Ciencias Naturales-CSIC, Madrid, Spain; Leibniz Institute for the Analysis of Biodiversity Change, Bonn – Hamburg, Germany; National Museum of the Czech Republic, Prague, Czech Republic; The Steinhardt Museum of Natural History, Tel Aviv, Israël.

Supp. file 1. List of all published and in Genbank (Sayers *et al.* 2021) stored COI and 28S sequences of *Niphargus aquilex* Schiødte, 1855, *Niphargus schellenbergi* S. Karaman, 1932, and the new species. https://doi.org/10.5852/ejt.2025.1011.3023.13555

Supp. file 2. A. Already published abbreviations of existing or newly described species. The "Region" line shows which region the corresponding publication is about. **B**. Used colors and color names following https://www.w3schools.com/colors/colors_names.asp.
https://doi.org/10.5852/ejt.2025.1011.3023.13557

Supp. file 3. Photos of type locality or collecting localities close to type locality.
https://doi.org/10.5852/ejt.2025.1011.3023.13559

Supp. file 4. Habitats of the individual species. https://doi.org/10.5852/ejt.2025.1011.3023.13561

Supp. file 5. Used primers. https://doi.org/10.5852/ejt.2025.1011.3023.13563

Supp. file 6. Finding list and ASAP results. https://doi.org/10.5852/ejt.2025.1011.3023.13565

Supp. file 7. COI tree. https://doi.org/10.5852/ejt.2025.1011.3023.13567

Supp. file 8. Description of COI tree. https://doi.org/10.5852/ejt.2025.1011.3023.13569

Supp. file 9. Full 28S rDNA fragment available, 2 sequences (A in column M); only part of 28S rDNA fragment available, 78 sequences (B in column M); data from Weber *et al*. (2023), full 28S rDNA fragment and full COI available, 195 sequences (C in column M); new data within this study, full 28S rDNA fragment available, 138 sequences (D in column M); new data within this study, only part of 28S rDNA fragment available, 2 sequences (E in column M).
https://doi.org/10.5852/ejt.2025.1011.3023.13571

Supp. file 10. All measured appendages for all species described.
https://doi.org/10.5852/ejt.2025.1011.3023.13573